1991

Instrumental development of novel detection methods for liquid chromatography and capillary electrophoresis

Xiaobing Xi
Iowa State University

Order Number 9126271

Instrumental development of novel detection methods for liquid chromatography and capillary electrophoresis

Xi, Xiaobing, Ph.D.

Iowa State University, 1991

U·M·I
300 N. Zeeb Rd.
Ann Arbor, MI 48106

Instrumental development of novel detection methods for liquid chromatography and capillary electrophoresis

by

Xiaobing Xi

A Dissertation Submitted to the

Graduate Faculty in Partial Fulfillment of the

Requirements for the Degree of

DOCTOR OF PHILOSOPHY

Department: Chemistry
Major: Physical Chemistry

Approved:

Signature was redacted for privacy.

In Charge of Major Work

Signature was redacted for privacy.

For the Major Department

Signature was redacted for privacy.

For the Graduate College

Iowa State University
Ames, Iowa

1991

TABLE OF CONTENTS

GENERAL INTRODUCTION

In 1954, H. H. Strain [1] wrote about chromatography:

> *This increase in the number and applications of these basic analytical tools and a concomitant multiplication of the workers versed in their use have stimulated progress in all aspects of science concerned with chemical substances and their reactions. The resultant expansion of knowledge has been so rapid, so great and so diverse that it cannot be cited here.*

What was written about chromatography in general over three decades ago is even more descriptive of modern liquid chromatography (LC) today. LC has, indeed, stimulated progress in all areas of chemistry, biology, food technology, genetic engineering, pharmaceutical industry, environmental science and medical science. LC is now widely used as a powerful separation and quantitative analysis technique in all of these branches of science and industry.

The reason why the development of LC is ahead of other separation techniques, particularly the long-dominant gas chromatography (GC), is that many samples simply cannot be handled by GC. Either they are thermally unstable or decompose under the conditions of separation. LC, on the other hand, is not limited by sample volatility or thermal stability. Thus LC is ideally suited for the separation of macromolecules and ionic species of biomedical interest, labile natural products, and a wide variety of other high molecular weight and/or less stable

compounds.

As a general rule, the amount of information that can be obtained from any LC separation depends on, to a large extent, the ability of the detector. It is generally accepted that detectors are the weakest link in LC systems. The lack of a truly satisfactory detector has probably been the greatest single impediment to the development of LC [2]. The problem of detection in LC is far greater than in GC because both the solute and the solvent are liquids, very often with similar physical and chemical properties. The low concentrations of a solute do not modify the overall physical characteristics of the solution to the same extent that low concentrations of vapor in the gas phase modify the physical properties of the gas. Even though only 10-15% of the 6 million compounds in the chemistry registry are suitable for GC analysis because of stability and volatility, roughly one-half of current routine problems are studied with GC [3]. The primary reason is that currently the detection methods in GC are substantially better than those in LC. The development of better detection methods in LC is therefore of great importance.

Perry et al. [4] described the necessary properties of an LC detector, requirements that serve as a basis for current detector evaluation. They stated that ideal detectors for LC should have the following characteristics:

1. Have high sensitivity and the same predictable response.
2. Respond to all solutes, or have predictable specificity.

3. Respond independently of the mobile phase.
4. Have a wide range of linearity.
5. Be unaffected by change in temperature and mobile phase flow.
6. Not contribute to extra column band broadening.
7. Be reliable and convenient to use.
8. Have a response that increases linearly with the amount of solute.
9. Be nondestructive of the solute.
10. Provide qualitative information on the detected peak.
11. Have a fast response.

Unfortunately, no LC detector devised so far nearly approaches the above specifications. The LC equivalent to the sensitive and universal thermal conductivity and flame ionization detectors of GC has not yet been produced.

Developments for LC detectors have been, and will continue to be, in designing detectors that provide either new or improved information on the analytes. LC detectors that provide new chemical information are slow to develop, primarily due to the conceptual and technical challenges of the novel instrument. However, the consequences of the efforts in developing new LC detectors can often be important and rewarding, taking into account the limitations of the existing LC detectors. It is interesting to note that the most popular detectors in the early 1970's, the UV absorbance detector, the refractive index detector and the fluorescence detector, are still the most commonly used LC detectors today, nearly

two decades later, even though the detector design has changed significantly to meet the challenges of highly efficient separations.

It is of interest, in the following, to discuss LC detectors in more detail. Following next section, detection methods for microcolumn LC and capillary electrophoresis (CE) will be briefly reviewed as well. This will provide a basis for further discussion. However, it is not the purpose of this chapter to give an exhaustive bibliography on all LC, microcolumn LC and CE detectors and their applications. For this purpose, a number of specialized books and comprehensive reviews are available [2,4-11]. In addition, the development of columns and separation techniques for LC, microcolumn LC and CE will not be reviewed here, since LC, microcolumn LC and CE themselves are only used in demonstration of the detection methods in each of the projects.

Liquid chromatography detectors

UV absorbance detection It was estimated that at least 65% of the samples analyzed by LC can absorb some light at 254 nm region (in which fixed wavelength UV detectors work) and more analytes will absorb somewhere in the range of the more sophisticated variable wavelength detectors. [12,13] This, combined with the relative ease of operation and reliability, makes the UV detector the most useful and widely used LC detector. Apart from being relatively universal, selectivity in the UV detector can be realized by using multi-wavelength detection. The presence

of unresolved peaks can be diagnosed from the shift of retention time as a function of detection wavelength [14-19]. The multi-wavelength detection can also provide the information on chemical properties and structures of the analytes by using a rapid-scanning spectrometer [20]. Multi-wavelength detection has significantly progressed with the development of the photodiode array as a multichannel detector for LC [21-24]. The improvements include larger spectral range, better resolution and faster data processing. The general acceptance and popularity of the photodiode array detector have arisen from several factors: (1) it is an information-rich detector; (2) it has multi-vendor availability; and (3) powerful and economical computer hardware and software became available. For this detector, peak spectra can be compared with those of standards to confirm the identity of unknowns, thus providing another dimension of information besides retention times. Peak purity can be easily ascertained through a variety of techniques to aid method development and to provide confidence in quantitative results. Chromatograms at multiple wavelengths can either be simultaneously stored or extracted post-run from the three-dimensional data matrix to enable quantitation of multiple peaks at each of their optimum wavelengths of detection. Although photodiode array detection presents very interesting and useful alternatives, it seems to be no danger that single-channel spectrophotometric detectors will be eliminated from the market-place. As with any analytical problem, the situation will dictate the choice of detector.

Refractive index detection The refractive index (RI) detector has a unique place in LC since it is one of very few universal detectors available [25]. RI is a definitive physical characteristic of all compounds. The RI detector measures the very small difference between the RI of the eluent and a solute. The highest sensitivity is obtained when the widest difference of RI exists between the sample and the mobile phase. Difficulty frequently arises in selecting a mobile phase that provides the desired separations and shows no significant interference. In complex mixtures, single components may cover a wide range of RI values and some may closely match that of the mobile phase. An additional detriment is the requirement for rebalancing the detector each time there is a slight change in the mobile phase composition. This factor is often severely limiting since it renders the RI detector unusable in gradient elution, where mobile phase constitution or concentration is changed during the analysis to effect the separation. Since the RI detector is a number density detector, any fluctuations in the number density of the eluent in the optical region will appear as a background signal, even when no analyte is eluted from the column. Eventually, this is the limiting factor in achieving good detectability. The effect of temperature can be determined from the coefficient of thermal expansion of the liquid. The temperature dependence, dn/dT, ranges from -1×10^{-4} K^{-1} for water to -6.4×10^{-4} K^{-1} for benzene at room temperature [26]. The pressure dependence of RI can be determined from the isothermal compress-ibility of the liquid. The dn/dP ranges from 0.16×10^{-9} m^2/N for water to 0.90 x

10^{-9} m^2/N for pentane [27].

The common RI detectors are based on refraction, reflection or interference of the light beam [28-30]. The interference RI detector provides the best concentration limit of detection in both commercial instruments and in research prototypes, because a long path length can be used to compensate for lower concentrations [9]. Spectral interference refractometry by diode array spectrometry has been developed [31,32]. The detection method provides the spectral dispersion curve instead of the standard absorbance spectrum. Recently RI gradient (RIG) detection is developing into a useful RI detector, since, in this technique, low-frequency noise due to temperature, pressure and eluent composition changes is minimized relative to the analyte signal [33-35].

Optical activity detection Optical activity detection is based upon either polarimetry, the rotation of plane polarized light, or circular dichroism, the differential absorption of left and right circularly polarized light [37,38]. The optical activity detector is very selective because only those molecules which have chiral centers can produce signal. This detection method is also important since most biological compounds have chiral centers. A laser-based polarimetric detector for LC has been developed with two order improvement on the limit of detection [39]. The detector is capable of detecting 10^{-5}° to 10^{-6}° of rotation. Although the laser-based polarimetric detector has the same general configuration of other polarimeters, certain components are responsible for the decreased detection limits. These

are the polarizers, the modulation and the laser. First, excellent quality Glan-Thompson prisms are required to have an extinction ratio of 10^{-6} or better. By judicious choice of locations for the laser beam to pass through, an extinction ratio of 10^{-10} is obtainable. Second, because measuring an AC signal is preferred over a DC signal in order to discriminate against noise, modulation is induced into the detection system. Modulation is introduced in the flow cell causing the polarization plane of the beam to oscillate between points equidistant from, but on the opposite side of, the plane which produces extinction of the beam. The light emerging from the analyzer is consequently intensity modulated. Third, the highly collimated laser beam makes it possible to select the specific positions on the polarizers and the pointing stability of the laser makes the positions stable. Further, since the specific rotations of molecules depend on wavelength, a monochromatic laser beam is desired for accurate measurement [40].

Fluorescence detection The high sensitivity and specificity of fluorometric measurements have made fluorescence the detector of choice for trace analysis of fluorescent compounds [41-47]. Because only a small number of compounds exhibit fluorescence, fluorescence detection offers a high degree of selectivity. Additional refinements in the detector optics can permit selection of excitation and emission wavelengths, which will enhance selectivity even more. There are many examples where such three-dimensional (excitation, emission and retention time) chromatograms have been used to distinguish species that are not chromatographically

resolved. Of course, selectivity is a double-edged sword, and the fact that only a few compounds fluoresce also limits the applicability of fluorescence detection. If an analyte does not fluoresce originally, various derivatization procedures, both on line and in sample preparation, have been devised to take advantage of the excellent detectability provided by fluorescence detection. Not only are fluorescence detectors selective, but they also offer about 100 times higher sensitivity than that of absorption detection.

A combination absorbance-fluorescence detector can provide simultaneous absorption and fluorescence detection [48]. Because excitation via the absorption of radiation must precede fluorescence emission, all the fluorescent components in a sample also give a response on the absorbance detector. This combination can provide the LC user with a highly sensitive specific detector and a moderately sensitive general detector [49].

Electrochemical detection Electrochemical detection in LC is growing rapidly in popularity. This is evidenced by the fact that electrochemical detection papers were the most reviewed among all LC detection methods in the last two Fundamental Reviews issues of *Analytical Chemistry* [50,51]. Electrochemical detection offers a unique approach to the detection of trace amounts of certain classes of compounds that can readily be oxidized or reduced. The detectors are based on an electrolysis reaction in which a constant potential is applied and the current is measured as a function of time. The current will vary as compounds are

oxidized or reduced, and the magnitude of the current will be directly proportional to the concentration of the compounds reacted. Normally, two approaches, coulometric and amperometric, are taken to electrochemical detectors [52-56].

Famed far and wide for their sensitivity (in many cases a picomole or less can be detected) electrochemical detectors also provide considerable selectivity, since only a few components in a complex sample are likely to be electroactive. The selectivity can be further enhanced by rapid-scanning and dual-electrode techniques [57]. Aromatic amines and phenolic compounds represent the most important classes of compounds to which electrochemical detection has been applied. These classes include a large number of biochemical compounds. It is in the analysis of metabolic products (such as catecholamides) that the sensitivity and selectivity of electrochemical detection have been best used [58-61].

The full potential of the electrochemical detector is still being explored. Improvements such as new equipment, electrochemical techniques such as pulsed coulometric, potential-sweep-pulsed coulometric [62], and chromatographic techniques like pre- and post-column reactions continue to be made. It is expected that electrochemical detectors will become a very powerful tool for certain, otherwise difficult, analyses.

Mass spectrometric detectors The mass spectrometer (MS) is a unique detector for LC, which offers a combination of three very important analytical features: sensitivity, selectivity and universality. None of 20 or so LC detectors

commonly used today can provide all of these features. The sensitivity for current LC-MS systems is on the order of 10 pg [63-64] if, instead of scanning the entire mass range, certain selected ions are monitored. In addition to the sensitivity performance of MS, the technique provides unequalled universality to most organic compounds.

An interface is necessary to combine the separation power of LC with the unique detection capabilities of MS to retain the chromatographic fidelity of a separated band, maintain the sensitivity of MS and respond linearly in a concentration range of several orders of magnitude. The difficulties in coupling LC with MS are well documented [65-68] with the most emphasis placed on the process of efficiently converting the solute to the gas phase with subsequent removal of the chromatographic eluent either prior to the source inlet or by supplementing the pumping ability of the existing MS. Various LC-MS interfaces have been developed such as moving belt [69-71], thermospray [72-75], direct liquid injection [76-79], MAGIC [80,81], atmospheric pressure ionization [82,83] and continuous-flow fast atom bombardment [84-87]. LC-MS offers the analytical community great potential for solving more problems than has ever been available previously. When MS becomes of comparable cost and simplicity as a conventional UV or similar detectors, LC-MS will be one of the most popular analytical instruments for sample analysis in complex matrices.

Detection in microcolumn liquid chromatography

One of the increasingly important trends in the field of separation sciences is the miniaturization of LC [88-91]. A comparison of the operating parameters between conventional LC and miniaturized LC is shown in table 1 [92]. Micro-column techniques offer the following advantages over conventional LC: (a) increased separation efficiency; (b) the ability to use "exotic" or expensive mobile phases because of the low flow rates; (c) increased mass sensitivity with concentration-sensitive detectors and (d) the chances to apply novel detection modes. The development of microcolumn LC detectors has paralleled that of detectors for general use in LC. The thrust of development started with detectors that have a more general applicability (such as UV/Vis and thermal lens spectrometry). In time other, more selective, detectors have been adapted for use in microcolumn LC (laser induced fluorescence, optical rotation, electrochemical, etc.). There appears to be two general forces driving the development of microcolumn detectors. One is adaptation of conventional LC detectors to more closely fit the requirements of microcolumn LC. The second force is the design of novel detection modes whose requirements closely match those of microcolumn LC [93].

The overriding concern in designing a useable microcolumn detector must always be the need to minimize extra-column variance while maintaining sensitivity, considering the extremely small peak volume. This is difficult for optical detectors since they depend on a finite volume being illuminated. For UV absorption

Table I. Comparison of operating parameters for liquid chromatography

	Conventional	Microbore	Packed capillary	Open tubular capillary
Column Diameter (μm)	4600	300	75	10
Peak Volume (μL)	500	5	2	0.01
Flow Rate (μL/min)	1000	10	3	0.05
Linear Flow Rate (mm/min)	60	140	680	600

detection, the path length dependence of absorption has limited the development for microcolumn LC. In an effort to maintain as long a path length as possible, without sacrificing chromatographic resolution in detection, both the spatial and polarization properties of the laser have been utilized to develop the state-of-the-art absorbance detectors capable of detecting low picogram amounts of injected analytes. These novel approaches include thermal lens [94-96], photothermal [97,98] and indirect absorbance detection [99]. In the last case, the laser-based polarimetric detector was modified for use with microcolumn LC. A 1 μL flow cell was constructed and the achiral solutes were detectable by employing indirect detection, which was demonstrated using a chiral mobile phase in a normal phase LC separation.

For fluorescence detection, microcolumn LC has benefitted by the

development of laser-based fluorescence detectors [91,100]. The ability to focus high intensity light into very small volumes has produced excellent fluorescence detectabilities. The femtomole analysis of prostaglandin pharmaceuticals using laser-excited fluorescence detection has been reported [101]. Proper design consideration has allowed detection cells for microcolumn LC to have volumes of less than 100 nanoliters [102,103]. Fluorescence spectra obtained in such small detection volumes provide a powerful qualitative tool for analyte identification for extremely small injected quantities.

In contrast to many optical detectors, electrochemical detectors are uniquely well-suited to be scaled down for microcolumn LC. One inherent advantage of any kind of electrochemical detector for microcolumn LC is that only the volume that the working electrode surface encompasses and the cell volume in front of this surface affect the elution band as extra-column variance. The amperometric-mode detectors, which usually have a small surface area for the working electrode, can easily be constructed to prevent excessive band broadening. In addition, the low flow rates of microcolumn LC reduces some of the noise produced by electrochemical detectors. An on-line electrochemical detector that has an effective volume of 100 nL has been reported [104]. The working electrode was a tubular length of carbon polymer. A tubular electrochemical cell with a single carbon fiber, 0.7 μm o.d. x 15 mm, as the working electrode provides an effective volume of 30 nL and a detection limit of 1-2 ng for catecholamines and their metabolites [105].

Detection limits of phenols is reported on the order of 100 fg for open tubular LC [106]. Rapid-scanning and dual-electrode techniques have provided a means to further enhance the selectivity already implicit in electrochemical detection [107].

The small size of the microcolumn allows small quantities of eluent to be used. This is especially beneficial to microcolumn LC-MS. The optimum flow rates of microcolumn LC systems are compatible with some conventional [108] and modified [109] chemical ionization MS pumping systems without the need for a flow splitter. Open tubular capillary LC has been directly coupled to the ion source of the MS [110,111]. For samples of low molecular weight, the direct inlet of column effluent from an unmodified capillary column is well suited for practical qualitative as well as quantitative analysis. The peak shape quality is comparable to those obtained from the UV detector and the detection limit of 100 pg is far better than that obtained from the UV detector. Detectabilities for state-of-the-art micro-column LC-MS systems are on the order of 1 to 10 pg with the interface of direct-liquid-injection (DLI) [112]. The flux of material due to the eluent flow for the microcolumn LC is found to be small enough for DLI. Microcolumn LC-MS is quite favorable for thermally labile species that could not survive a GC-MS analysis, but can be analyzed by LC-MS procedures [113-115]. The electron-impact (EI) spectra have also been obtained for species eluted from open tubular capillary columns [116]. The source pressures could be kept sufficiently low to obtain EI spectra due to the extremely low flow rates used with the capillary columns.

Detectors for capillary electrophoresis

Capillary electrophoresis (CE) has developed into an important technique in the repertoire of liquid-phase separations [117-121]. Many of the problems in the development of CE can be related to convection and detection [122]. The concept of CE includes the alleviation of the convection problems by using narrow-bore capillary columns as the separation chamber, thereby allowing rapid dissipation of the Joule heat generated by the applied electric field. This approach brought about the realization of a powerful instrumental version of electrophoresis [123], analogous to modern column chromatography. With regard to the above mentioned detection problem, it is similar to that associated with microcolumn LC. The small capillary dimensions and the minuscule peak volumes create a system in which sensitive detection without introducing peak dispersion is a major challenge. For example, with a 25 μm i.d. capillary 100 cm long, a peak exhibiting 500,000 theoretical plates would have a peak volume of only 3 nl.

The small peak volumes encountered in CE are best dealt with by performing detection in an on-column mode. Even with its limited sensitivity, on-column UV absorption is still the most popular detection system owing to its more universal nature. A high-frequency excited electrodeless low pressure iodine discharge lamp [124] and a cadmium "pen-ray" lamp [125], that emits radiation from both sides, have been used to eliminate the problems encountered with modifying commercial instruments. An on-column UV absorption detection system

has been designed, in which two optical fibers are butted against an exposed portion of the capillary [126]. The detection limits of UV absorption detection are limited to about 10^{-5} M due to the small path length.

Fluorescence detection is most easily adapted to CE in an on-column configuration, since its sensitivity is not path length dependant. The laser based fluorescence detector can provide a typical detection limit of 10^{-7}M. While fluorescence detection can provide excellent detection limits, this technique is less versatile because many solutes of interest do not exhibit native fluorescence and must be derivitized with some type of fluorophore. One alternative to derivitization of nonfluorescent compounds is to perform indirect fluorescence detection [127,128], which is used in an on-column fashion by incorporating a fluorescent ion in the electrophoretic buffer. Ionic analytes will interact with the fluorophore and result in either displacement or ion pairing with the fluorophore. The signal produced in this system is therefore independent of the spectral properties of the analyte. This technique should be useful for any ionic species ranging from monatomic ions to viruses and bacteria. The detection limits are in the range of 10^{-5} M for negatively charged amino acids.

The earliest form of electrochemical detection used in CE was via solution conductivity. A sophisticated conductivity detector has recently been reported [129]. The detection limit is as low as 10^{-7} M for Li^+, although detection limits are considerably higher for most ions. Even in the most advanced form, the major

difficulties with conductivity are baseline drift and relatively high detection limits for most species. These factors can often be overlooked, however, in view of the system's universal usefulness for CE detection. For amperometric detection [130-132], the detection volume is minimized by placing the carbon fiber working electrode (5 μm o.d.) directly into the end of the capillary. In contrast to the optical detection methods, the performance of the electrochemical detector is optimized by miniaturizing both the separation column and the detector, which minimizes the annular flow around the electrode and increases the coulometric yield. A detection limit of 10^{-9} M is obtained for catecholes.

CE-MS is still in the early stages of development. Electrospray ionization techniques have developed for CE-MS interfacing [133-135]. The key of the interface is the realization that the cathodic end of the capillary need not be situated in a buffer reservoir as long as it is biased negative of the cathode potential. The dead volume in the interface (<10 nL) is minimized by using a sheath flow to make electrical contact with the CE effluent [136]. The detection limit is in the 10^{-7} M range for quaternary ammonium salts. The latest development of CE-MS detection is a continuous-flow fast-atom bombardment interface [137,138]. The impressive MS and MS/MS spectra of as little as 32 fmol of peptides is reported.

SECTION I

UNIVERSAL DETECTOR BASED ON MAGNETO-OPTICAL ROTATION FOR HIGH-PERFORMANCE LIQUID CHROMATOGRAPHY

INTRODUCTION

Significant advances in instrumentation and application of high performance liquid chromatography (HPLC) have been made in recent years. However, the problems of detection in terms of sensitivity and selectivity still exist in many applications of HPLC. The need for further development of HPLC detectors is obvious, especially those that are based on entirely different physical or chemical properties from those normally associated with standard instruments.

The most commonly used HPLC detector is the absorption detector. When the samples of concern do not absorb in a convenient wavelength region, various derivatization methods [1] have been developed to attach desirable chromophores to molecules so that the absorption detector can be used. However, derivatization is not always desirable, e.g. when the analyte has to be preserved after separation. In addition, in the survey of impurities in samples, one is often faced with analytes with unknown chemical properties. A universal detector will therefore be necessary for the analysis of truly unknown samples. It is thus of interest to utilize the refractive index (RI) detector, which is one of the very few universal detectors available. Unfortunately, the RI detector suffers from such problems as poor sensitivity, incompatibility with gradient elution, and extreme sensitivity to temperature and pressure. It is therefore desirable to develop new methods for universal detection in HPLC.

In 1845, Faraday discovered that the plane of polarization of linearly

polarized light was rotated on passage through substances placed in a magnetic field with non-zero component in the direction of the light beam. Effectively, a longitudinal magnetic field made all substances appear optically active. This Faraday effect is a general physical property for all substances. It has been observed in wide electromagnetic spectrum covering the region from microwave to x-rays [2-3]. Fig.1 shows the Faraday effect.

The Faraday effect can be expressed as a complex equation [4]:

$$\hat{\alpha} = \alpha - i\theta = \hat{\Lambda} \int_0^l H(l)\,dl \qquad (1)$$

The magneto-optical rotation (MOR) α is the rotation of the polarization plane of a light beam after passing through a substance of length l parallel to a magnetic field H. The magnetic circular dichroism (MCD) θ measures the corresponding ellipticity of the beam. α and θ are related by exactly the same Kramers-Kronig transformation which apply in natural optical activity. In the regions of non-absorption, $\theta = 0$, the MOR is the only contributor and is given by:

$$\alpha = \Lambda \int_0^l H(l)dl \qquad (2)$$

where the Verdet constant Λ is characteristic of a given substance and is frequency and temperature dependent.

The Faraday effect, like the related Zeeman effect, results from the influence of the magnetic field upon the electron movement within the atoms. The sign of the effect depends on the direction of the magnetizing current in the

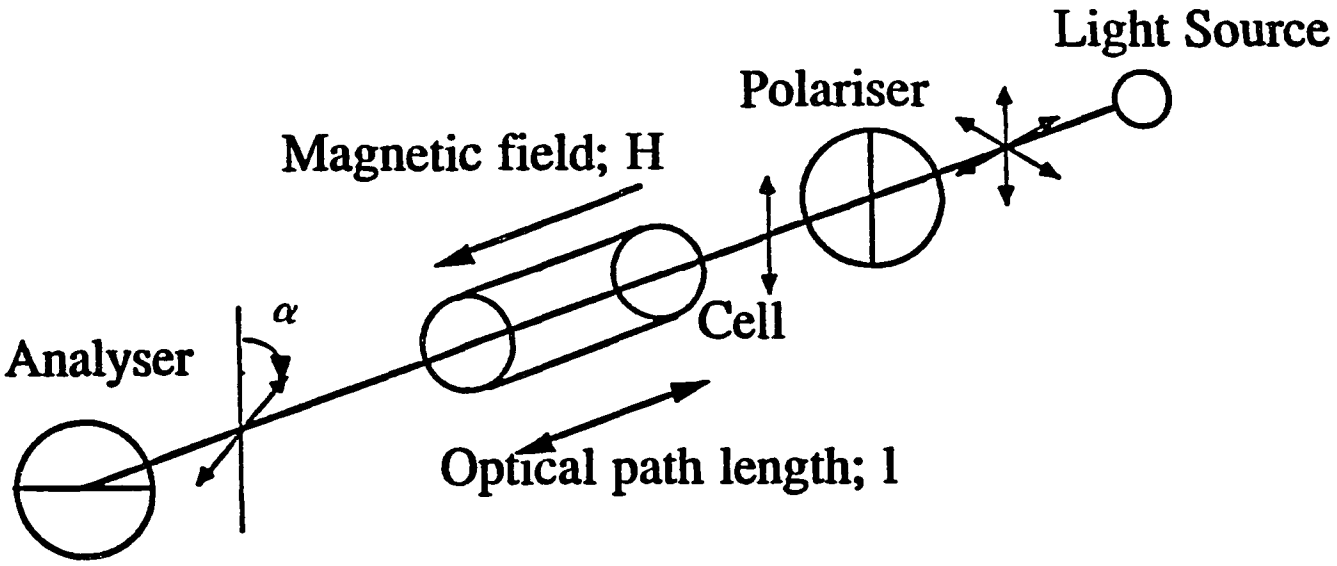

Figure 1. The Faraday effect. The magneto-optical rotation α depends on the property of the substance inside the cell, magnetic field strength and cell path length

solenoid. For most substances, the MOR has the same direction as the magnetizing current, as illustrated in Fig.2. The effect is then defined positive.

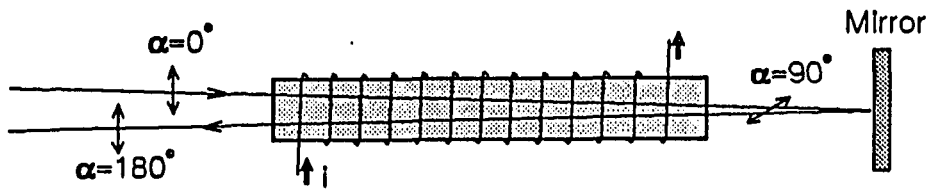

Figure 2. The dependence of magneto-optical rotation on the magnetizing current

It is obvious from Fig.2 that the dependence on the direction of current leads to a different characteristic property of the Faraday effect from natural optical activity. If the light beam travels twice through the substance in opposite direction by reflecting back along the original path, the MOR will be doubled. The rotation of the polarization plane due to natural optical activity, on the hand, will be annulled since the rotation is fixed relative to the direction of light propagation.

It is interesting to notice that an optically active substance observed in a longitudinal magnetic field will therefore exhibit two types of rotation, a natural

optical rotation upon which is superimposed a MOR. Whether the field exerts a measurable influence upon the natural optical rotation itself is still an open question.

The polarization rotation is also observed when the magnetic field is perpendicular to the light beam (Cotton-Mouton effect). This phenomenon is related to the transverse Zeeman effect, just as the Faraday effect is related to the axial Zeeman effect. The Cotton-Mouton effect is proportional to the square of the magnetic field strength and is generally much smaller than the Faraday effect.

Although MOR was first observed about one-and-a-half centuries ago and substances exhibiting a well measurable MOR are much more numerous than those having natural optical activity, the Faraday effect has found relatively little application to chemistry in comparison with natural optical activity until the 1960s. Early studies on MOR were mainly focused on the MOR of semiconductors [5] and its application to light modulation [6]. Following the success of natural optical rotatory dispersion and circular dichroism in yielding useful structural information for organic compounds [7-9], the dispersion of MOR and MCD were extensively studied [10-12], with the aim of obtaining similar information. These studies were very powerful means for clarifying spectroscopic assignments and characterizing the symmetry and angular momentum properties of both ground and excited states of molecules and ions. More recently, MOR has been applied to atomic spectroscopy [13-18]. Atomic magneto-optical rotation spectroscopy, or coherent forward-

scattering spectroscopy, has been shown to be a sensitive and selective method for trace-element analysis. With this technique, plane polarized resonant radiation is incident upon a magnetized atomic vapor. The magnetically induced birefringence and dichroism then rotates the plane of polarization of the transmitted radiation. The magnitude of the rotation is dependent on the number of analyte atoms in the path of the beam and so can be used for quantitative determination of the analyte. Kawazumi and coworkers [19] were the first to apply MOR for detection in liquids. Incorporating a modulating-solenoid into the detection cell of a laser-based polarimeter, they were able to detect 180 μg of injected phenol in a flow injection scheme. Their study, however, was severely limited by the poor detectability of the polarimetric system, low magnetic field strength from the solenoid, and modulation instabilities. Since there will be further dilution after the chromatographic column, that particular approach is not compatible with HPLC.

In the following, we present the first working detector based on MOR for universal detection in HPLC. As demonstrated later, both theoretical and experimental studies show a linear relationship between the MOR signal and the concentration of the analyte. Submicrogram quantities of analytes can be detected following the HPLC separation, and further improvements are expected.

THEORY

To apply MOR to quantitative determinations in HPLC, the rules governing Verdet constants for mixtures have to be known. The MOR of a mixture is not necessarily equal to the sum of the MOR of its pure components. Verdet [20] investigated the MOR of solutions and concluded that the contributions of the solvent and the solute to the total MOR are additive, and each component of the solution behaves as if it alone were present in the total volume of the solution. This is known as Verdet additivity law. Actually, the Verdet constant of the individual components does not have additive character, whereas a constant D has. D is derived from the electromagnetic theories of MOR [21] based on the dispersion theory, and is defined by:

$$D = \frac{9n}{(n^2+2)^2} \frac{M}{d} \Lambda \qquad (3)$$

where n is the refractive index, M is the molecular weight and d is density. Waring and coworkers [22] studied MOR of carbon disulfide in a number of organic solvents, including toluene and cyclohexane. Broersma et al. [23] investigated MOR of a number of binary hydrocarbon mixtures. To calculate the Verdet constants of mixtures, they used the equation:

$$D = \Sigma_i D_i G_i \qquad (4)$$

where G_i is the weight fraction of component i. They confirmed this equation in

general even though some small deviations were observed when a large change in density and refractive index occurred on mixing or if association was present.

Since density and refractive index of the solution have to be experimentally determined, it is inconvenient to use Eq. 3 in applications of MOR for mixtures. Several simplified equations were used in the literature for calculating MOR of solutions [24,25]. However, the derivations of the equations were not clear and some of the results were of doubtful validity. For example, Chuckerbutti [26] found that the equation in ref. 25 did not hold and that it was dependent on the additivity of partial volumes of the solution.

We shall derive an alternative expression suitable for quantitation in HPLC. Here we have assumed that the value of n in Eq. 3 is constant, as in the case of minor solutes in the chromatographic eluent. Since MOR is a number density property, it could be expressed as:

$$\alpha = [\Lambda] C \int_0^l H(l)\, dl \qquad (5)$$

where C is the concentration of the substance with units of mol/ml and [Λ] is molar magnetic rotivity: $[\Lambda] = \Lambda M/d$. Obviously, for a pure substance, $[\Lambda]C = [\Lambda]d/M = \Lambda$, while Verdet constant of a mixture is:

$$\Lambda = \sum_i [\Lambda]_i C_i = \sum_i \Lambda_i M_i C_i / d_i \qquad (6)$$

where C_i is the concentration of component i as if it alone were present in the

whole volume of the mixture and $[\Lambda]_i$ is the molar magnetic rotivity of component i.

Since $V_i d_i/V = W_i/V$ and $M_i C_i = W_i/V$, we have:

$$V_i d_i/V = M_i C_i \tag{7}$$

where V_i and W_i are volume and weight of component i, respectively, and V is the total volume of the mixture. Substituting Eq. 7 into Eq. 6:

$$\Lambda = \sum_i \frac{V_i}{V} \Lambda_i \tag{8}$$

This equation shows a simple expression for additivity of Verdet constants in a mixture.

Since a single chromatographic peak consists of one solute and the eluent, we can consider a binary mixture:

$$\Lambda = \frac{V_1}{V} \Lambda_1 + \frac{V_2}{V} \Lambda_2 \tag{9}$$

where 1 and 2 symbolize solute and solvent, respectively.

In our experiment, the polarization analyzer was physically rotated to compensate for the MOR of the pure solvent. Therefore, the signal from the output of the lock-in amplifier is proportional to the difference in MOR between the solution and the solvent:

$$\Delta\alpha = (\Lambda - \Lambda_2)\int_0^1 H(l)dl = \left[\frac{V_1}{V}\Lambda_1 + \left(\frac{V_2}{V} - 1\right)\Lambda_2\right]\int_0^1 H(l)d(l) \qquad (10)$$

Assuming that the mixture is an ideal solution, $V_1 + V_2 = V$, we then have:

$$\Delta\alpha = \frac{V_1}{V}(\Lambda_1 - \Lambda_2)\int_0^1 H(l)dl \qquad (11)$$

The signal is thus proportional to the volume fraction of the solute and to the Verdet constant difference between the solute and the solvent.

However, mixtures of polar substances are usually non-ideal solutions and volume additivity has large deviations. Note that $W_i = V_i d_i$ and $W = Vd$ where W is the total weight of the solution. Then, the weight fraction of component i is:

$$G_i = \frac{W_i}{W} = \frac{V_i d_i}{Vd} \qquad (12)$$

Substituting Eq. 12 into Eq. 9:

$$\frac{\Lambda}{d} = \frac{G_1}{d_1}\Lambda_1 + \frac{G_2}{d_2}\Lambda_2 \qquad (13)$$

For very dilute solution, $d \approx d_2$, we then have:

$$\Lambda \approx G_1\frac{d_2}{d_1}\Lambda_1 + G_2\Lambda_2 \qquad (14)$$

and

and

$$\Delta\alpha = (\Lambda - \Lambda_2) \int_0^1 H(l)dl = G_1\left(\frac{d_2}{d_1}\Lambda_1 - \Lambda_2\right) \int_0^1 H(l)dl \qquad (15)$$

where $G_1 + G_2 = 1$ is used.

Since the parameters inside the parenthesis and the integration are constants for a giving system, this equation shows an important linear relationship between the MOR signal and the weight fraction of the solute, without the complications of volume additivity of non-ideal solutions. Because no physical properties of the solution have to be measured, this equation is very convenient for the application of MOR measurements in mixtures. The linear dependence of signal on analyte concentration make MOR feasible for analytical applications. We will show later that this linear relationship is confirmed in HPLC detection and the experimental detection limit is approximately equal to that calculated from the equation.

EXPERIMENTAL SECTION

Apparatus

As we discussed before, both natural optical rotation and the MOR can utilize a similar detection technique. The laser-based optical activity detector for HPLC was first reported by Yeung's group [27]. The present work used a similar experimental arrangement with several major modifications. Fig. 3 shows a schematic diagram of the instrument and chromatographic system. About 2-3 mW of 442 nm line from a He-Cd laser (Liconix, Sunnyvale, CA, model 4240NB) was used as light source. A 50 cm f.l. lens couples the laser beam into the modulation and detection cells. The modulation cell was the same as the detection cell used earlier but without water cooling [28]. The cell was filled with acetonitrile for a larger modulation. The modulation frequency of 210 Hz was chosen to provide larger signal to noise ratio.

A stable, longitudinal magnetic field must be generated within the analytical volume of the detection cell for reproducible MOR signal to be obtained. This magnetic field was generated by a permanent magnet assembly designed and constructed in our laboratory. Fig. 4 shows a schematic diagram of the permanent magnet-detection cell assembly. The assembly consisted of two neodymium-iron-boron permanent magnets of 30 MGOe (2" x 2" x 0.5", Tridus International, Carson, CA, model 085). The magnets were magnetized along the smaller dimension. Holes (1/8" diameter) were drilled with an abrasive drill through the center of the

magnets to permit the laser beam to travel through the detection cell. The conical pole pieces were made from Armco, a soft magnetic material with high saturation magnetization. The conical pole pieces taper from 50 mm diameter (in contact with the magnets) to 3 mm diameter (at the tip). The conical shape made it possible to achieve high field strength inside the gap. The U-shaped yoke was made from low-carbon 1018 steel (2" x 0.5" plate) which held the magnets and pole pieces in position and provide a magnetic flux path between the magnets. One of magnets was held together with a cylinder made from Armco. The cylinder can move along the central axis of the assembly to allow the gap width between the two magnets to be varied. The detection cell consisted of two brass plates and one stainless steel tube (1/8" o.d. and 1/16" i.d.). The tube was first inserted into the magnets and then soldered together with two brass plates. The procedure for selecting windows was the same as that for the modulation cell [27]. The field strength was measured by using a gauss meter (F. W. Bell Inc., Orlando, FL, model 615) with a Hall-effect probe (F. W. Bell Inc., model HTB1-0608).

The radiation exiting the analyzer was passed through a 442 nm line filter and detected with a photomultiplier tube (PMT) (Hamamatsu, Middlesex, NJ, model R928) biased at -800 V. The current from PMT was terminated in a 10 kΩ resistor and the voltage was monitored by a lock-in amplifier (Stanford Research, Stanford, CA, model SR510 or EG&G, Princeton, NJ, model 5209) which was operated with a 1-s time constant. The output of the lock-in amplifier was

Figure 3. Schematic diagram of magneto-optical rotation detection system for HPLC. (He-Cd) helium-cadmium laser, (M) mirror, (L) lens, (PO) polarizer, (AI) air core solenoid, (RE) chart recorder, (DC) DC power supply, (MO) modulation cell, (WG) waveform generator, (MA) permanent magnet-detection cell assembly, (AN) analyzer, (LI) lock-in amplifier, (PMT) photomultiplier tube, (CU) HPLC column, (IN) injector, (PU) pump.

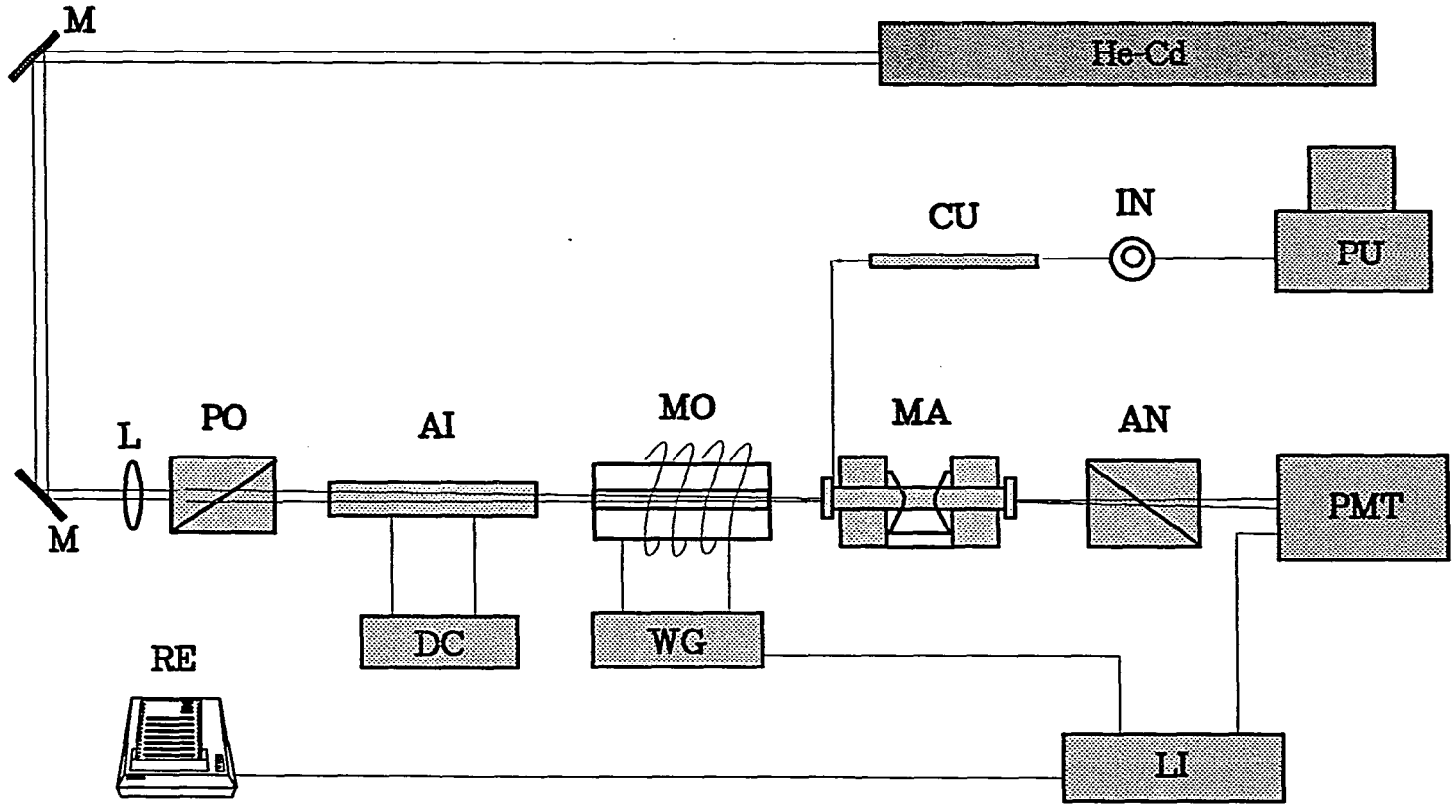
M
He-Cd
CU
IN
PU
L
PO
AI
MO
MA
AN
M
PMT
DC
WG
RE
LI

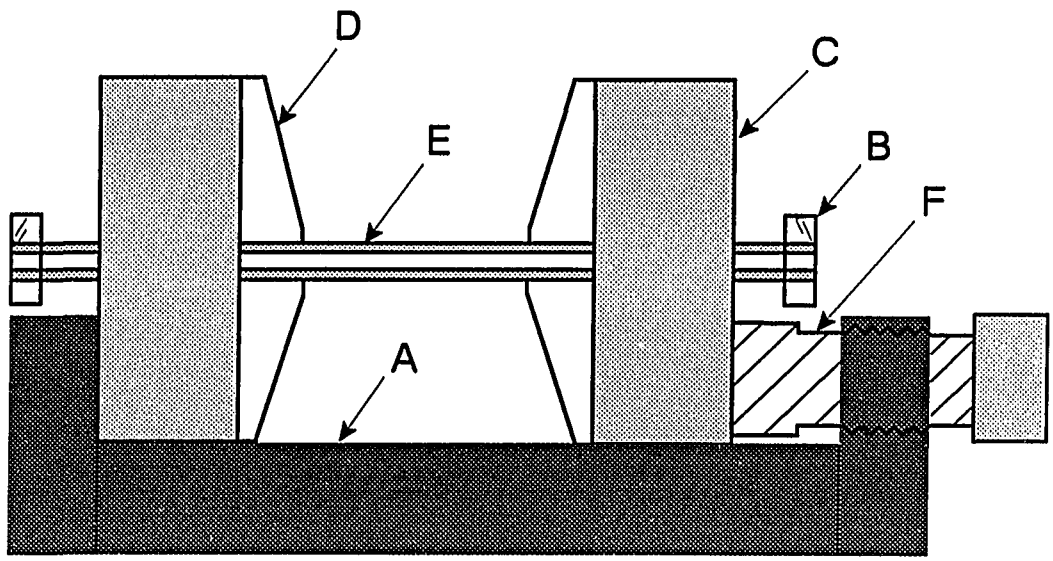

Figure 4. Cross section through the permanent magnet-detection cell assembly. (A) steel yoke, (B) brass plate, (C) neodymium-iron-boron permanent magnet, (D) iron pole piece (E) stainless steel tube, (F) iron cylinder. The stainless steel tube was inserted into the magnets and then soldered together with the brass plates.

displayed on a chart recorder (Measurement Technology Inc., Denver, CO, model CR 452) or sent to a data acquisition system consisting of an analog to digital I/O interface (Data Translation, Marlborough, NH, model DT 2827) and a microcomputer (IBM, Boca Raton, FL, model PC/AT).

Chromatography

Chromatography was performed in a standard arrangement. A syringe pump (ISCO, Lincoln, NE, model LC-2600) was operated at about 0.47 ml/min and about 750 psi pressure. A 0.5 μm line filter (Alltech, Deerfield, IL, model SSI05-1005) was connected before the injector (Rheodyne, Cotati, CA, model 7101) which has a 50 μL injection loop. The column was a 3-μm C_{18} reverse phase column (15 x 0.46 cm, Alltech, model 287092). Water, acetonitrile and methanol were used as mobile phases in this work.

Analytical reagents

All chemicals were reagent grade and were used as supplied. The water used came from a Barnstead Nanopure II system (Boston, MA). All solutions were degassed in an ultrasonic bath before use. This procedure is important since any residual bubble inside the modulation or detection cells will degrade the performance of the system.

RESULTS AND DISCUSSION

Design of magnet-detection-cell assembly

Since the rotation angle of the polarized light is proportional to the strength of longitudinal magnetic field and the pathlength, it is desirable to have magnets with as high a field strength along the axial direction over as large a distance as possible. The magnetic field should also be stable to eliminate noise introduced by fluctuations in the field strength. On the other hand, the high homogeneity of the magnetic field in this experiment is not as critical as that in such experiments as atomic magneto-optical rotation spectroscopy. Most previous studies on the applications of MOR and MCD utilized solenoids to generate the magnetic field. In our earlier work on laser-based polarimetric detection for HPLC [27-28], solenoids were used to provide both static and modulated magnetic fields. However, the dissipative (non-superconducting) solenoids are usually quite bulky and require high power or high current to generate magnetic fields with moderate field strength. For example, an ideally designed solenoid needs about 1000 watts of power to generate a magnetic field of 3600 Gauss [29]. In practice, even higher power is required. It has been found [28] that ohmic heat from even a very small amount of power (2 W) will severely degrade the performance of polarimetric detection for HPLC because the RI of the solution is so sensitive to temperature changes that the exiting light beam will be distorted. This deflection of the light beam will be converted into intensity fluctuations, i.e., detection noise, after passing

through the analyzer. Even though coupling cooling water into the solenoid would partially improve the performance, the efficient cooling for the high power solenoids is difficult to achieve and the system would become much bulkier. If modulation is incorporated, an associated problem is that the field strength would sharply decrease as the modulation frequency increases, due to the strong inductance generated in the solenoid [28,30]. This inductance puts an upper limit on the field strength for solenoids.

On the other hand, recent advances in the researches of permanent magnetic materials based on rare earth metals have provided new permanent magnets with high field strength. The rare earth metal based permanent magnets have been widely applied in the researches of physics and engineering. In recent years, these strong and compact samarium-cobalt and neodymium-iron-boron permanent magnets have found use in atomic magneto-optical rotation spectroscopy [31,32], light microscopy, x-ray and light-scattering studies of macromolecular assemblies [33]. These permanent magnets can provide similar field strengths to those of solenoids with 1000 watts power, but without the inconvenient cooling requirements. The field strength of permanent magnets is also more stable than that of solenoids, which is affected by the stability of the power supply and environmental temperature. In this work, we utilized two pieces of neodymium-iron-boron permanent magnet to produce a longitudinal magnetic field. The field strength was dependent on the distance between the two pole pieces of the

magnets. The relationship between the gap spacing and the field strength is shown in Fig. 5. The field strength was measured both at the center of the gap and on the pole piece surface. It can be seen that the magnetic field is quite inhomogeneous. This, however, should not be critical in our work since the MOR signal is proportional to the integrated magnetic field strength along the optical axis of the assembly. Note that only the part of detection cell between magnet pole pieces is inside the magnetic field. This implies that there is an optimal gap spacing which maximizes Eq. 1 for a given set of pole pieces. Fig. 5 shows that H x l is relatively constant for this particular cell. Another consideration for designing the magnet-detection-cell assembly was that the physical length of the assembly should be kept as short as possible since a long path of light beam through the cell would amplify the effect of beam deflection caused by RI change of solution, flow disturbance, temperature fluctuations, etc. [28], even though the signal may be higher. In HPLC one further needs to consider band broadening when the cell length, and thus the cell volume, gets too large. Here, we used a gap spacing of 16 mm for a total cell length of 6.5 cm due to physical constraints.

Limit of detection

The limit of detection of the HPLC detector based on MOR is dependent on the limit of detection (LOD) of the polarimetric system according to Eq. 15. For the laser-based polarimetric detector for HPLC [27], if the detectability is expressed as the rotation angle at a signal-to-noise ratio (S/N) = 3, the best

Figure 5. Strength of magnetic field as a function of magnet pole-gap distance. (A) at center of gap, and (B) at pole piece surface.

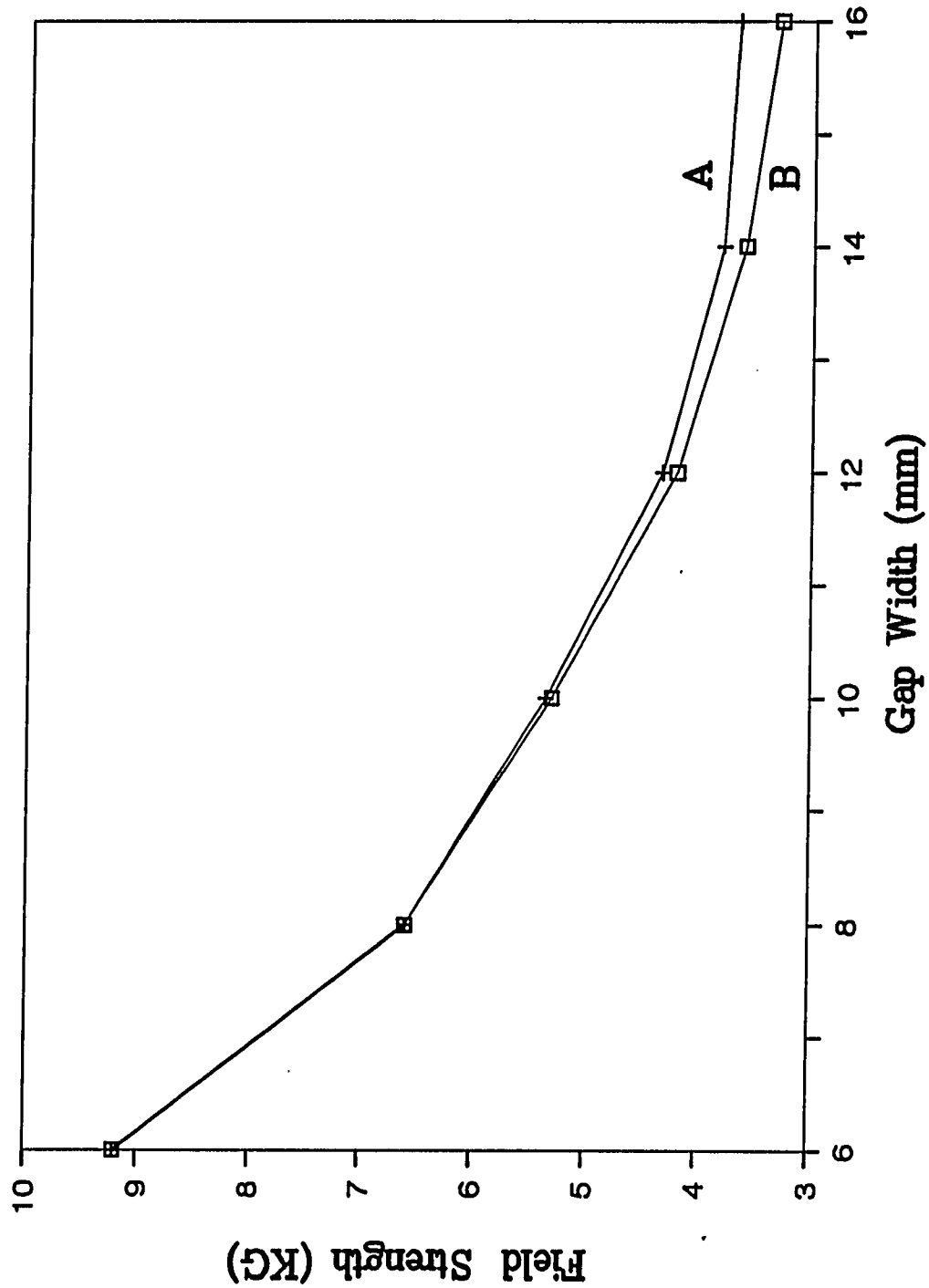
Field Strength (KG)
Gap Width (mm)
A
B
10
9
8
7
6
5
4
3
6
8
10
12
14
16

detectability was about 3.0 x 10^{-6} degree with 1-s time constant. This is achieved by using either high frequency modulation [30] or optimized solenoid design, water cooling and laser power stabilization [28], while a theoretical analysis [34] predicted a shot-noise-limited detectability of 10^{-6} degree.

To simplify the experimental set-up in this work, we did not incorporate high frequency modulation, water cooling, or laser stabilization into the system. The detectability was about 1.5 x 10^{-5} degree without the magnet-detection cell assembly in position. When the assembly was in position, the polarization plane of the laser beam was rotated due to the MOR of the liquid and windows. When this MOR was compensated by rotating the analyzer (ca. 1°), the detectability of the polarimetric system was degraded to about 3.0 x 10^{-5} degree. The degradation of the detectability was mainly due to the slight change of the location of the laser beam at the analyzer, since the extinction ratio of the polarimetric system is highly dependent on the laser beam location on the polarizers [27]. Other possible reasons include stray magnetic field interacting with air turbulence in the optical path of the system.

Assuming the inhomogeneous field in our cell (Fig. 5) can be approximated by a linear function, we have $\int_0^l H(l)dl \approx 6000$ gauss.cm. We can now use Eq. 15 to calculate the theoretical limit of detection:

$$G_{LOD} = \frac{\Delta\alpha}{\left(\frac{d_2}{d_1}\Lambda_1 - \Lambda_2\right)\int_0^l H(l)\,dl} = \frac{3.0 \times 10^{-5} \times 60}{6000\left(\frac{d_2}{d_1}\Lambda_1 - \Lambda_2\right)} = \frac{3 \times 10^{-7}}{\frac{d_2}{d_1}\Lambda_1 - \Lambda_2} \quad (16)$$

The factor of 60 was introduced to convert from minutes to degrees. Table I shows the results of calculated LOD for phenanthrene and water when methanol was used as the solvent.

It should be noted that all Verdet constants used for the calculation were for the sodium D line. On the other hand, it is known that, similar to natural optical rotatory dispersion, MOR dispersion is normal in nearly all cases, i.e. the MOR increases with decreasing wavelength [35]. The MOR dispersion (wavelength dependence) can be approximately represented by a formula similar to Drude's equation for optical rotatory dispersion [36]:

$$\Lambda = \sum_i \frac{K}{\lambda^2 - \lambda_i^2} \qquad (17)$$

where K is the dispersion constant and λ_i is the absorption wavelength. From Foehr and Fenske's measurements [37] of the MOR of hydrocarbons at different wavelengths, we can estimate that at 442 nm, Verdet constants of the compounds in Table I should be larger than those at 589 nm by a factor of about two. This means that the calculated limit of detection in Table I should be about two times lower.

Fig. 6 shows a chromatogram of the separation of three polynuclear aromatic hydrocarbons: phenanthrene, pyrene and benzo(b)fluoranthene using MOR detection. These analytes were chosen so that they can be also monitored by a conventional UV detector in this work. Naturally, the real advantage of MOR is

Table I. Density, Verdet Constant, and Calculated Limit of Detection

Substance	d_{20} (g/cm^3)	$10^2 \Lambda_D$ (min G^{-1} cm^{-1})[a]	G_{LOD} (W/W)[b]
Methanol	0.791	0.96	---
Water	0.998	1.31	2.82×10^{-4}
Phenanthrene	0.980	5.84[c]	8.82×10^{-6}

[a] At sodium D line
[b] Methanol as solvent
[c] At 578 nm

Figure 6. Chromatogram of (A) phenanthrene, (B) pyrene and (C) benzo(b)fluoranthene, 50 μl injection of 5×10^{-5} (w/w) of each compound in methanol. Eluent: pure methanol, flow rate: 0.47 ml/min.

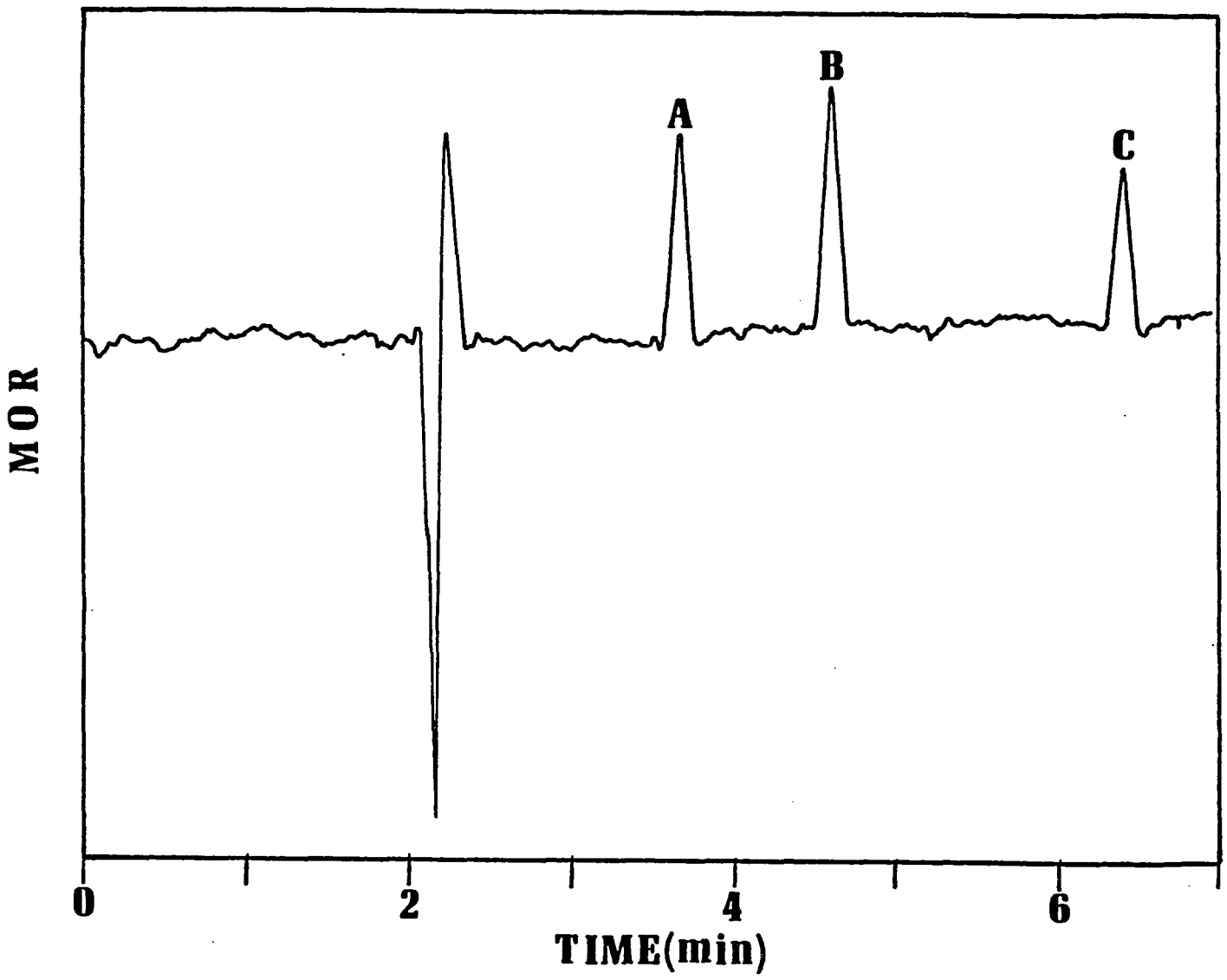
A
B
C
MOR
0
2
4
6
TIME(min)

in its ability to monitor nonabsorbing analytes. In general, Verdet constants for organic materials range from ~1 to ~7 x 10^{-2} min. G^{-1} cm^{-1}. The sharp negative peak and the adjacent positive peak are probably system peaks due to the relatively high total amount of injected analytes. We used pure methanol instead of a mixture with water as the mobile phase to rule out the possibility that these two peaks were due to the MOR of the solvent, which might have different composition from the mobile phase due to the vaporization. These two peaks were reproducible in the chromatographic runs. The chromatogram represents 2.0 μg (40 ppm) of each compound injected. So the detection limits are 0.19 μg (3.8 ppm), 0.16 μg (3.2 ppm) and 0.24 μg (4.8 ppm) for phenanthrene, pyrene and benzo(b)fluoranthene, respectively. The value for phenanthrene reasonably matches the detection limit calculated from Eq. 15, with the consideration of MOR dispersion and the dilution factor from the peak volumes and the injector loop size. The Verdet constants of the other two compounds in Fig. 4 are not available in the literature.

Another interesting point drawn from Eq. 15 is that the MOR signals should show different polarities, depending on the sign of the value ($d_2 \Lambda_1/d_1 - \Lambda_2$). To confirm this point, we injected 20% (w/w) water in methanol, and pure methanol, respectively, with 10% (w/w) water in methanol as the mobile phase. We did observe that the two MOR signals showed opposite polarities. It has to be emphasized that the same experimental conditions must be maintained during injection of the two samples because the polarity of the magnetic field, modulation

polarity, analyzer rotation direction, and lock-in amplifier phase setting can all affect the polarity of the observed MOR signals.

Linearity

From our previous discussion on the additivity of Verdet constants of mixtures, we can expect a linear relationship between the MOR signal of the solution and the weight fraction of the solute. We studied the chromatograms of five samples with different concentrations ranging from $G_1 = 1.0 \times 10^{-5}$ to $G_1 = 3.3 \times 10^{-4}$. The compositions of the samples were the same as that in Fig. 6. Fig. 7 shows the plot of log(MOR) vs. log(G_1) for the three components. It can be seen from the plot that, as expected, the MOR signals are proportional to the respective weight fractions of the compounds in the range of low concentrations. However, for higher concentrations the MOR signals become far lower than those expected. It is the RI change in the detection cell that caused this nonlinearity. Whenever there is a sudden, large change in RI, such as when a relatively high concentration of sample passes through the detection cell, the laser beam is distorted by defocusing and deflection, is partially blocked by apertures and thus cannot pass through the analyzer properly. This problem has been observed in previous work on laser-based polarimeters [27], and a similar problem also exists when absorption causes thermal lensing [38]. Fig. 8 shows the effect of RI change on the MOR signal when high concentrations of samples were separated and then detected by MOR detector. Those negative peaks were artifact signals due to the

Figure 7. Log (MOR signal) vs. log G_1 (weight fraction of solute). (A) phenanthrene, (B) pyrene, and (C) benzo(b)fluoranthene. The three best-fit lines have slopes of 1.11 ± .02, 1.12 ± 0.04 and 1.14 ± 0.02 respectively. For a linear-linear plot, the correlation coefficients are r^2 = 0.997, 0.995, and 0.995, respectively.

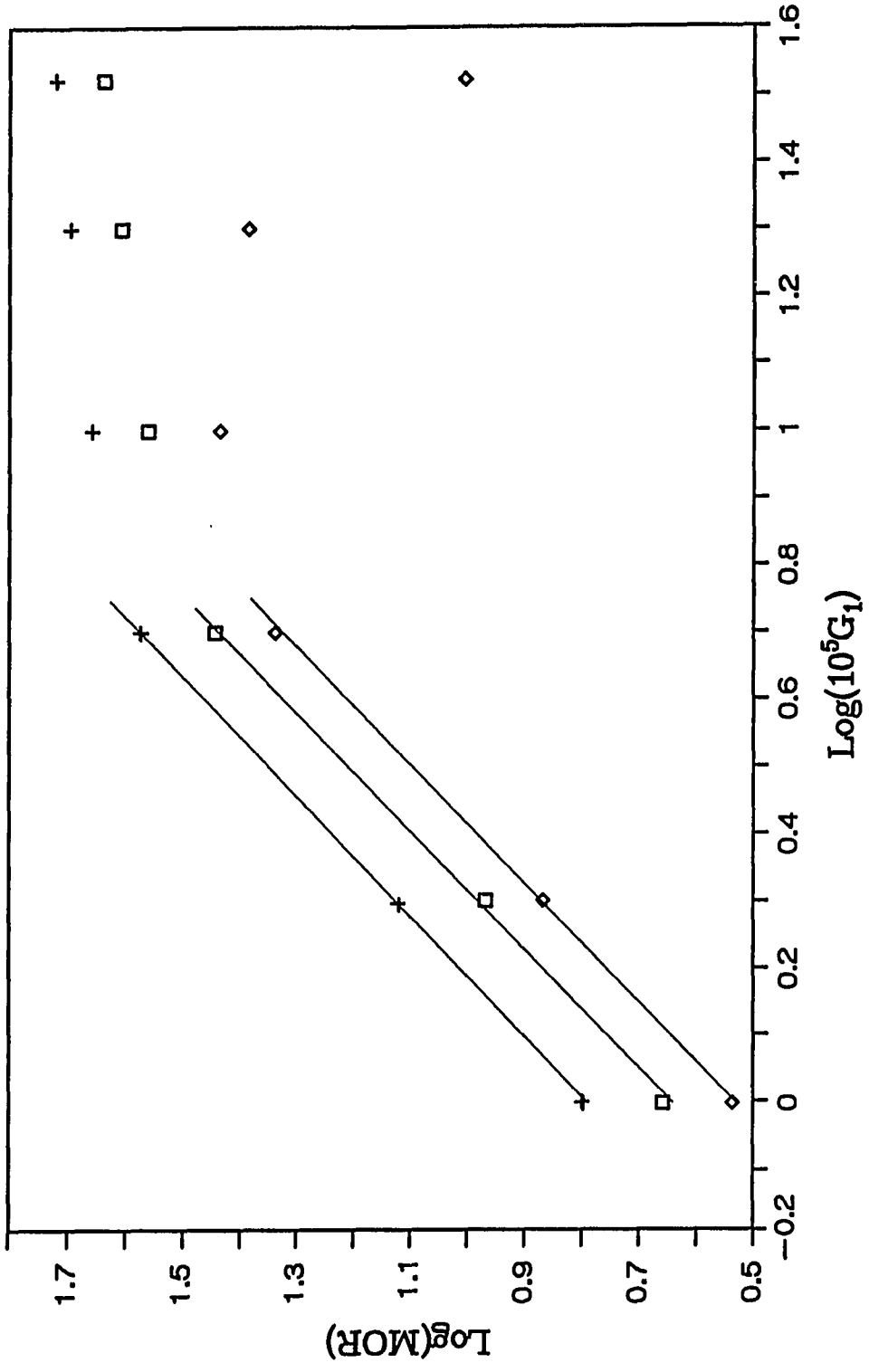
Log(MOR)
1.7
1.5
1.3
1.1
0.9
0.7
0.5
−0.2
0
0.2
0.4
0.6
0.8
1
1.2
1.4
1.6
Log(10⁵G₁)

Figure 8. Chromatograms of (A) phenanthrene, (B) pyrene, and (C) benzo(b)fluoranthene showing negative peaks caused by refractive index changes in the detection cell. Upper trace: 2×10^{-4} (w/w) of each, lower trace: 3.33×10^{-4} (w/w) of each. Other experimental conditions were the same as in Fig. 4.

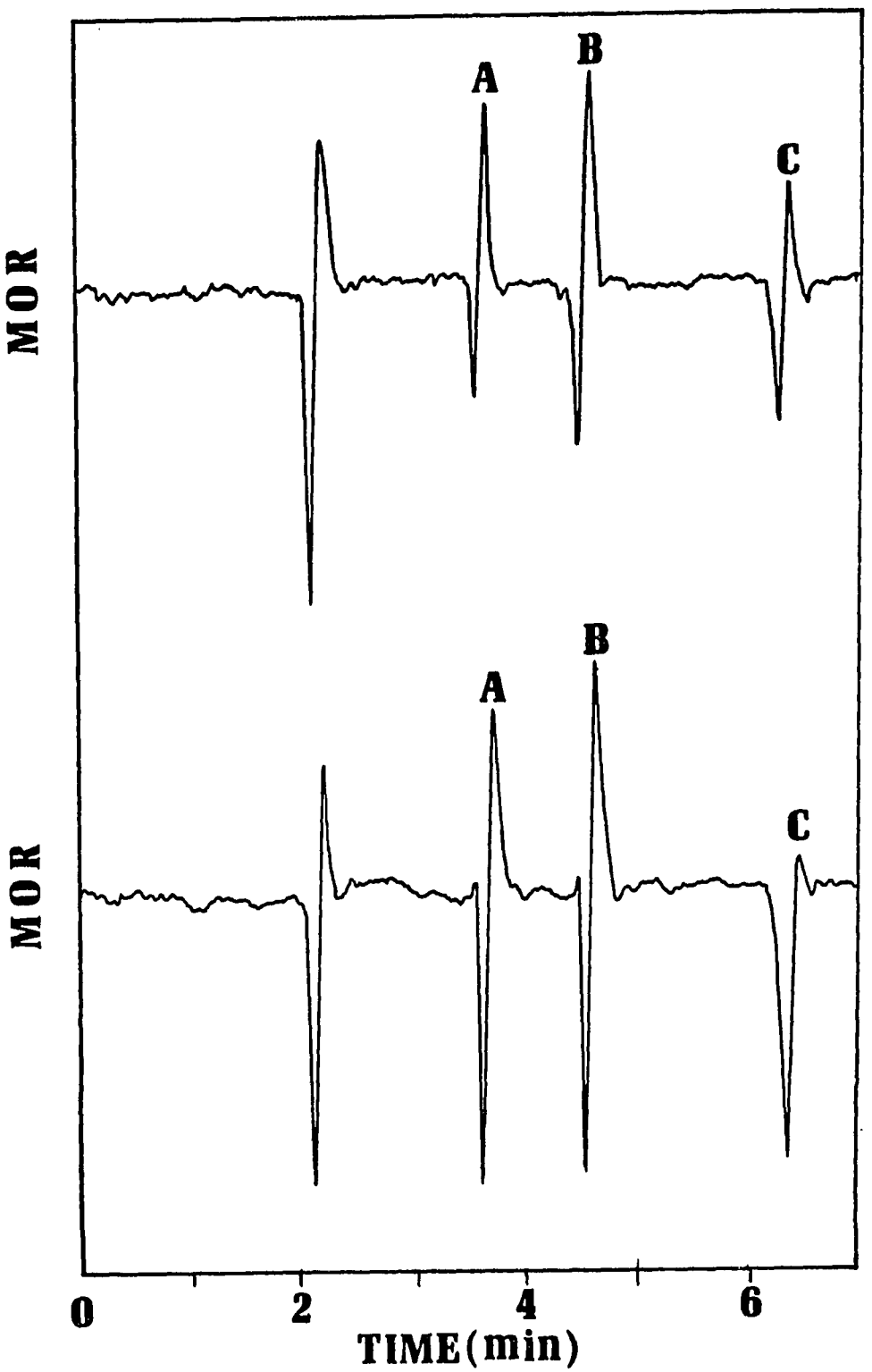
A
B
C
MOR
A
B
C
MOR
0
2
4
6
TIME(min)

RI change. The higher the concentration, the larger is the artifact signal. It is obvious that the artifact signals offset the MOR signal and cause non-linearity.

It has to be emphasized that no attempt was made in this work to further minimize the effect of the RI change and to optimize the system for a larger linearity range. With proper design of the detection cell one should be able to control the flow pattern of the solution in the cell and to reduce the effect of the RI change. In addition, it was shown [19] that careful optical alignment could reduce the defocusing and disturbance of the laser beam caused by the RI change, and solutions of as high concentration as 1% could be used.

It should be noted that in Fig. 8 the experimental conditions were so selected that the artifact and MOR signals had opposite polarities. It was found to be very difficult to distinguish the MOR signals from the artifact signals when both of them had the same polarity since they overlapped each other.

Other Considerations

The contribution of the detector volume to peak broadening is an important issue. The physical dimension of the active region, i.e. the region of the flow cell under the influence of the magnetic field, is estimated to be 19 μL (1.27 mm i.d., 15 mm long). This is not too different from commercial absorption or RI detectors. Using a standard UV detector, we obtained N = 11,200 plates for the phenanthrene peak under identical column conditions but with a 5 μL injection loop. In Fig. 4, we measure N to be 8010 plates. So, there is a slight degradation of the

separation efficiency due to the use of the larger (50 μL) sample loop, which is needed for the best concentration detectability.

It is worth comparing MOR and RI for the universal detection in HPLC. First, the RI detector is extremely sensitive to temperature and pressure changes. It was shown [39] that the LOD of a RI detector using Fabry-Perot interferometry was limited by fluctuations of pressure and temperature. On the other hand, the influence of temperature and pressure on MOR is not as pronounced. This can be explained by the Verdet constants in Table I. The signal due to phenanthrene relative to the solvent (methanol) at equal concentrations is (5.84 - 0.96)/0.96 = 5.1. On the other hand, for RI detection, the relative signal is (1.59 - 1.33)/1.33 = 0.20. Therefore MOR is roughly 26 times more immune to temperature and pressure fluctuations, which change the density of the solvent and thus the background signal. Second, RI and MOR are distinct molecular properties. For HPLC detection, the two are therefore complementary as far as qualitative information (selectivity) is concerned. Third, the RI detector is practically incompatible with gradient elution because of the difficulty of matching the refractive indices of the reference and sample streams. For the same reasons stated above, a mismatch in temperature or pressure between the two flow cells will be less of a problem for MOR. The change of the background MOR signal in the detection cell is then better compensated by the reference cell. In fact, Forsythe et al. [40] have demonstrated the application of this idea in an automatic MOR spectropolarimeter.

Thus, the MOR detector, in principle, could be used with gradient elution if a second flow cell for the reference stream is incorporated into the system. This reference cell has an opposite magnetic field to that of the detection cell. Finally, the commercial RI detectors have a typical detectability of 3×10^{-7} RI units, which is roughly equal to 1 μg of analytes. We have shown in this work that MOR detector has somewhat better detectability and further improvement seems possible. One of the promising methods for improvement is to incorporate a compact superconducting magnet into the polarimetric system. We can expect at least one order of magnitude improvement in the detectability since a normal superconducting magnet can provide a magnetic field of 50,000 to 100,000 gauss, which is about 15 to 30 times higher than that used in this work. A more straightforward modification is to introduce high frequency modulation, water cooling, and intensity stabilization to improve the detectability of the polarimeter by a factor of 10 [28,30].

In conclusion, we have for the first time developed a novel method for universal detection in HPLC based on magneto-optical rotation, which is a general physical property for all substances and in wide electromagnetic spectrum. The working HPLC detector is capable of determining sub-microgram quantities of analytes. This detector can also be used for the normal polarimetric detection in HPLC, where a combined MOR-ORD signal will be obtained. The theoretical study derived a simplified equation for calculating Verdet constants of mixtures and it has been verified experimentally. The linearity is limited by the artifact signals

caused by RI change at high concentrations. The experimental results reasonably match the LOD calculated from Verdet constants. With expected further improvement on LOD, the MOR detector will be developed into a new and better method for universal detection in HPLC.

LITERATURE CITED

1. Umagat, H.; Kucera, P.; Wen, L. F. J. Chromatogr. 1982, *239*, 463-474.

2. Wilson, C.; Hull, G. F. Phys. Rev. 1948, *74*, 711.

3. Kartschagin, W.; Tschetwerikowa, E. Z. Physik 1926, *39*, 886-900.

4. Schatz, P. N.; McCaffery, A. J.; Suëtaka, W.; Henning, G. N.; Ritchie, A. B. J. Chem. Phys. 1966, *45*, 722-734.

5. Mason, S. F. Quart. Rev. (London) 1963, *17*, 20-66.

6. Moscowitz, A. Advan. Chem. Phys. 1962, *4*, 67-112.

7. Djerassi, C. Optical Rotatory Dispersion, McGraw-Hill, N.Y., 1960.

8. Stephens, P. J. Ann Rev. Phys. Chem. 1974, *25*, 201-232.

9. Djerassi, C.; Bunnenberg, E.; Elder, D. L. Pure Appl. Chem. 1971, *25*, 57-90.

10. Shashova, V. E. J. Amer. Chem. Soc. 1960, *82*, 5505-5506.

11. Pidgeon, C. R.; Smith, S. D. Infrared Phys. 1964, *4*, 13-28.

12. Bloembergen, N.; Shen, Y. R. J. Opt. Soc. Amer. 1964, *54*, 551-552.

13. Church, D. A.; Hadeishi, T. Appl. Phys. Lett. 1973, *24*, 185-187.

14. Ito., M.; Murayama, K.; Kayama, K.; Yamamoto, M. Spectrochim. Acta Part B 1977, *32B*, 347-355.

15. Kitagawa, K.; Shigeyasu, T.; Takeuchi, T. Analyst 1978, *103*, 1021-1030.

16. Kersey, A. D.; Dawson, J. B. Anal. Proc. Roy. Soc. Chem. 1981, *18*, 187-189.

17. Debus, H.; Hanle, W.; Scharmann, A.; Witz, P. Spectrochim. Acta Part B 1981, *36B*, 1015-1021.

18. Yamamoto, M.; Murayama, S.; Ito, M.; Yasuda, M. Spectrochim. Acta Part B 1980, *35B*, 43-50.

19. Kawazumi, H.; Nishimura, H.; Ogawa, T. Anal. Sci. 1990, *6*, 135-136.

20. Partington, J. R. "Advanced Treatise on Physical Chemistry", Longmans, Green & Co., London, 1954, p. 602.

21. Hougen, J. T. J. Chem. Phys. 1960, *32*, 1122-1125.

22. Waring, C. E.; Hyman, H.; Steingiser, S. J. Am. Chem. Soc. 1940, *62*, 2028-2031.

23. Broersma, S.; Waterman, H. I.; Westerdijk, J. B.; Wiersma, E. C. Physica 1943, *10*, 97-129.

24. Washburn, E. W. International Critical Tables, Vol. VI, McGraw-Hill, N.Y., 1926, p. 425.

25. Schrönrock, V. O. Z. Phys. 1932, *78*, 707-721.

26. Chuckerbutti, B. N. Indian J. Phys. 1932, *8*, 387-395.

27. Yeung, E. S.; Steenhoek, L. E.; Woodruff, S. D.; Kuo, J. C. Anal. Chem. 1980, *52*, 1399-1402.

28. Xi, X.; Yeung, E. S. Appl. Spectrosc. 1989, *43*, 1337-1341.

29. Montgomery, D. B. in Solenoid Magnet Design, Robert E. Krieger, Huntington, N.Y., 1980, p. 6.

30. Bobbitt, D. R.; Yeung, E. S. Anal. Chem. 1986, *40*, 407-409.

31. Monnig, C. A.; Madison, R. T.; Heiftje, G. M. Appl. Spectrosc. 1990, *44*, 216-219.

32. Monnig, C. A.; Heiftje, G. M. J. Anal. Atom. Spectrosc. 1988, *3*, 679-682.

33. Oldenbourg, R.; Phillips, W. C. Rev. Sci. Instrum. 1986, *57*, 2362-2365.

34. Yeung, E. S. Talanta 1985, *32*, 1097-1100.

35. Stephen, M. J. Mol. Phys. 1958, *1*, 301-304.

36. Partington, J. R. "Advanced Treatise on Physical Chemistry" Longmans,

Green & Co., London, 1954, p. 607.

37. Foehr, E. G.; Fenske, M. R. Ind. Eng. Chem. 1949, *41*, 1956-1966.

38. Dovichi, N. J.; Harris, J. M. Anal. Chem. 1979, *51*, 728-731.

39. Woodruff, S. D.; Yeung, E. S. Anal. Chem. 1982, *54*, 2124-2125.

40. Forsythe, J. G.; Kieselbach, R.; Shashoua, V. E. Appl. Phys. 1967, *6*, 699-702.

SECTION II

AXIAL-BEAM ON-COLUMN ABSORPTION DETECTION FOR OPEN TUBULAR CAPILLARY LIQUID CHROMATOGRAPHY

INTRODUCTION

Recently, the subject of open tubular capillary liquid chromatography (OTCLC) has received considerable interest [1-3]. Using "separation impedance", a criterion introduced by Bristow and Knox [4], to assess the theoretical performance of conventional and capillary columns in liquid chromatography, Knox [5] predicted that OTCLC could have the smallest theoretical plate height and best performance. It is generally accepted that OTCLC with inner diameters of less than 10 μm and employing detectors with low nanoliter volumes and high sensitivities will produce high separation efficiencies in a reasonable time with superior limits of detection [6-8].

The advantages of OTCLC with respect to separation speed and efficiency can be exploited only when the external contribution to peak broadening is minimized [6,9]. Since the inner diameters of OTCLC columns are normally about 10 μm, the injection and detection volumes have to be substantially reduced, compared with conventional liquid chromatography, to maintain the column efficiency. As far as the injection volume is concerned, this is readily achieved by using techniques such as split injection [10], microsyringe injection [11] or stopped flow injection [12]. However, the reduction of detection cell volume to below 1 nl is a more difficult task. Controlling the shape of the detector is also a challenge. The ideal focusing of a Gaussian light beam will give [13]:

$$V = 16Z^2 \lambda \quad (1)$$

where V is the minimum volume, Z is the path length (the range of collimation of the focused beam) and λ is the wavelength of light. To provide a volume of 1 nl, the maximum path length is about 0.2 mm at 300 nm excitation, which is almost two orders of magnitude shorter than the path length of conventional absorption cell.

A variety of detection methods have been utilized in the development of OTCLC, including UV-vis absorption [14-17], fluorescence [18-20], electrochemistry [21-23], mass spectrometry [24], flame photometry [25], flame ionization [26], and thermal lens detection [27], etc. Most of the reported research in OTCLC has utilized absorption, fluorescence or electrochemistry detection. Although it has relatively poor sensitivity compared with fluorescence and electrochemistry detection, absorption detection is more versatile and is most widely used in the research of OTCLC. The early studies of OTCLC with absorption detection employed the post-column scheme by miniaturizing detectors of conventional liquid chromatography. However, the volumes of flow cells which were about 100 nl were still far from the optimum for OTCLC.

The problems were approached in a different way by Yang [28] who developed an on-column absorption detector for OTCLC. This new detection method utilized a segment of the fused silica capillary column for its detection cell. This on-column absorption detection scheme was later extended to detection for open tubular capillary zone electrophoresis [29], which has a similar detection

problem to OTCLC. An on-column fluorescence detector was also developed for OTCLC based on the idea of on-column absorption detection [30-31]. The major advantage of on-column detector over post-column detector based upon miniaturization of conventional flow cells was the elimination of zone broadening effects caused by extra column volumes inherent to detector cells and associated coupling fittings. However, since on-column absorption detectors rely on a cross-beam arrangement (i.e. the light beam crosses the capillary column at right angles), the absorption path length was severely limited to that of the inner diameter of capillary columns, ranging from 10 μm to 50 μm. In turn, the absorbance and thus the concentration limits of detection were also limited. For example [32], if one assumes an absorbance detection limit of 5×10^{-4} for a high quality commercial chromatographic detector interfaced to a capillary column, and an analyte with molar absorptivity of 10^4 1 mol^{-1} cm^{-1}, then concentration limits of detection range from 5×10^{-5} M to 1×10^{-5} M for path lengths of 10 μm to 50 μm, hardly state-of-the-art in trace analysis.

On the other hand, it is known that the theoretical plate height in OTCLC is roughly equal to two times the inner diameter of capillary column [33], and so the number of available theoretical plates, $N \approx L/2d$, where L is the column length and d is the column inner diameter. Also, from the plate theory of chromatography $N = 5.54 (t_R/w_{1/2})^2$ where T_R and $w_{1/2}$ are retention time and width of a peak at half its maximum, respectively. Notice that t_R is proportional to column length L

and $w_{1/2}$ is proportional to the length of sample zone inside the capillary column b. We then have an approximation of relating T_R and $w_{1/2}$ to L and b:

$$N = 5.54 (t_R/w_{1/2})^2 \approx 5.54 (L/b)^2 \quad (2)$$

Consequently, b is dependent on d by the equation:

$$b^2 \approx 11.08 \, d \, L \quad (3)$$

For a typical 100 cm long and 10 μm i.d. capillary column, b equals 10.5 mm, which is 1050 times longer than the inner diameter of the column.

If one can couple a light source into one end of the capillary column and guide the beam through the whole column, the light signal detected at the other end of the column will be a measure of the absorption of the samples. One therefore will be able to take full advantage of the length of sample bands inside the capillary column and increase the path length, and so the absorbance, by a factor of 1000. We refer to this detection scheme for OTCLC as "axial-beam" on-column absorption detection, with the potential of providing 1000-fold improvement on the concentration limits of detection over the cross-beam on-column absorption detection.

In this section, we report the results of the first experiments of axial-beam on-column absorption detection for OTCLC. The interface between light source and the capillary columns will be explored and discussed. The intensity profiles of

light beams traveling through the capillary columns are measured to explore the possibilities of guiding light through long capillary columns with inner diameters ranging from 10 μm to 75 μm. We will also demonstrate the feasibility of applying this detection method to reversed phase OTCLC using an optical waveguide capillary column.

EXPERIMENTAL

Apparatus

A schematic diagram of the axial-beam on-column absorption detector for OTCLC is shown in Figure 1. The detector utilized as a light source a 3mw He-Ne laser (Uniphase Corp., San Jose, CA, Model 1105P) which operated at 632.8nm and was linearly polarized. The laser beam was passed through a laser power stabilizer (Cambridge Research and Instrumentation, Cambridge, MA, Model LS100), was reflected by two mirrors (Newport, Fountain Valley, CA, Model 10D10.ER3) and was then focused by a 25mm focal length lens (Newport, Model KPX076) into the end of the capillary column. The laser beam power after the focusing lens was about 1mw. The transmitted laser beam at the other end of the capillary column was collected by a 5X microscope objective lens. The image was passed through a 632.8nm line filter (Corion Corp., Holliston, MA, Model P1-633-FR) and then detected by a photodiode (Hamamatsu Corp., Middlesex, NJ, S1790) or a photo-multiplier tube (Hamamatsu, R928) which was operated with a bias potential of 250 V to 550 V. The output of the photomultiplier tube was fed to a digital multimeter (Keithley Instruments, Cleveland, OH, 160B) which amplified and converted the signal to a voltage output. This output was then sent either to a chart recorder (Houston Instruments Corp., Austin, TX, Model B5117-5I) or to a data acquisition system consisting of an analog to digital I/O interface (Data Translation, Marlborough, NA, Model DT2827) and a microcomputer (IBM, Boca Raton, FL, Model

PC/AT).

The lens was mounted on a precision x-y positioner (Newport, 462 series) for fine alignment of the laser beam focal point. The entrance end of the capillary column was inserted into one port of a 1/32" stainless steel tee (Valco Instruments Corp., Houston, TX, Model ZT.5) and tighten by a one-piece fused silica adaptor (Valco Instruments Corp., Houston, TX, Model FS.25, 1/32"). The output end of the capillary column was held by a fiber optic positioner (Newport, Model FP1) and was adjusted to slightly touch the tip of a drill bit (1/20") to direct the liquid flowing out of the capillary column to drain. The capillary column was either sandwiched between two pieces of foam plastics sheets or taped on a solid mount to prevent any vibrations.

Chromatography

The chromatographic system employed in this work is shown in Figure 1. A microsyringe pump (ISCO, Lincoln, NE, Model μLC-500) was used in the constant flow mode to propel the eluent through the column. A 0.5-μm line filter (Alltech, Deerfield, IL, Model SSI 05-1005) was connected before the injector (Rheodyne, Cotati, CA, Model 7520) which had a rotor volume of 0.5 μl or 1.0 μl. Since the majority of the mobile phase was diverted from the column by a split-flow system, the flow rate in the open tubular capillary column was typically 20 nl/min. A 1/16" stainless steel splitting tee (Valco Instruments Corp., Model ZT1C) was positioned after the injector and a section of fused silica capillary tubing (150 μm

Figure 1. Schematic diagram of axial-beam on-column absorption detector for open tubular capillary liquid chromatography. He-Ne, Helium-Neon laser; LS, laser power stabilizer; M, mirror; L1, 25 mm f.l. lens; T1, 1/32" tee; T2, 1/16" tee; CT, fused silica capillary tubing; IN, injector; FL, filter; PU, syringe pump; CC, capillary column; PN, optical fiber positioner; L2, 5X microscope objective; PMT, photomultiplier tube; PS, power supply; DMM, digital multimeter; CM, microcomputer; CR, chart recorder.

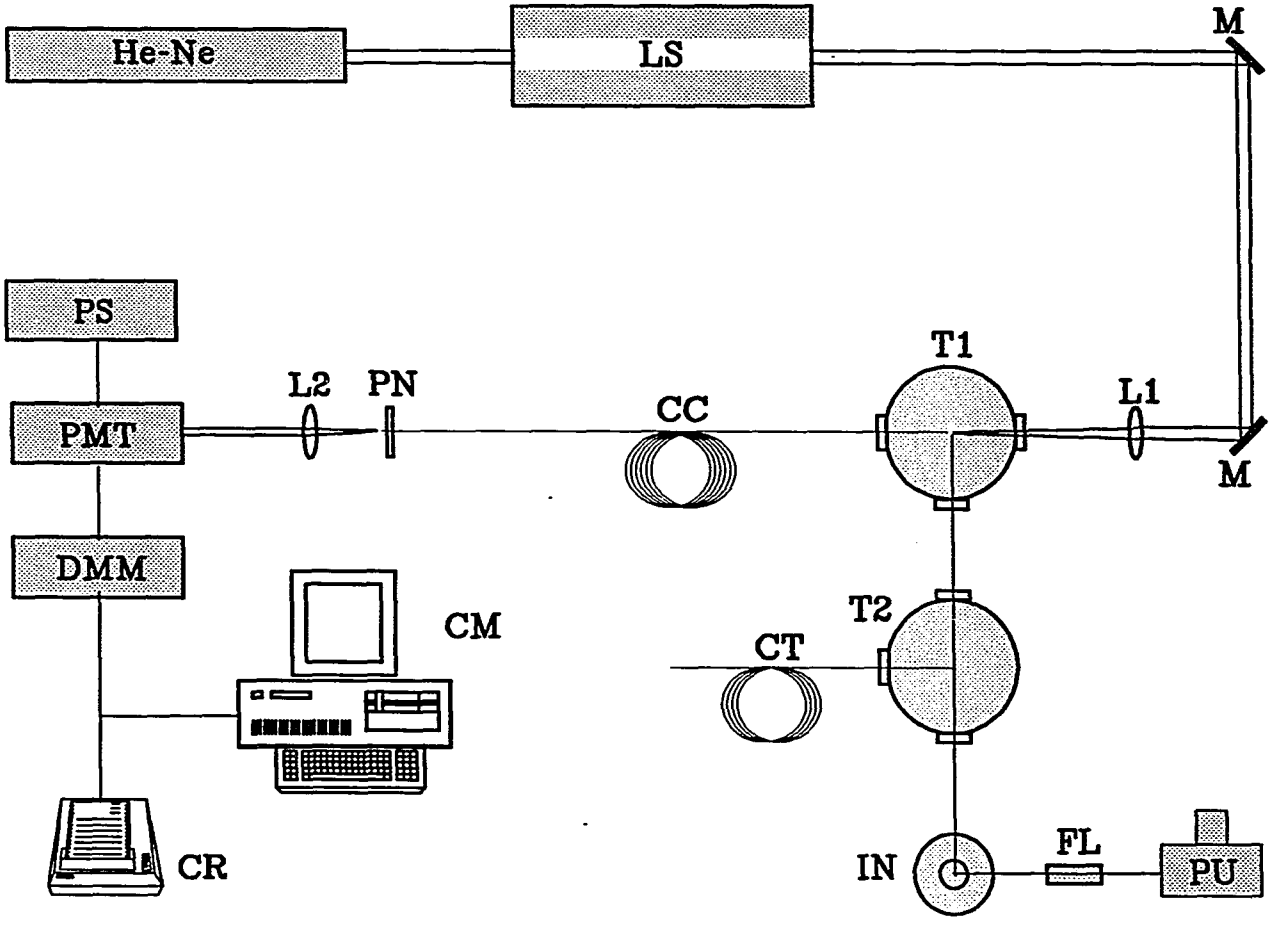
He-Ne
LS
M
PS
PMT
L2
PN
CC
T1
L1
M
DMM
CM
T2
CT
CR
IN
FL
PU

o.d. and 10 μm to 25 μm i.d., Polymicro technologies Inc., Phoenix, AZ) was inserted into the tee and drew off most of the flow from the open tubular capillary column. Another piece of fused silica capillary tubing was employed to connect the splitting tee and the light-coupling tee. By proper choice of the lengths and inner diameters of both capillary tubings, the desired splitting ratios were obtained.

Columns

The open tubular capillary column used in this work were prepared using a procedure adapted from Farbrot et al. [34]. The reverse-phase stationary phases were coated on the inside of fused silica capillary columns (150 μm o.d. and 10-12 μm i.d., Polymicro Technologies Inc.) by cross-linking vinyl silicone gums. The details of the column coating procedure have been described elsewhere [35].

Reagents

The mobile phases used in this work were either 93% by volume pyridine (Fisher, Fair Lawn, NJ) in water, dimethyl sulfoxide (Fisher) or methanol (Mallinckrodt, Paris, Kentucky). Bromocresol green was supplied by Baker (Phillipsburg, NJ) and azulene was obtained from Aldrich (Milwaukee, WI). The water used was purified using a Barnstead Nanopure II system (Boston, MA). All chemicals were reagent grade and used as supplied. All solutions were filtered with a disposable Nylon 66 filter (Alltech, 0.2 μm) and degassed in an ultrasonic bath.

Axial coupling of light source with capillary columns

The interface between the light source and the open tubular capillary column is shown in Figure 2. The column and fused silica capillary tubing were inserted into a 1/32" stainless steel tee and were tighten by fused silica adapters as described above.

A quartz window that permitted the insertion of He-Ne laser light into the end of the open tubular capillary column was held by a 1/32" polyimide ferrule (Valco Instruments Corp., Model ZF.5). The quartz window was home-made using a high quality synthetic fused silica rod (Dynasill Corp., Berlin, NJ, Selected Grade 4100) and was 1.6 mm thick and 0.78 mm in diameter. The quartz window, with surfaces of good quality, could transmit about 80% of light. The gap between the end of capillary column and the quartz window was estimated to be 1 mm, which allowed mobile phase to flow into the column.

Beam profile measurement

To measure the profiles of laser beams passing through the columns, a 5X microscopic objective was used to image the beams at the output end of the column to a white screen about two meters away. The 30 x 30 and 50 x 50 pixel images were digitized using a cooled CCD camera system (Photometrics Ltd., Tucson, AZ, Series 200) equipped with a 90 mm macro-lens (Tamron, Tokyo, Japan). The images were then transferred to a microcomputer (Compuadd, Austin, TX, Model Standard 286) for storage and analysis.

Figure 2. Schematic diagram of axial coupling of light beam with capillary column. L, 25 mm f.l. lens; W, Quartz window; T, 1/32" tee; CT, capillary tubing; CC, capillary column; F, polyimide ferrule; A, fused silica adapter; N, nut.

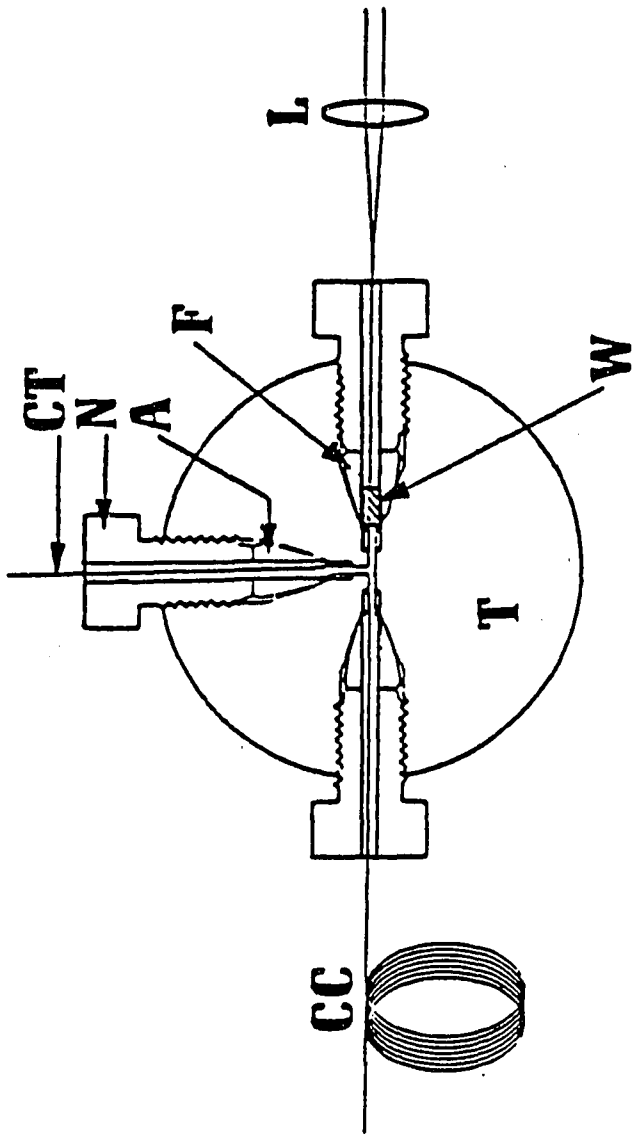
L
F
W
CT
N
A
T
CC

RESULTS AND DISCUSSION

Source light coupling with capillary columns

One of keys for success in developing an axial-beam on-column absorption detector for OTCLC was the interface between the light source and the small columns. An interface is required which can not only transmit light with high optical quality, i.e. high transmittance and small scattering and wavefront distortion, but also withstand the relatively high pressure produced in the chromatographic system. The interface used in our experiment was a home-made quartz window hold in position by a flexible polymide ferrule. This system readily tolerated 1500 psi pressure, which is sufficient for most experiments in OTCLC. On the other hand, high optical quality in the window was difficult to achieve. We found that the quartz windows with low optical qualities provided poor transmittance, large wavefront distortion and severe scattering when coupling light into the columns with inner diameters ranging from 10 μm to 75 μm. These problems were mainly controlled by the flatness and scratch and dig numbers of the window surfaces, the refractive index homogeneity and the numbers of inclusions, bubbles and seeds in the window material. Compared with the commercial grade fused silica, the Selected Grade 4100 fused silica provided much better refractive index homogeneity and more than 100 times less inclusions, bubbles and seeds. This in turn efficiently reduced the wavefront distortion and scattering. To make flat and scratch and dig free surfaces for the quartz window, we tried to grind and polish the surfaces using

600 grit paper and then 0.3 μm aluminum oxide abrasive. However, due to the difficulty of handling the small quartz window, grinding and polishing did not produce satisfying surfaces. We then used normal glass-drawing technique and cut the quartz windows with a sharp knife. With practice, it was possible to make quartz windows with relatively flat and scratch and dig free surfaces. Even though it was tedious to prepare, a quartz window with high optical quality could be used for a long period of time.

Profiles of transmitted laser beams

Lei et al. [36] developed a long capillary cell with 1 mm i.d. to enhance the detection power of ordinary colorimetry for the determination of phosphorus in natural water. They found that changing the capillary cell shape, i.e. curving or looping the cell, resulted in serious attenuation of the incident light. A 70-cm looped capillary cell could transmit only 2.8×10^{-6} of the light energy compared to a linear capillary cell of same length. Similarly, we found it absolutely necessary for capillary columns with 10 μm to 75 μm i.d. to be at a linear arrangement to efficiently transmit light. No light energy could be detected for a 85 cm x 75 μm looped capillary column (1 turn loop, 12 cm diameter).

Figure 3 shows the intensity profile of a laser beam transmitted through a linear 85 cm x 75 μm capillary column. It can be seen that most of light energy was distributed inside the liquid core of the column. That is, transmission through the fused silica wall plays a minor role. To quantitatively determine the percentage of

light energy distributed inside the core, the output end of the column was immersed in a cell containing pyridine (refractive index n=1.51). This caused the light energy distributed inside the wall of the column to refract out, so that only light traveling through the core of the column was detected. We found this percentage to be about 78%. This naturally depends on the alignment of capillary column and focusing of the light source.

For applications in OTCLC, columns with inner diameters smaller than 75 μm have to be utilized. Figure 4 shows the intensity profile of a laser beam transmitted through a 85 cm x 25 μm capillary column. In this case, the vast majority of light energy was distributed along the wall of the column. Obviously, this arrangement is useless for absorption detection. One of the reasons for light to preferentially travel through the wall instead of the core was the difficulty in focusing light into the exact center of the column with 25 μm i.d. and 150 μm o.d. Wavefront distortion and scattering caused by the imperfect window made focusing more difficult. Another reason was that the cross-sectional area of the wall was 35 times larger than that of the core.

An optical waveguide using hollow glass fiber as the cladding and liquid (with a higher refractive index) as the core was developed for long distance optical communication [37-38]. Later, this technique was employed for signal enhancement in Raman spectroscopy [39], colorimetry[40] and fluorimetry[41]. If one uses mobile phases in LC with higher refractive indices than that of the column material,

light will travel exclusively through the core of the column by total internal reflection. Figure 5 shows the intensity profile of laser light traveling through a 85 cm x 25 μm column filled with pyridine by total internal reflection. All the light energy was distributed inside the core and the Gaussian profile was nicely retained. The column can be looped since the transmittance was independent of the column shape.

Optical waveguide capillary columns

According to Snyder and Kirkland [42], about 30% of the most often used solvents for liquid chromatography have refractive indices larger than that of the column material (fused silica, refractive index n=1.458). These all could be used in OTCLC with total internal reflection. In our work, we chose pyridine and dimethyl sulfoxide (refractive index n=1.477) as the mobile phases based on their relatively high polarity, low viscosity, large water solubility and transparency at the operating wavelength.

Figure 6 shows a typical chromatogram of OTCLC using a axial-beam on-column absorption detector with total internal reflection. I_0 was the light intensity detected when only mobile phase ran through the column. I_1 was due to the absorption of the component with larger retention time. I_2 results from the absorption of both components. In Figure 6, AZ was azulene and BG was bromocresol green which had a larger retention time. For quantitative determination, it can be seen that $A_{AZ} = \log(I_1/I_2)$, $A_{BG} = \log(I_0/I_1)$ and $A = A_{AZ} +$

Figure 3. Intensity profile of transmitted laser beam. Column: 85 cm x 75 μm, 150 μm o.d.; mobile phase: methanol; flow rate: 200 nl/min.

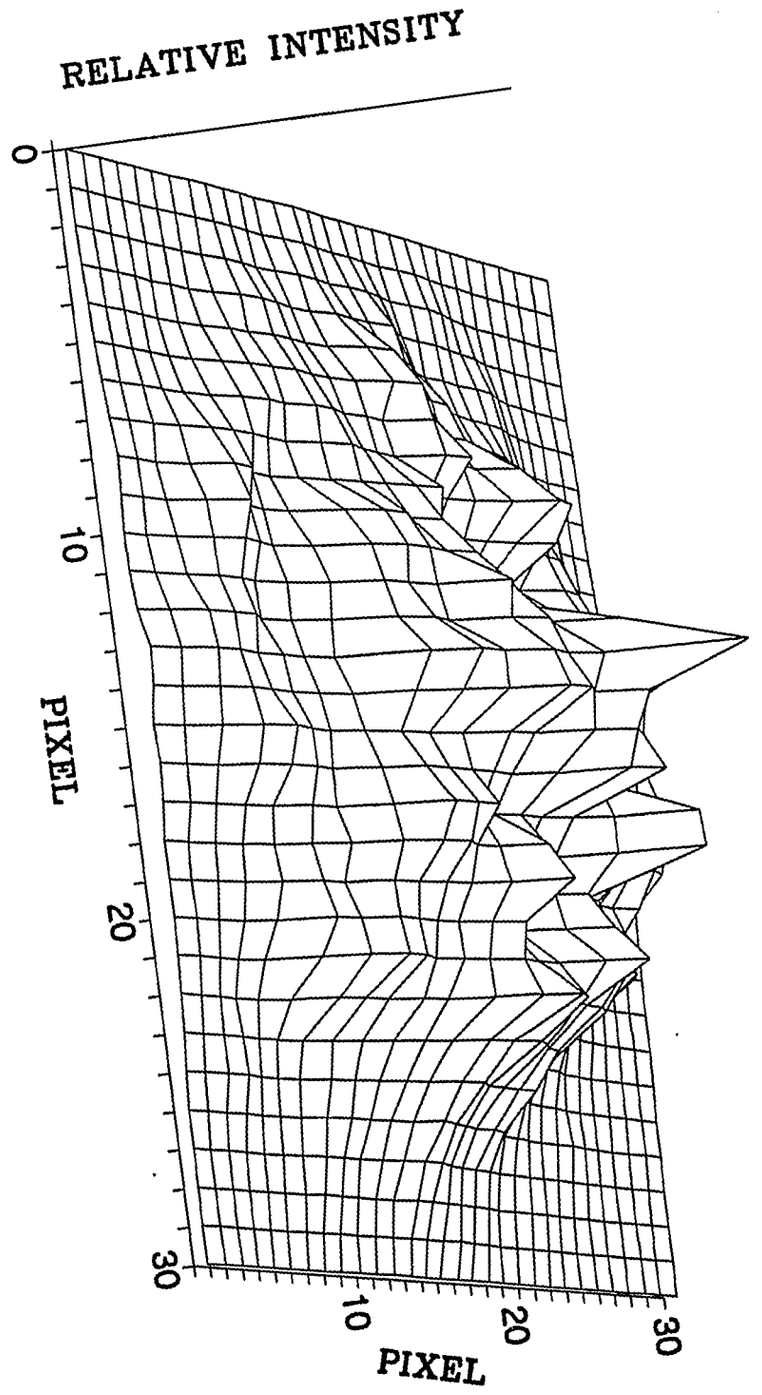
RELATIVE INTENSITY
0
10
20
30
PIXEL
10
20
30
PIXEL

Figure 4. Intensity profile of transmitted laser beam. Column: 85 cm x 25 μm, 150 μm o.d.; mobile phase: methanol; flow rate: 70 nl/min.

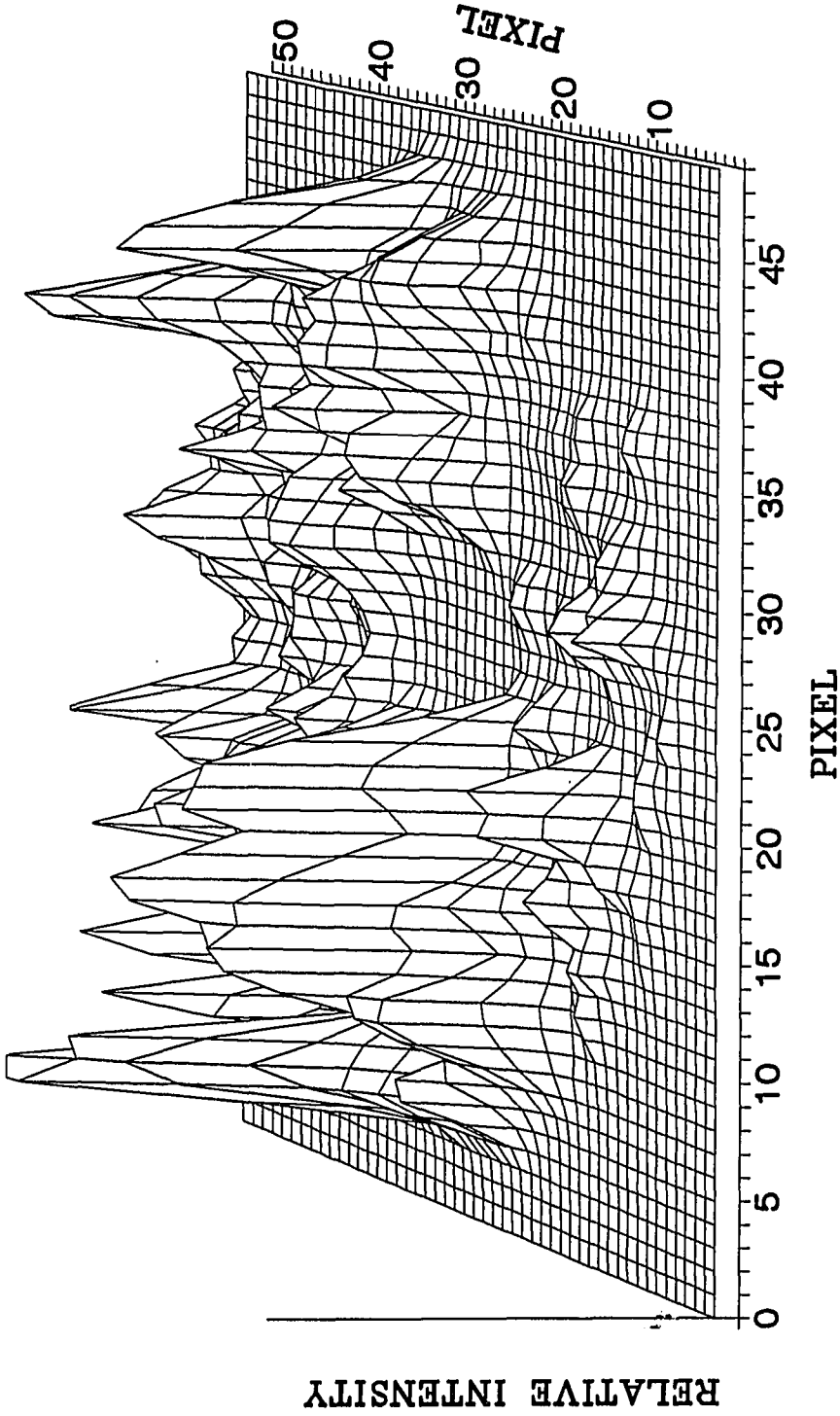
RELATIVE INTENSITY
PIXEL
0
5
10
15
20
25
30
35
40
45
PIXEL
10
20
30
40
50

Figure 5. Intensity profile of transmitted laser beam. Column: 85 cm x 25 μm, 150 μm o.d.; mobile phase: 93% pyridine in water; flow rate: 70 nl/min.

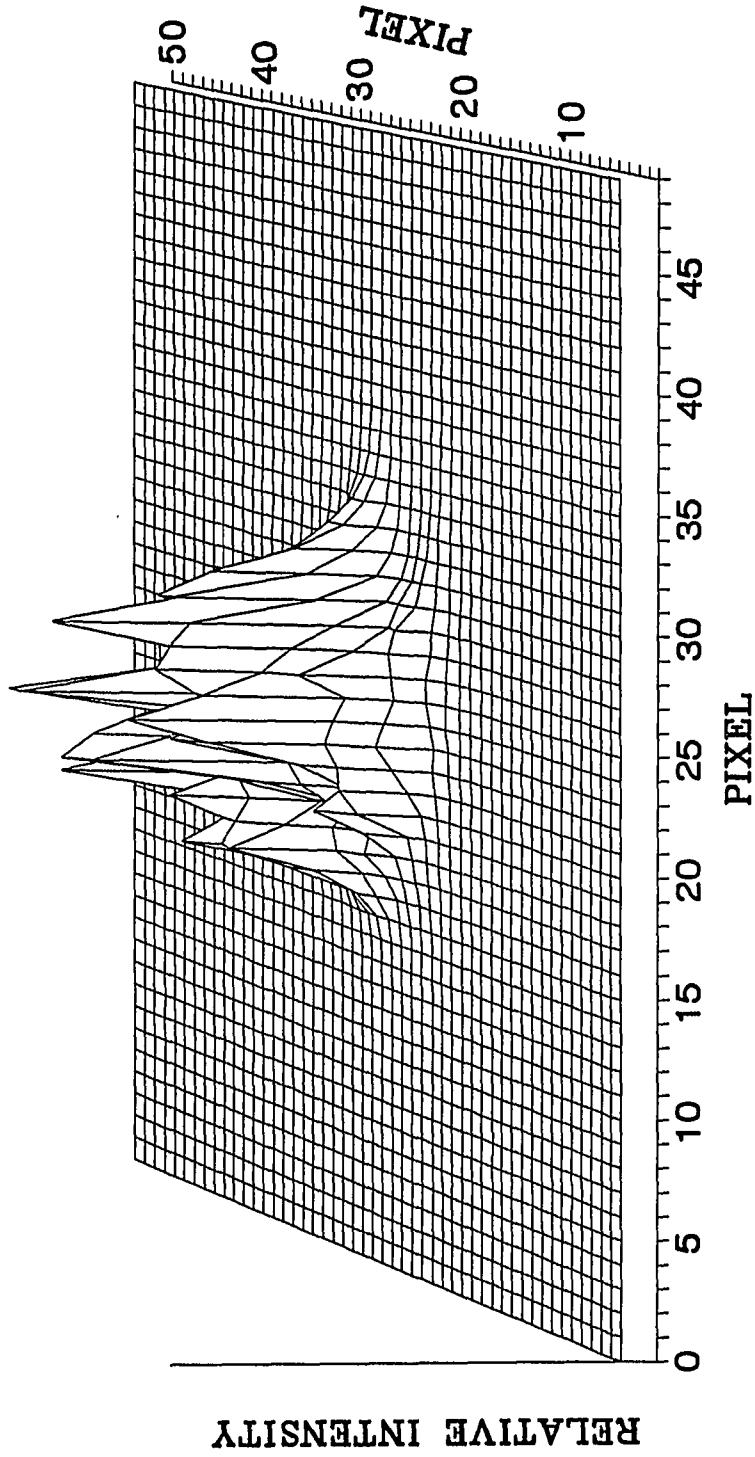
PIXEL
50
40
30
20
10
0
5
10
15
20
25
30
35
40
45
PIXEL
RELATIVE INTENSITY

$A_{BG} = \log(I_0/I_2)$. The retention time of azulene and of bromocresol green was measured as the time between the first and the second inflection point and between the first and the third inflection point, respectively. The rise time at the slopes of the two plateaus provides information about the peak widths.

Although Figure 6 shows a chromatogram appearing different from the "normal" chromatogram, it is nothing more than an integrated plot derived from a normal chromatogram. To demonstrate this, we took a 21-point quadratic first derivative on Figure 6, using a least squares differentiation method introduced by Savitzky and Golay [43]. Figure 7 shows the result, which is in the form of a normal chromatogram. Peak A in Figure 7 was a system peak due to injecting the sample into the column. It is not surprising that one obtains an "integrated" chromatogram by axial-beam on-column detection. Only when absorbing components enter or leave the column will there be a change in transmission. At any given time, the cumulative absorbance within the column is recorded. Synovec and Yeung [44] developed an integration method to improve the limits of detection (LOD) in chromatography. The relation between Figs. 6 and 7 here is identical to the transformation discussed in ref. [44], except that integration is inherent to the optical scheme here and not performed mathematically. In the earlier work, a LOD enhancement ratio of 5 to 20 could be obtained for a typical chromatographic system by using an integration procedure. We have confirmed this conclusion in this work. Figure 7 shows noticeably larger noise levels than Figure 6 even though

a 21-point smooth has been applied to the former. The superior signal to noise ratio in Figure 6 shows an inherent advantage of using the raw data rather than converting back to a "normal" chromatogram. As pointed out earlier [44], chromatographic resolution and quantitative accuracy are retained in the integrated chromatogram. Finally, it should be noted that for simplicity the intensities were plotted in Fig. 6 and 7. For quantitation, these chromatograms should first be converted to absorbance units. One would then be able to avoid nonlinearity when a trace analyte is present with other strongly absorbing components. Naturally, the dynamic range will eventually be affected if the baseline stability begins to degrade when the transmitted intensity becomes too low.

Limit of detection

The LOD of the axial-beam on-column absorption detector is dependent on the baseline stability of the transmitted intensity. Several factors affecting the baseline stability were identified. First, flow turbulence in the mobile phase immediately before entering the column will change the focal point of the incident light and cause fluctuations in light intensity. However, we found that the baseline stability was independent of flow rate ranging from 0 to 35 nl/min for a 10-12 μm i.d. column in the split flow arrangement. Second, any vibrations in the column will change the alignment and introduce noise. Taping the column on a solid mount overcomes this problem. Finally, the formation, growth and release of the liquid drop at the exit end of the column can produce a periodic optical distortion. The

Figure 6. Axial-beam on-column absorption detection of azulene (AZ) and bromocresol green (BG). I_0: baseline intensity; I_1: intensity with BG; I_2: intensity with AZ and BG. AZ: 4×10^{-4} M; BG: 5.5×10^{-5} M; eluent: 93% pyridine in water; flow: 20 nl/min; injection volume: 0.93 nl.

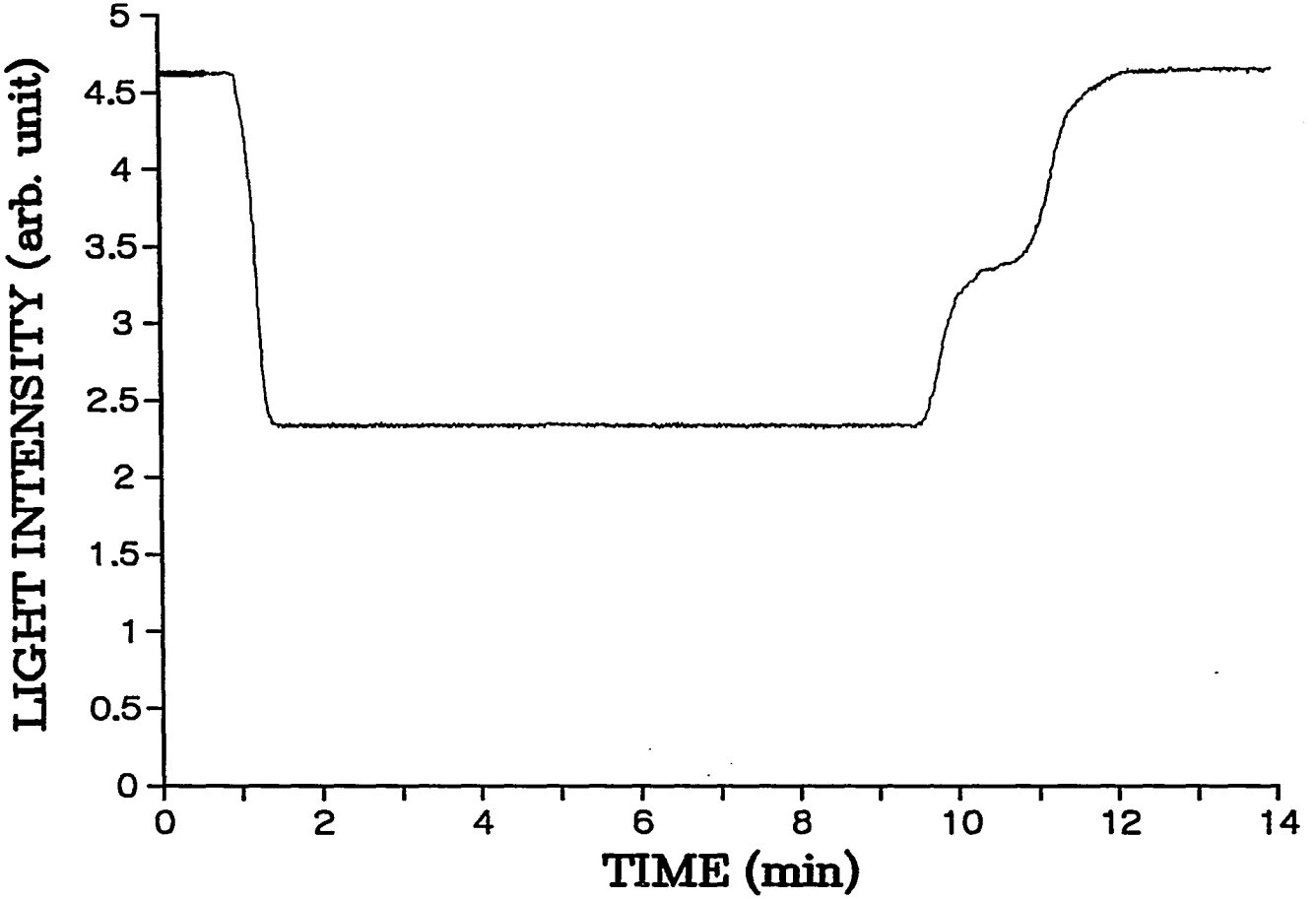
LIGHT INTENSITY (arb. unit)
5
4.5
4
3.5
3
2.5
2
1.5
1
0.5
0
0
2
4
6
8
10
12
14
TIME (min)

Figure 7. Chromatogram of B, azulene; C, bromocresol green; A is the system peak. The plot is a 21-point quadratic-smoothed first derivative of Figure 6.

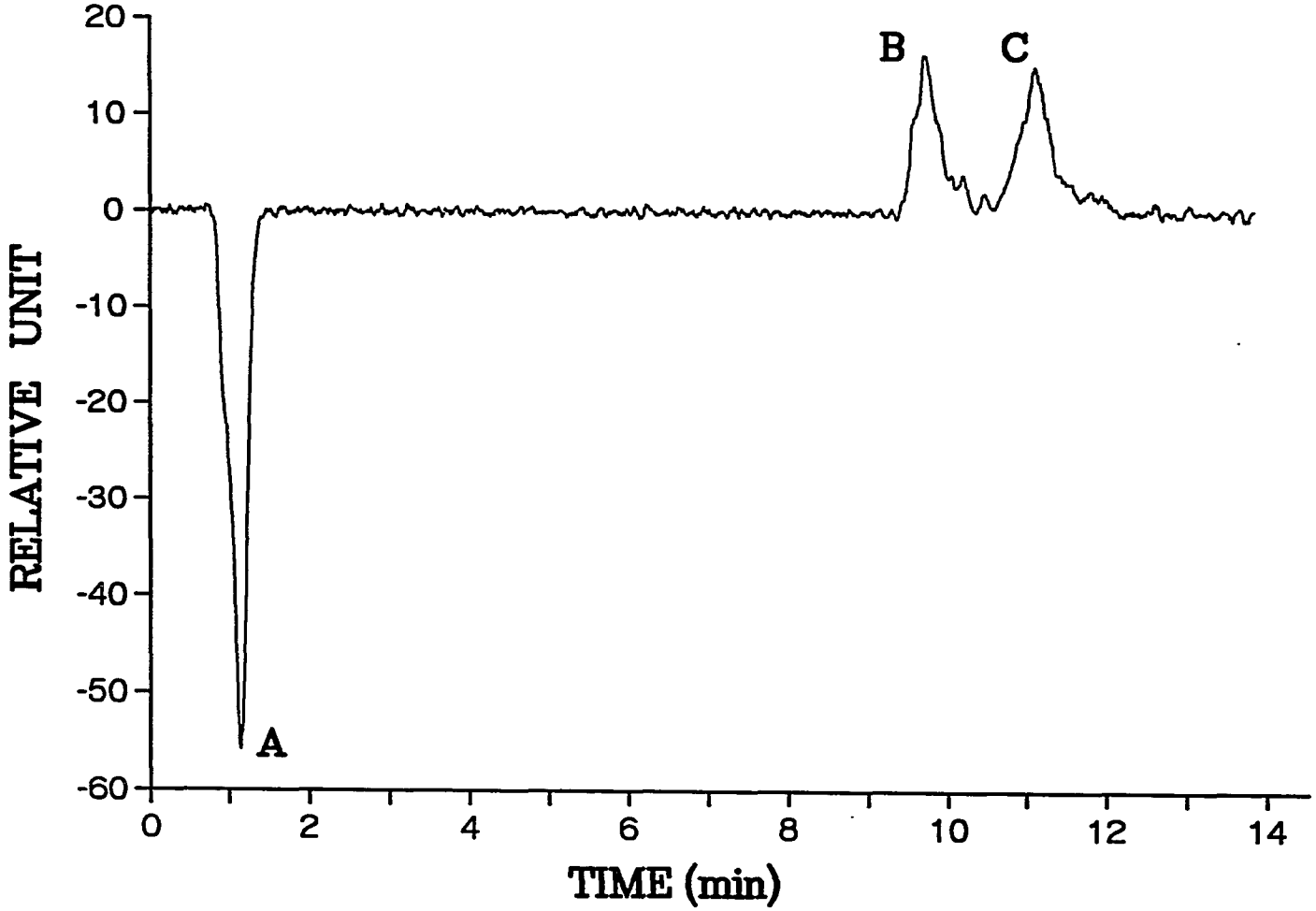
20
10
0
-10
-20
-30
-40
-50
-60
RELATIVE UNIT
A
B
C
0
2
4
6
8
10
12
14
TIME (min)

noise level became larger with increasing mobile phase viscosity. This problem was solved by touching the column end to the tip of a drill bit to direct the liquid flow. The baseline stability in our work was found to be limited by the residual fluctuations at this interface.

A laser power stabilizer was used to minimize the intensity fluctuations. In the end, we were only able to obtain a baseline stability of 1 part in 500 instead of the 1 part in 2000 after the stabilizer. This equals a baseline stability of 8.7×10^{-4} absorbance unit (a.u.) or a LOD of 2.6×10^{-3} a.u. at S/N=3. To determine the concentration LOD of the detector for a given absorber (given molar absorptivity), we use the ratio of absorbance to path length A/b as the criterion. For a 10 μm capillary column, a LOD of 5×10^{-4} a.u. at S/N=3 is estimated for a cross-beam on-column absorption detector. So A/b is 0.5 cm^{-1} for that system. For the axial-beam on-column absorption detector with a 10 mm sample zone length, this ratio is 2.6×10^{-3} cm^{-1}. Therefore, even though the baseline stability in our system is worse, the concentration LOD is better by a factor of 192, due to the increased path length. It should be noted that although a He-Ne laser was used in our experiment, such a source is not essential and can be replaced by a non-coherent source such as a xenon lamp, provided one can couple sufficient light energy to the entrance of the capillary. In using uv lasers or the uv output of arc lamps, one will have to be concerned about photobleaching because the analytes will be exposed to radiation for much longer periods than in normal detectors.

Other considerations

The band broadening of the chromatogram in Figure 7 was caused partly by column to injector connection and the dead volume inside the light coupling tee. No attempt was made in this work to further minimize the band broadening and to optimize the system. Further effort on developing axial-beam on-column absorption detection has to address this problem.

The requirement that mobile phases with large refractive indices must be used limits the applicability of axial-beam on-column absorption detection. To overcome this limitation, a couple of approaches can be pursued. Tsunoda et al. [45] have recently employed a poly(tetrafluoroethylene-co-hexafluoropropylene) (FEP) tubing as a waveguide cell for liquid absorption spectrometry. The refractive index of FEP is only 1.338, close to that of water (1.333). If FEP capillary columns with inner diameters about 10 μm are available, most solvents, including aqueous solutions, can be used in the optical waveguide mode. On the other hand, the possibility of successive total reflection at the outer wall of a capillary cell has been demonstrated in an application to colorimetry [46]. It was shown that a considerable fraction of the light energy could be distributed in the core of the column if all the light was introduced into the center of the column. As previously indicated, this is confirmed here even for capillary columns with inner diameters smaller than 25 μm. We expect that the percentage of light energy distributed in the core will be enhanced if the ratio of cross-sectional areas of the core to the wall of column

is larger. With capillary columns with smaller o.d., say 50 μm, the total reflection at the outer column surface may be employed for axial-beam on-column absorption detection using mobile phases of any refractive index. Although the axial-beam arrangement was only applied to OTCLC in this work, it can be extended to the detection of other chromatographic systems using open tubular capillary columns, such as supercritical fluid chromatography and capillary electrophoresis.

Finally, we note that transmission here is by total internal reflection. There is no fundamental limit to the length of the columns used. When gradient elution is used, provided that at no time the solvent refractive index becomes smaller than that of the capillary wall, the chromatogram will maintain its stable baseline. Contributions due to absorption by the changing solvents, however, will be magnified in this scheme.

In conclusion, a novel approach has been developed for absorption detection in open tubular capillary liquid chromatography. The axial coupling of source light with the capillary columns and the use of optical waveguide capillary columns made it possible to utilize the full length of the sample bands inside the capillary columns as the path length for absorbance measurement. Comparing with the cross-beam arrangement, the axial-beam on-column absorption detection provides up to 1000 times increase in path length and 192-fold associated improvement on the concentration limits of detection. This new detection method allows investigation

of substantially lower sample concentrations and quantities than conventionally feasible for absorption detection in open tubular capillary liquid chromatography.

LITERATURE CITED

1. Kucera, P. ed.; Microcolumn High Performance Liquid Chromatography; Elsevier: Amsterdam, 1984.

2. Yang, F. J. ed.; Microbore Column Chromatography: A Unified Approach to Chromatography; Marcel Dekker: NY, 1989.

3. Novotny, M. Anal. Chem. 1988, 60, 500A.

4. Bristow, P. A. and Knox, J. H. Chromatograhia, 1977, 10, 279.

5. Knox, J. H. J. Chromatogr. Sci. 1980, 18, 453.

6. Knox, J. H. and Gilbert, M. T. J. Chromatogr. 1979, 186, 405.

7. Yang, F. J. J. Chromatogr. Sci. 1982, 20, 241.

8. Jogenson, J. C. and Guthrie, E. J. J. Chromatogr. 1983, 225, 335.

9. Sternberg, J. C. Adv. Chromatogr. 1966, 2, 205.

10. Yang, F. J. J. Chromatogr. 1982, 236, 265.

11. Kennedy, R. T. and Jogenson, J. W. Anal. Chem. 1988, 60, 1521.

12. Manz, A. and Simon, W. J. J. Chromatogr. 1987, 387, 187.

13. Yeung, E. S. in Microbore Column Chromatography: A Unified Approach to Chromatography; Yang, F. J. ed.; Marcel Dekker: NY, 1989, p. 117.

14. Hirata, Y.; Novotny, M.; Tsuda, T.; and Ishii, D. Anal. Chem. 1979, 51, 1807.

15. Krejci, M.; Tesarik, K.; and Pajurek, J. J. Chromatogr. 1980, 191, 17.

16. Ishii, D. and Takeuch, T. J. Chromatogr. Sci. 1980, 18, 462.

17. Tsuda, T. and Nakagawa, G. J. Chromatogr. 1983, 268, 369.

18. Hirata, Y. and Novotny, M. J. Chromatogr. 1979, 186, 521.

19. Tsuda, T.; Katsugoshi, T.; Nakagaw, G. J. Chromatogr. 1981, 214, 283.

20. Folestad, S.; Johnson, R.; Josefsson, B.; and Galle, B. Anal. Chem. 1984, 54, 925.

21. Hirata, Y.; Lin, P. T.; Novotny, M.; and Wightman, R. M. J. Chromatogr. 1980, 181, 287.

22. Slais, K. and Kreci, M. J. Chromatogr. 1982, 235, 21.

23. Knecht, L. A.; Guthrie, E. T.; and Jogenson, J. W. Anal. Chem. 1984, 56, 479.

24. Niessen, W. M. A. and Poppe, H. J. Chromatogr. 1985, 323, 37.

25. McGuffin, V. L. and Novotny, M. Anal. Chem. 1981, 53, 946.

26. Krejci, M.; Tesarik, K.; Rusik, M.; and Pajurek, J. J. Chromatogr. 1981, 218, 167.

27. Sepaniak, M.; Vargo, J. D.; Kettler, C. N.; and Maskarinec, M. P. Anal. Chem. 1984, 56, 1252.

28. Yang, F. J. J. HRC & CC 1981, 4, 83.

29. Walbroech, Y. and Jorgenson, J. W. J. Chromatogr. 1984, 315, 135.

30. Guthrie, E. J. and Jorgenson, J. W. Anal. Chem. 1984, 56, 483.

31. Guthrie, E. J. and Jorgenson, J. W. J. Chromatogr. Sci. 1984, 22, 171.

32. Dovichi, N. J.; Zarrin, F.; Nolan, T. G.; and Bornhop, D. J. Spectrochimica Acta 1988, 43B, 639.

33. Novotny, M. in Microcolumn High Performance Liquid Chromatography, Kucera, P. ed.; Elsevier: Amsterdam, 1984, Chapter 7.

34. Farbrot, A.; Folestad, S.; and Larson, M. J. HRC & CC 1986, 9, 117.

35. Pfeffer, W. D. and Yeung, E. S. J. Chromatogr., in press.

36. Lei, W.; Fujiwara, K.; and Fuwa, K. Anal. Chem. 1983, 55, 951.

37. Stone, J. Appl. Phys. Lett. 1972, 20, 239.

38. Stone, J. IEEE J. Quantum Electron., 1972, EQ-8, 386.

39. Stone, J. J. Chem. Phys. 1978, 69, 4349.

40. Fuwa, K.; Wei, L.; and Fujiware, K. Anal. Chem. 1984, 51, 164.

41. Fujiware, K.; Simeonsson, J. B.; Smith, B. W.; and Winefordner, J. D. Anal. Chem. 1988, 60, 1065.

42. Snyder, L. R. and Kirkland, J. J. Introduction to Modern Liquid Chromatography; John Wiley: NY, 1979, pp. 249-250.

43. Savitzky, A. and Golay, M. J. E. Anal. Chem. 1964, 36, 1627.

44. Synovec, R. E. and Yeung, E. S. Anal. Chem. 1985, 57, 2162.

45. Tsunoda, K.; Nomura, A.; Yamada, J.; Nishi, S. Appl. Spectrosc. 1990, 44, 163.

46. Tsunoda, K.; Nomura, A.; Yamada, J.; Nishi, S. Appl. Spectrosc. 1989, 43, 49.

SECTION III

OPTIMIZATION OF DETECTABILITY IN LASER-BASED POLARIMETRIC DETECTOR FOR HIGH PERFORMANCE LIQUID CHROMATOGRAPHY

INTRODUCTION

The rotation of polarized light by naturally optically active molecules is an interesting optical phenomenon since it indicates the existence of asymmetry in the medium. Measuring optical rotation is then a unique way to selectively detect chiral molecules. Molecules with chiral centers are important because they are generally associated with biological activity. However, these molecules are normally present in trace quantities, and commercial polarimeters simply do not have low enough detectability to detect them. If the detectability of a polarimeter is expressed as the minimum detectable angle of optical rotation at a level of signal-to-noise ratio (S/N) = 3, the best performance for a commercial polarimeter is in the 10^{-2} degree range (1-4), which corresponds to a concentration of 0.1 mg/ml of an analyte with a typical specific rotation of 100° in a 10 cm cell. For the applications in HPLC separation of complex samples of clinical, geological or biological importance, the extremely high selectivity of optical rotation is very useful for the selective detection. However, the detectability of 10^{-2} degree is far from acceptable for most applications of HPLC detection. It is obvious that the usefulness of the polarimetric detection in HPLC depends on its detectability.

A laser-based polarimetric detector for HPLC has been developed (5) and applied to the studies of HPLC separations of sugars in urine (6), cholesterol in serum (7), components in shale oil (8) and extracts of coal (9). It has also been used to measure absorption indirectly for detection in microbore liquid chromatog-

raphy (10). The key to success of this laser-based detection method is the better rejection of stray light and the reduction of birefringence in the optical components by using a small, collimated laser beam. The detectability is then substantially improved. The first generation laser-based polarimetric detector (5) used two 20-cm air-based solenoid (16750 turns) to modulate the signal. The large current (0.5A) was required to produce a 10^{-3} degree modulation due to the very small Verdet constant of air. The detectability was about 1×10^{-4} degree for a 1 s time constant (11). Later, a modified design used a liquid-based solenoid, typically with a 5 cm cell length, 60 turns/cm and about 0.1A current. Smaller size and current were required to produce the same extent of modulation because liquid has much larger Verdet constant than air. This design gave an improved detectability of 4.7×10^{-5} degree. A better detectability, 2.6×10^{-5} degree at a 1 s time constant, was reported later with a similar liquid-based solenoid (12). For a 10 cm cell and an analyte with specific rotation of 100°, this detectability implies a concentration of 26 ng/ml, which is a useful concentration level for most HPLC applications.

A theoretical analysis (13) on S/N optimization in laser-based polarimetric detectors indicated a shot noise limited detectability of 2.8×10^{-7} degree. It was found that the detectability of the earlier designs was limited by the intensity fluctuations in the laser beam (flicker noise), characteristic of the ion laser used as probe beam. An attempt was then made to improve the noise level by using high-frequency modulation to minimize the laser amplitude noise (14). As low as 3 x

10^{-6} degree of rotation (1 s time constant) could be detected at the modulation frequency of 100 kHz. However, the use of high modulation frequencies severely limited the design of the flow cell for impedance matching. The inductance induced by high modulation frequencies caused problems on the selection of cell material. The low signal levels also put great demands on the lock-in amplifier and on signal transmission (rf interference).

To improve S/N of the polarimetric detection without the problems associated with high frequency modulation, we can produce a larger signal by increasing the angle of modulation (5). This, in turn, can be accomplished by using a larger modulation current and/or larger solenoid with more wire turns. The parameters related to solenoid design, however, are not independent of each other. Arbitrarily varying the parameters will not necessarily provide improved results. A model is therefore needed to relate these parameters, and simulations based on the model will provide optimized parameters and so optimized S/N. In this section, we report improvements of detectability in laser-based polarimetric detector for HPLC, based on the results of simulations. Feedback-controlled stabilization of laser power provided further improvements. These improvements have resulted in detectability approaching the shot noise limit.

MODEL

The signal strength of a polarimetric detector with lock-in amplifier detection is proportional to (5)

$$Signal = I_0 [\sin^2(\alpha+\beta) - \sin^2(\alpha-\beta)] \quad (1)$$

where I_0 is the input light intensity, α is the modulation angle and β is the extent of rotation of the sample. For small angles,

$$Signal = 4 I_0 \alpha \beta \quad (2)$$

The modulation angle (magnetic rotation) in a solenoid is

$$\alpha = VlH \quad (3)$$

where V is the Verdet constant of the medium, l is the length of the solenoid, and H is the magnetic field strength:

$$H = \frac{4\pi nI}{10} \quad (4)$$

where n is the number of solenoid turns per unit length and I is the current passed through the solenoid. Combining equations 2, 3 and 4, we have

$$Signal = (\frac{16\pi I_0 \beta V}{10}] \; nlI \tag{5}$$

The terms inside the parenthesis are constants for a given system. We then have

$$Signal \propto nlI \tag{6}$$

At first glance, it seems from equation 6 that the signal could be enhanced by simply providing a larger modulation current, longer solenoid length or more solenoid turns per unit length. However, there are practical limits on increasing the signal by these methods. One of the limits is the geometric dimensions of the solenoid, which has to be of a reasonable size for practical applications in liquid chromatography. More importantly, the modulation current is limited by the ohmic heat generated in the solenoid (see discussion below). The maximum allowable ohmic heat can be expressed as:

$$I^2R = C \tag{7}$$

where R is the resistance of the coil and C is a constant which depends on solenoid length, cell material (heat capacity) and cooling ability. Since the coil resistance R depends on the total length and the type of magnet wire wound on the solenoid, for a constant voltage driver, I is a function of solenoid turns n, length l and wire

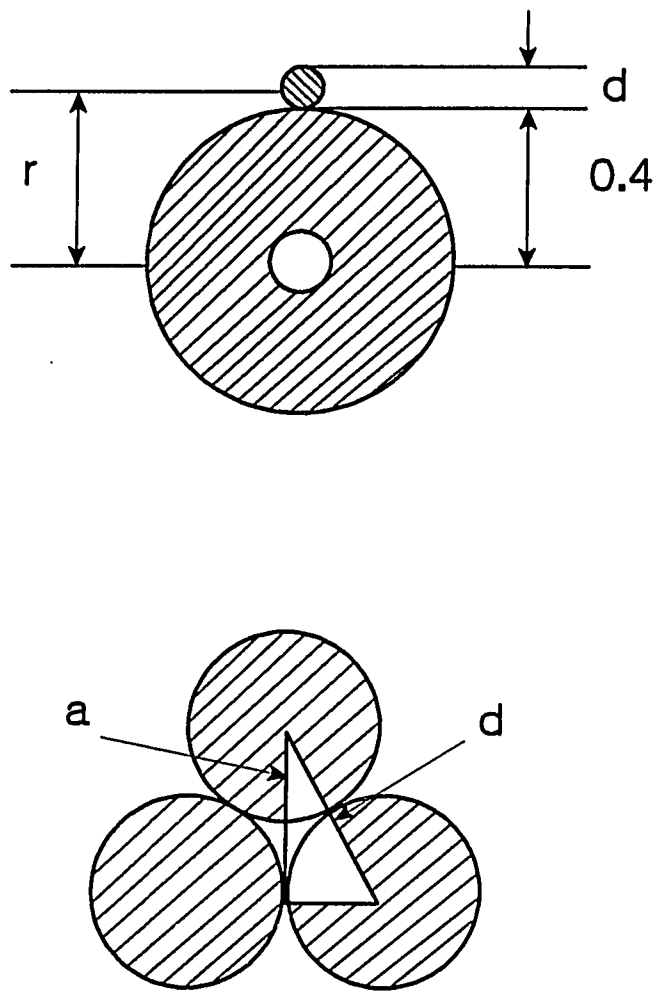

Figure 1. Cross-section of the solenoid. r, inner radius; a, layer thickness; d, wire diameter.

diameter d. Since there are nl total turns and l/d turns per layer, there are a total of nd layers of wires. The total length of magnet wire can be calculated as:

$$L = 2\pi nl\left[r + \frac{a}{2}nd - \frac{a}{2} \right] \tag{8}$$

where r and a are the inner diameter of the solenoid and the thickness of each layer, respectively. Now, considering close packing,

$$a = \frac{\sqrt{3}d}{2} \tag{9}$$

Substituting equation 9 into 8 and taking r = (0.4 + d/2) cm, the actual dimensions of our cell,

$$L = \left(\frac{\pi ln}{2}\right)\left[1.6 + (2 - \sqrt{3})d + \sqrt{3}nd^2\right] \tag{10}$$

The resistance per unit length of magnet wire is proportional to l/d^2, so

$$\frac{R}{L} = \frac{2.2 \times 10^{-6}}{d^2} \tag{11}$$

Substituting equation 10 into 11:

$$R = 3.45 \times 10^{-6} nl \frac{[1.6 + (2 - \sqrt{3})d + \sqrt{3}nd^2]}{d^2} \qquad (12)$$

Combining equations 6, 7 and 12:

$$Signal \propto d \sqrt{\frac{Cnl}{1.6+(2-\sqrt{3})d+\sqrt{3}nd^2}} \qquad (13)$$

The maximum C value for a given system has to be determined by experiments. Considering the physical limit on the solenoid diameter, we have:

$$\frac{\sqrt{3}}{2} nd^2 \leq (b - 0.4) \qquad (14)$$

where b is the outer radius of the solenoid.

This model has simplified the whole problem to optimizing equation 13 with the constraints in equation 14. Simulations based on these two equations will provide optimized cell parameters.

EXPERIMENTAL

Instruments

The arrangement of the laser-based polarimetric detector used in this work has been described previously (5,8). Briefly, 15-20 mW of the 488-nm line from an argon ion laser (Laser Ionics, Orlando, FL, Model 554A) was used as the probe beam. The beam was focused into the detection cell which was between a pair of selected polarizer and analyzer. Signal passing through the analyzer was detected by a photomultiplier tube (Hamamatsu, Middlesex, NJ, model R928). The photoelectric output was then demodulated by a lock-in amplifier (EG&G, Princeton, NJ, Model HR-8) and displayed on a chart recorder (Measurement Technology Inc., Denver, CO, model CR 452).

The solenoid cell was wound on either an aluminum core or a quartz tube with the help of a winding machine. Quartz tubes have the advantage of low heat conductivity and small waveform distortion caused by the inductance at high modulation frequency (14). But the stray light produced in the quartz tube was much stronger than that in the aluminum core. A 1/8" o.d., 1/16" i.d. copper tube was wound on top of the solenoid for water cooling, and silicon grease was used to help efficient dissipation of ohmic heat produced in the coil. The modulation was driven by a wave generator (Wavetek, San Diego, CA, Model 184) and a 150 W audio amplifier (Zenith Radio Corp., Chicago, IL, Model MC 7040). The audio amplifier was

superior to other current amplifier because of its small signal distortion and high power output. A 10 cm, 8000 turn, air-based coil was used to provide a standard signal in this study. A 0.25A current provided a 2.5×10^{-4} degree rotation. The noise was taken as the peak-to-peak variation of the baseline before and after the measurement of dc rotation. The stabilization of laser power was realized by using a laser power stabilizer (Cambridge Research and Instrumentation, Cambridge, MA, Model LS100). The noise power spectra were collected by using a 5 MHz spectrum analyzer with digital storage (Tektronix, Beaverton, OR, Model 7L5). The spectra were displayed on the oscilloscope (Tektronix, Beaverton, OR, Model 7704A) to select the modulation frequencies with minimum noise.

Procedures

The various components in the polarimetric system were carefully optimized during the experiments since the best extinction ratio and sensitivity of the system were very critical for the improvements on S/N. The laser beam was directed through the specific positions on the polarizer and analyzer previously selected to give optimum extinction ratio. The sensitivity of the system was checked at the same time by rotating the analyzer a small angle away from the extinction. The cell windows were selected to minimize the induced birefringence and depolarization and to maintain the optimum extinction ratio and sensitivity.

RESULTS AND DISCUSSION

According to equation 6, a very direct way to produce a larger signal, thus an improved S/N, is to increase the modulation current. This assumes that the modulation waveform itself is stable to the same level as other limiting noise sources. In previous studies, this current was limited to about 0.2A, depending on the load resistance, by the voltage output ability of the wave generator. Using an audio amplifier, as described in the experimental section, we can obtain currents larger than 3A with little distortion of the waveform and modulation stability. However, as shown in Fig. 2, the dependence of the magnitude of the signal on modulation current did not follow equation 6. After reaching a maximum, the signal decreased with increasing current. The current at maximum signal depends on various parameters of the solenoid. To optimize S/N of the polarimetric system, the noise power spectra were also collected using a frequency spectrum analyzer. Several modulation frequencies were chosen based on the noise power spectra, at which the noise powers were at a minimum. Fig. 3 shows a plot of the magnitude of the signals vs. modulation frequencies. It is interesting that the signal first increases and then decreases with increasing frequency. To explain the observation, the currents at the corresponding frequencies were then measured and plotted in the same figure. It is due to the inductance of the solenoid that the current decreases at high frequency (14). It is clear that

Fig. 2. Dependence of signal on modulation current. Signal is a dc rotation of 2.5×10^{-4} degree. n=600 cm^{-1}, l=2.8 cm, d=0.0254 cm, laser power: 20 mW, modulation frequency: 1 kHz, without water cooling.

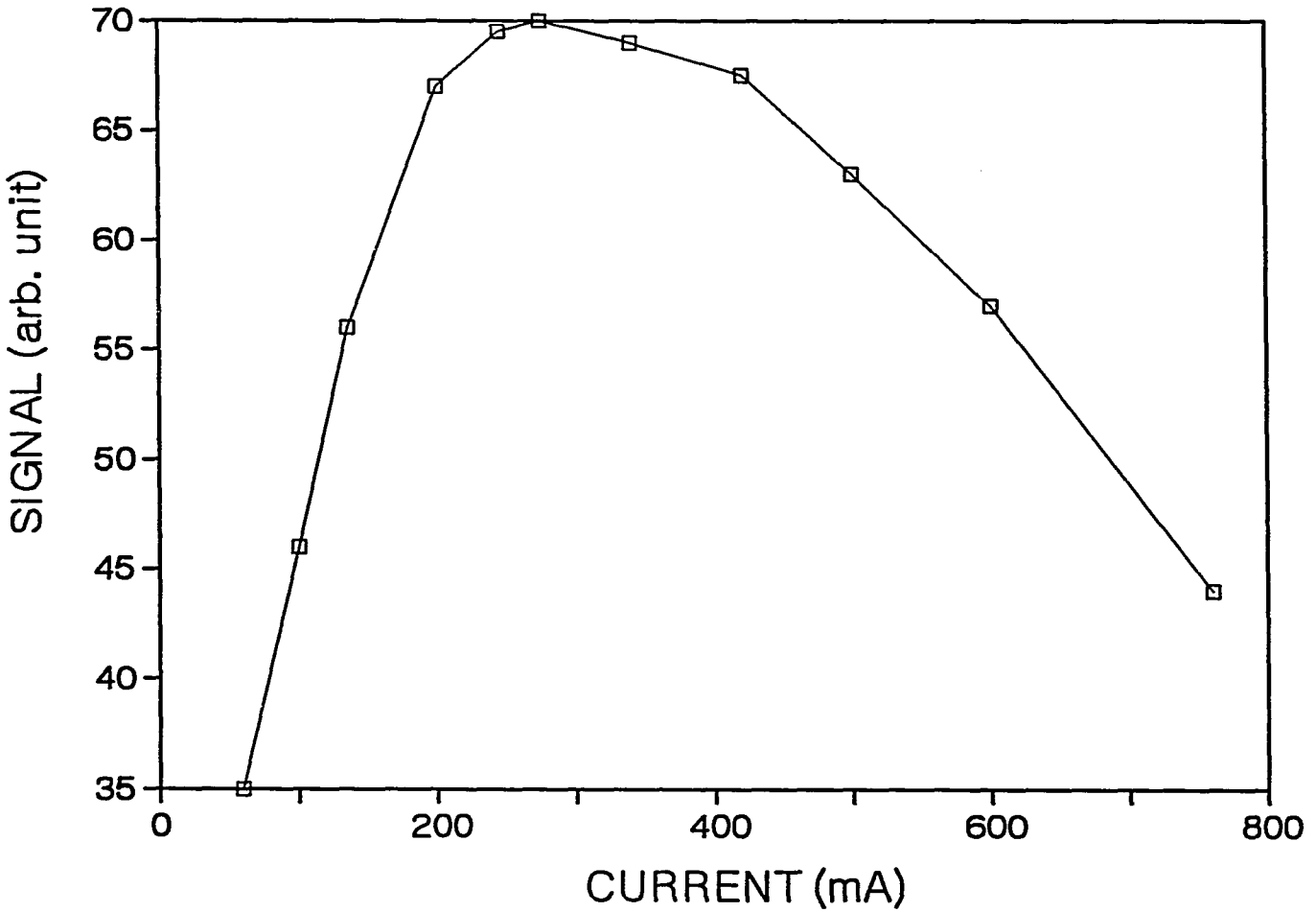
70
65
60
55
50
45
40
35
SIGNAL (arb. unit)
0
200
400
600
800
CURRENT (mA)

Figure 3. Dependence of signal and coil current on modulation frequency. Same conditions as in Fig. 2.

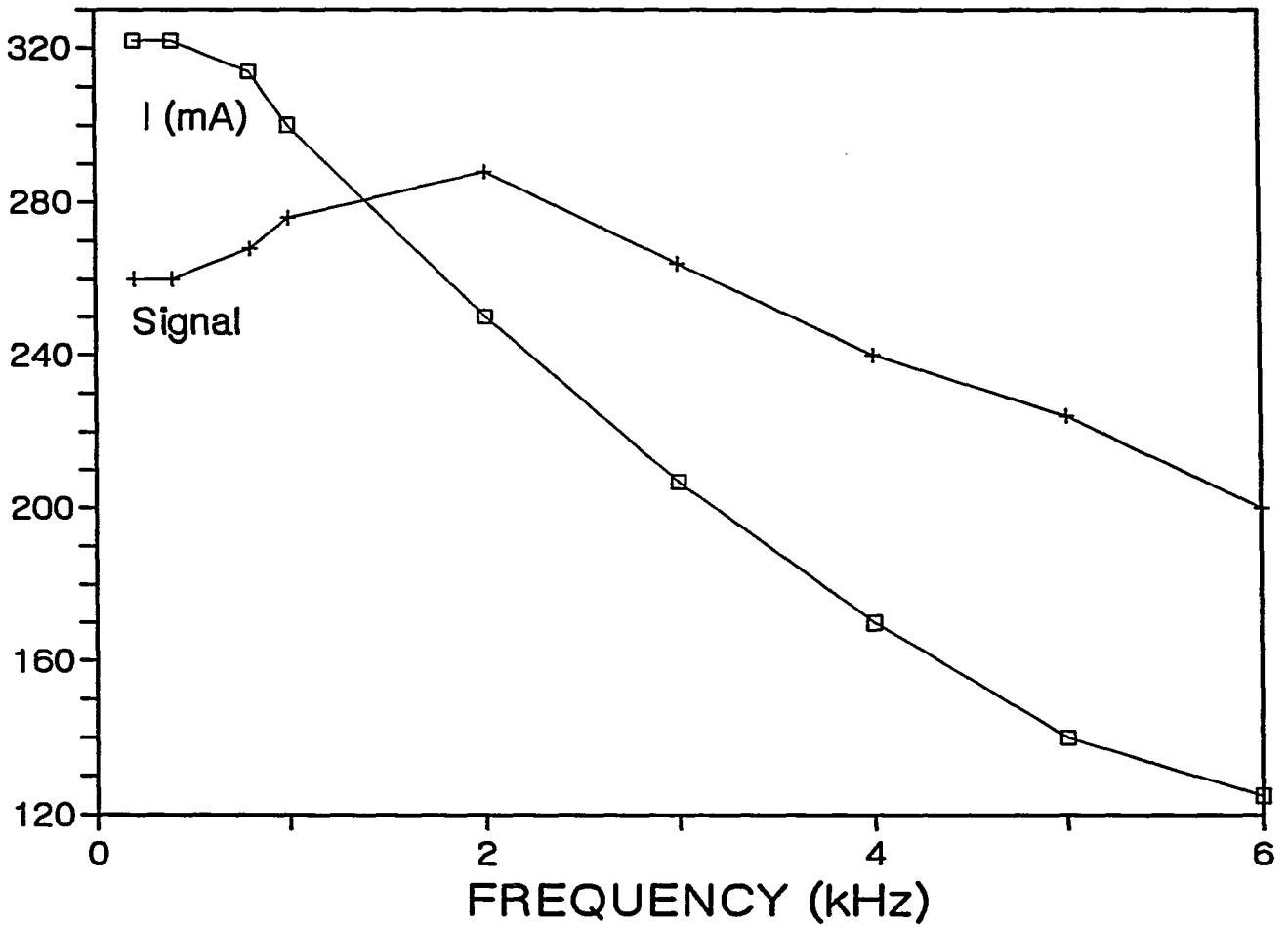
320
280
240
200
160
120
I (mA)
Signal
0
2
4
6
FREQUENCY (kHz)

Fig. 2 and Fig. 3 showed similar dependence of signal on current. These results indicate that it is the ohmic heat, I^2R, generated in the solenoid at high currents that caused a decrease in signal.

The effects of ohmic heat could be in a variety of ways. Temperature increase caused by ohmic heat will change the refractive index of the solvent inside the cell. This then deflects the laser beam and changes the position of the laser beam on the analyzer. This will reduce the magnitude of the signal because the sensitivity as well as the extinction ratio of the laser-based polarimeter are highly dependent on the laser beam positions on the polarizers (5,11). In fact, the beam deflection could be so severe at high currents that the beam became partially blocked by the pinholes which were used in the system to eliminate stray light. Also, increasing temperature caused by ohmic heat will change the birefringence of the cell windows and the Verdet constant of the solvent in the cell.

To apply equations 13 and 14 for optimization, ohmic heat must be evaluated. From the expression $I^2R=C$, ohmic heat limits the maximum current applicable to a given cell (given R and C) as $I = \sqrt{C/R}$. Since the extent of beam deflection will be affected by the path length of the laser beam inside the cell and the heat capacity of the cell will depend on cell material and cooling ability, C is a function of cell length, cell material and cooling ability. However, C is independent of the number of solenoid turns and the wire diameter. Maximum tolerable C values from experiments of several typical cells are summarized in

Table I. Experimentally determined maximum C values (W)

	Coil Length l (path length) (cm)			
Core Material	2.0 (3.5)	2.8 (5.0)	4.0 (6.5)	5.0 (9.0)
Without water cooling				
Aluminum	----	1.40	----	0.52
Quartz	1.79	1.92	1.28	----
With water cooling				
Aluminum	----	1.57	----	0.81
Quartz	2.00	2.18	1.53	----

Table I. Since quartz has a smaller heat conductivity than aluminum, a cell with quartz core will have a larger C value than that with aluminum core. However, quartz cells usually produce large amounts of stray light, therefore reducing the sensitivity. Marginal differences were found for C values for these two kinds of cells. On the other hand, the dissipation of ohmic heat by circulating cooling water around the cell allowed a larger C value and, as expected, a larger signal. Finally, the cell length showed a noticeably larger impact on the C value than the other two factors. Longer path lengths of the laser beam through the solvent amplified the effect of beam deflection, therefore, the C values were smaller.

It is quite surprising that such a small amount of heat, usually smaller than 2W, produced persistent effects on the polarimetric system. This can be explained by considering the very small volume of the solvent in the cell (about 90μl). Although it is impossible to calculate the exact temperature increase of the solvent because of the unknown heat capacity of whole cell, a several degree increase in temperature is expected. In a previous study of the polarimetric detector using high frequency modulation to minimize the laser flicker noise(14), the large modulation currents did not translate into improved S/N. It was concluded that the instability of the modulation depth (due to the limited capability of the driver) was the reason. However, it is very possible that ohmic heat also played an important role there because the severe baseline drift (Fig. 3, reference 12) is a definite indication of temperature changes.

With experimentally determined C values, simulations on the cell parameters n, l and d were carried out using equations 13 and 14. Fig. 4 shows the signal dependence on the number of turns n for a typical cell. At the beginning, the signal increased proportionally to the number of turns. The increase in signal is less pronounced at large n and almost reaches the maximum at about 1500 turns/cm, which was also about the practical limit for typical dimensions of a cell. Further increase in the number of turns will have little improvement on the signal because lower applied current, due to the higher resistance, will simply offset any improvement by more turns in equation 6. It is clear from Fig. 4 that about fivefold increase in signal can be obtained using a solenoid with 1500 turns/cm, compared to the previously used cells with a typical n value of 60 turns/cm. This improvement in signal is a result of increasing the modulation angle. The theoretical dependence of signal strength on wire diameter can also be calculated. Note that maximum n values were different for different wires because of the fixed dimensions of the cells. Equation 14 give the relationship between n and d. Fig.5 shows that signals are almost independent of wire diameters because thinner wires (larger n) have larger resistance (smaller I), and the two effects offset each other. A general simulation on the relationship between signal and solenoid length l is difficult since C is a function of l and the relation is unknown. Table II shows the calculated results for five cells of different path length and cell material with known C values.

Figure 4. Simulation of signal dependence on coil turns n. C=1.40 W, l=2.8 cm.

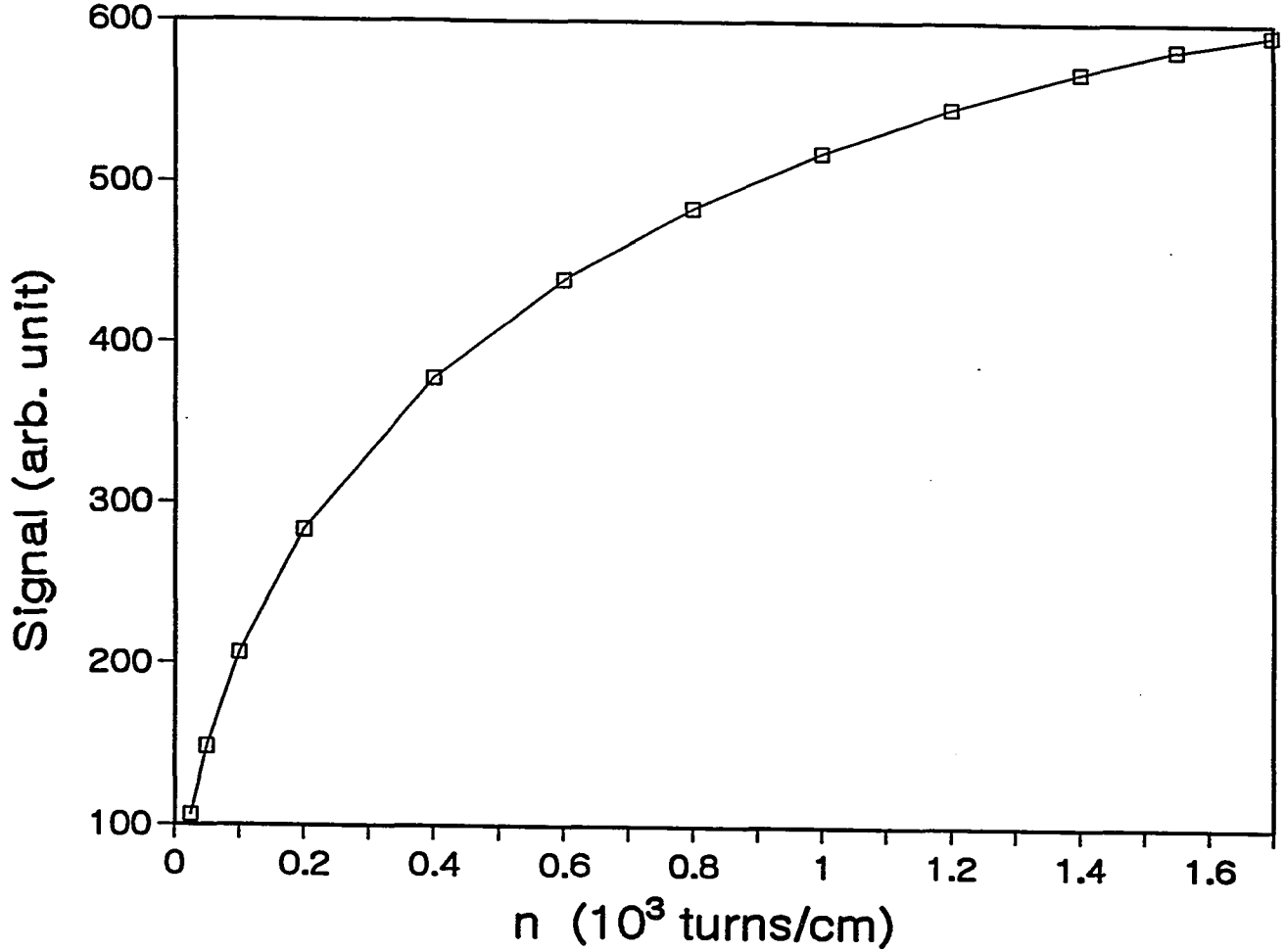
600
500
400
300
200
100
Signal (arb. unit)
0
0.2
0.4
0.6
0.8
1
1.2
1.4
1.6
n (10³ turns/cm)

Figure 5. Simulation of signal dependence on wire diameters. Note that maximum coil turns n changes with wire diameter d, which is decided by equation 14 in the text. (a) $l = 2.8$ cm; (b) $l = 5.0$ cm.

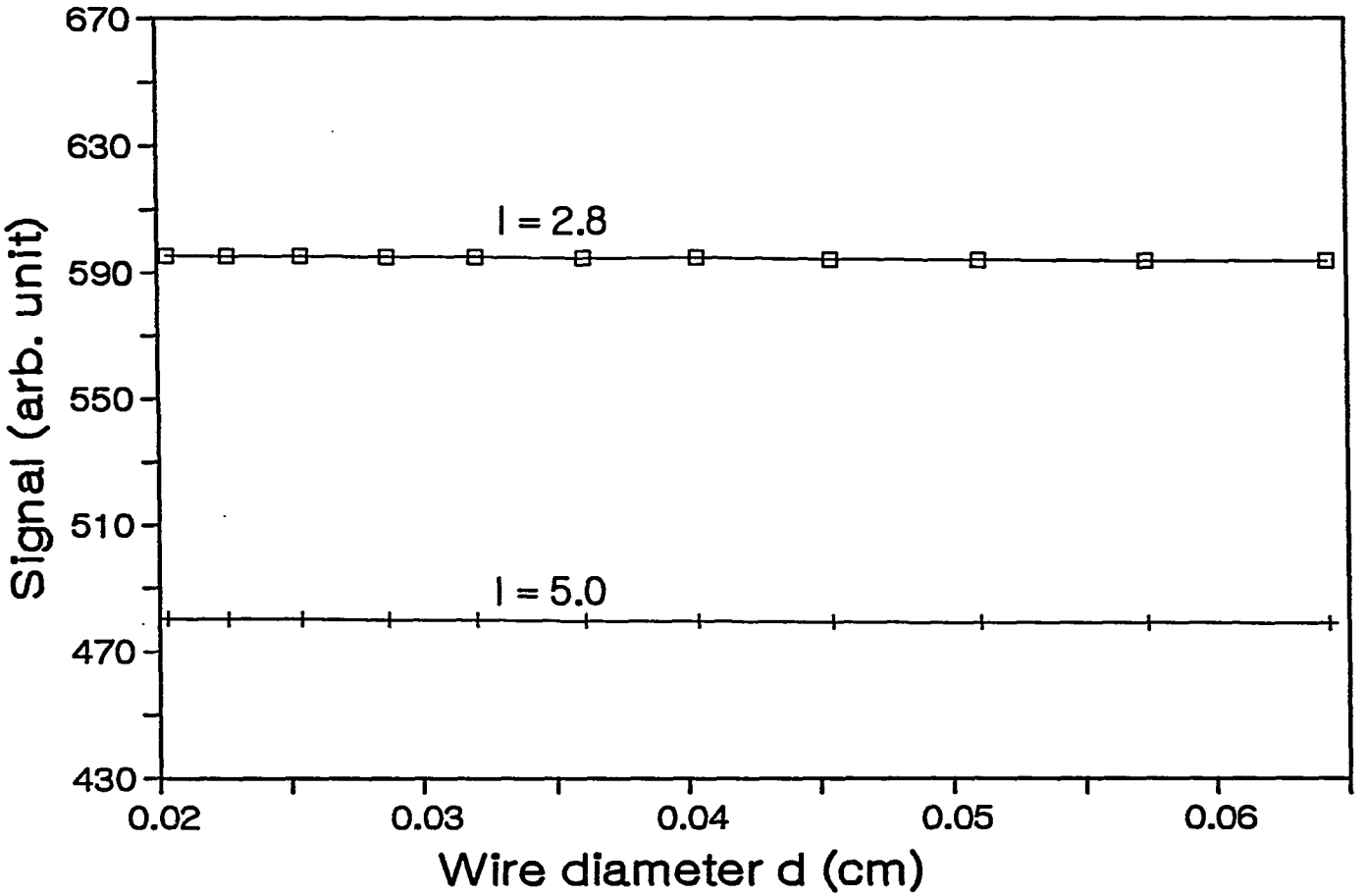
670
630
590
550
510
470
430
Signal (arb. unit)
I = 2.8
I = 5.0
0.02
0.03
0.04
0.05
0.06
Wire diameter d (cm)

Table II. Dependence of signal on cell length*

	Cell length l (path length) (cm)			
Core material	2.0 (3.5)	2.8 (5.0)	4.0 (6.5)	5.0 (9.0)
Quartz	78	100	93	--
Aluminum	--	86	--	69

*n = 600 cm^{-1}, d = 0.0254 cm, without water cooling, signal in arbitrary units.

On the basis of the simulation results, one set of optimized cell parameters can be chosen to provide the largest signal and the best S/N. The S/N for two optimized cells are 170 and 160 for n = 1550 cm^{-1} (#30 wire) and n = 617 cm^{-1} (#26 wire), respectively. More than fivefold improvement on S/N was achieved over previous work for low-frequency modulation. This improvement is significant in practice since no complication was introduced and it is easy to apply.

A theoretical study (13) of the sources of noise affecting the polarimetric system concluded that the dominant source of noise for the laser-based polarimeter was the flicker noise of the laser beam. If this laser flicker noise could be reduced to 10^{-4}, a detectability of 2.8×10^{-7} degree would be realized. One simple, but very

efficient way to minimize laser power fluctuation is to use a commercial laser power stabilizer. For example, it has been shown (15) that stabilization of laser power by a commercial power stabilizer improved both the detection limit and the dynamic reserve in a capillary zone electrophoresis system with indirect fluorescence detection. However, at the beginning of this study, little improvement on S/N was observed in the polarimetric system, even though the laser power stability was improved twenty-fold by a laser power stabilizer (from 200 to 4000). The laser power stability at different positions in the polarimetric system was then measured to explain the observation. As shown in Table III, stabilization of the laser power was greatly degraded by the flow cell and the analyzer. This is due to a variety of reasons. First, the temperature fluctuations in the cell caused by laser heating and ohmic heat produced instantaneous deflection of the laser beam, and this was converted into laser power fluctuations after passing the analyzer. Second, the rejected laser beam in the analyzer (about all of the input power) heated the holding cement, and thermal relaxation of the cement caused the analyzer to rotate minutely and randomly (11). Finally, the vibration of both the cell and the analyzer caused by unstable mounts and environmental noise could also introduce significant fluctuations.

To reduce laser power fluctuations caused by the cell and the analyzer, the analyzer was moved toward the cell as close as physically possible to minimize the effect of laser beam deflection, heavy springs were used for the flow cell mount to

Table III. Laser power stability at different positions in the polarimetric system

Before cell	After analyzer and cell	After analyzer without cell
4000	100	650
2000	100	620
180	80	130

reduce cell vibration, and the data were collected with minimized environmentally introduced vibration on the polarimetric system. With all these incorporated, a laser power stability of 200 after the analyzer can routinely be realized when the laser power stabilizer was used. This level of stabilized laser power provided another two-fold improvement on S/N: ~320 for the 2.5×10^{-4} degree rotation at 1 s time constant. This is equal to a detectability of 2.3×10^{-6} degree, which is an order of magnitude improvement over previous work for normal (~1 kHz) frequency modulation.

In summary, a model relating the modulation cell parameters of the laser-based polarimetric detector has been derived to optimize the signal-to-noise ratio. Since the cell parameters could be systematically chosen with simulation, the performance of the system has been optimized. Combined with a stabilized laser power, one order of magnitude of improvement in detectability of the system has

been achieved, without the complications associated with high frequency modulation. The result is approaching the theoretical limit. Further improvement is possible by isolating the system from vibrations.

LITERATURE CITED

1. Baumann, A. Z. Anal. Chem., 1977, 284, 31.

2. Rossi, P. Analyst (London), 1975, 100, 25.

3. Scott, B. S. and Dunn, D. L. J. Chromatogr., 1985, 319, 419.

4. Levy, G. B.; Schwed, P. and Fergus, D. Rev. Sci. Instr., 1950, 21, 693.

5. Yeung, E. S.; Steenhoek, L. E.; Woodruff, S. D. and Kuo, J. C. Anal. Chem., 1980, 52, 1399.

6. Kuo, J. C. and Yeung, E. S. J. Chromatog., 1981, 223, 321.

7. Kuo, J. C. and Yeung, E. S. J. Chromatog., 1982, 229, 293.

8. Kuo, J. C. and Yeung, E. S. J. Chromatog., 1982, 253, 199.

9. Bobbitt, D. B.; Reitsman, B. H.; Rougvie, A.; Yeung, E. S.; Aida, T.; Chen, Y.; Smith, F.; Squires, T. G. and Venier, C. G. Fuel, 1985, 64, 114.

10. Bobbitt, D. B. and Yeung, E. S. Anal. Chem., 1985, 57, 271.

11. Kuo, J. C. Ph.D. Thesis, Iowa State University, 1982.

12. Bobbitt, D. B. and Yeung, E. S. Anal. Chem., 1984, 56, 1577.

13. Yeung, E. S. Talanta, 1985, 32, 1097.

14. Bobbitt, D. B. and Yeung, E. S. Applied Spectroscopy, 1985, 32, 1097.

15. Kuhr, W. G. and Yeung, E. S. Anal. Chem., 1988, 60, 2642.

SECTION IV

AXIAL-BEAM ABSORPTION DETECTION FOR CAPILLARY ELECTROPHORESIS WITH CONVENTIONAL LIGHT SOURCE

INTRODUCTION

Capillary electrophoresis (CE) is a highly efficient instrumental technique for separation and quantitative analysis of a wide range of compounds in complex mixtures. Because capillaries with small inner diameters can provide efficient heat dissipation and suppress convection, one million theoretical plates within 30 minutes can be generated in CE (1-3). CE has been applied to separations of many ionic and non-ionic species that are important in biological, pharmaceutical and genetic engineering processes (4-8). The recent availability of commercial instruments from several manufacturers is an indication of the increasing popularity of CE.

The principal limitation for CE development has been identified as detection (3), primarily due to the extremely small sample volumes. In order to maintain the high efficiency of CE separation, on-column detection methods have been almost universally utilized, including UV absorption (9,10), fluorescence (11,12), radioisotope (13), mass spectroscopy (14-17) and electrochemistry (18-20). Among these detection methods, UV absorption, though less sensitive than fluorescence detection, is the most popular one because it is more universal than other detection methods. Specifically, most analytes of interest absorb in the 210 nm region. The first on-column UV absorption detector was constructed by Yang (21), who stripped the polymer coating of a segment of the fused silica capillary column and directed the light beam perpendicular to the capillary column window. While this cross-beam arrangement has provided reasonable detection limits owing to high intensity

stability of the conventional light source, the short absorption path length, which equals the inner diameter of the capillary (typically 50 μm), severely limits the absorbance and thus the concentration limits of detection.

Recently, we have developed an axial-beam on-column absorption detector for open tubular capillary liquid chromatography (OTCLC) (22). A laser beam was axially coupled into one end of a 10 μm i.d. fused silica capillary column, and light was transmitted through the column by total internal reflection. The signal was detected at the other end of the capillary column. At any given time, the total absorbance was the sum of the absorbances of the individual components within the column. When absorbing components eluted out from the column, the change of light transmittance could be detected and an integrated chromatogram was observed. This axial-beam detection method made it possible to utilize the full length of sample bands inside the capillary column as the pathlength for absorbance measurement. It provided 1000 times increase in path length and 192-fold improvement on the concentration limit of detection. The degradation of the improvement on the detection limit was mainly due to the poor intensity stability of the laser beam.

Comparing with OTCLC, CE avoids the high pressure interface in the system and can use larger diameter capillary columns. CE is therefore more compatible with axial-beam detection. Since the injection of sample bands up to 3 mm long inside the capillary column would cause little loss of separation

efficiency (1,23), axial-beam absorption detection could provide up to 60-fold improvement on the detection limit over the conventional cross-beam arrangement for a typical 50 μm i.d. capillary column. More recently, the axial-beam design has been utilized for both direct and indirect absorption detection in CE (23,24). Similar to the axial-beam absorption detection for OTCLC (22), a He-Ne laser beam was focused into a 50 μm i.d. fused silica or teflon capillary column (23). Light beam entering the column was transmitted by either partial or total internal reflection, with the proper choice of the buffers. A 15-fold improvement on detection limit over the cross-beam arrangement was observed. The main sources of noise limiting the signal-to-noise ratio of the transmitted light beam were capillary vibration and laser intensity fluctuation, even though a laser intensity stabilizer was used. In the other application (24), an extended pathlength UV absorbance detector was demonstrated by using laser-induced fluorescence which acted as a tool for indirectly determining the absorbance within a given length of the capillary. Fluorescein was added into the buffer as the fluorescent marker, and a laser beam was coupled into the end of the column to induce fluorescence. The intensity of the fluorescence was related to the absorbance of sample band inside the capillary. Even though this arrangement had longer absorption pathlength by a factor of 50 over the cross-beam detection, little improvement on detection limit was realized. It was concluded that the long pathlength could not be exploited due to the high background noise which was caused by poor intensity stability of the

laser beam. Bleaching of the fluorophore by the laser beam is another problem. Also the maximum allowed absorption pathlength is restricted to a small fraction of the length of the analyte zone, or else band broadening will occur. This is in contrast to irradiation of the entire column (22,23) to take advantage of the entire zone length.

The standard spectrophotometric detector is very desirable in CE applications since it allows selected detection at the absorption maximum of a solute, or at a wavelength that provides maximum selectivity. We describe here an axial-beam on-column absorption detector using a conventional light source which has high intensity stability and variable wavelength. An interface is designed and constructed to couple the light beam from a UV spectrophotometer into the entrance of the 50 μm i.d. capillary. The feasibility of this detection method is demonstrated. With minor modifications, both cross-beam and axial-beam on-column absorption detection can be achieved by using the same commercial capillary electrophoresis system.

EXPERIMENTAL SECTION

Instrument

A commercial capillary electrophoresis system (ISCO, Inc., Lincoln, NE; model 3850) was modified for this study. The sample introduction system of the instrument was based on the split injection technique, which had been developed previously for small-volume injection in OTCLC (22,25). A syringe was also used to flush and fill the capillary. The optical detection system of the instrument was basically the same as the CV^4 variable wavelength absorbance detector for liquid chromatography (ISCO, Inc.), except that a ball lens was placed in front of the capillary column to focus the light beam down to ~100 μm. A deuterium lamp, combined with a 1200 groove/mm diffraction grating monochromater, provided a range of wavelengths between 190 nm to 360 nm. The noise level was specified as 2×10^{-5} a.u. ASTM. A capillary column clamping plate held the column firmly against an aluminum retaining block, on which a groove was machined to align the capillary column window perpendicular to the focused light beam.

Fig. 1 shows a schematic diagram of the axial-beam on-column absorption detector. The light beam focused by a ball lens was coupled into the capillary end through an interface block which could be aligned in all three dimensions to optimize light coupling. Light transmitted to the buffer reservoir end of the capillary was collected by an optical fiber and sent to a photomultiplier tube (Hamamatsu, Middlesex, NJ; model R928, at 900 V). The photocurrent was then

Figure 1. Schematic diagram of the axial-beam absorption detector for capillary electrophoresis with a conventional light source.

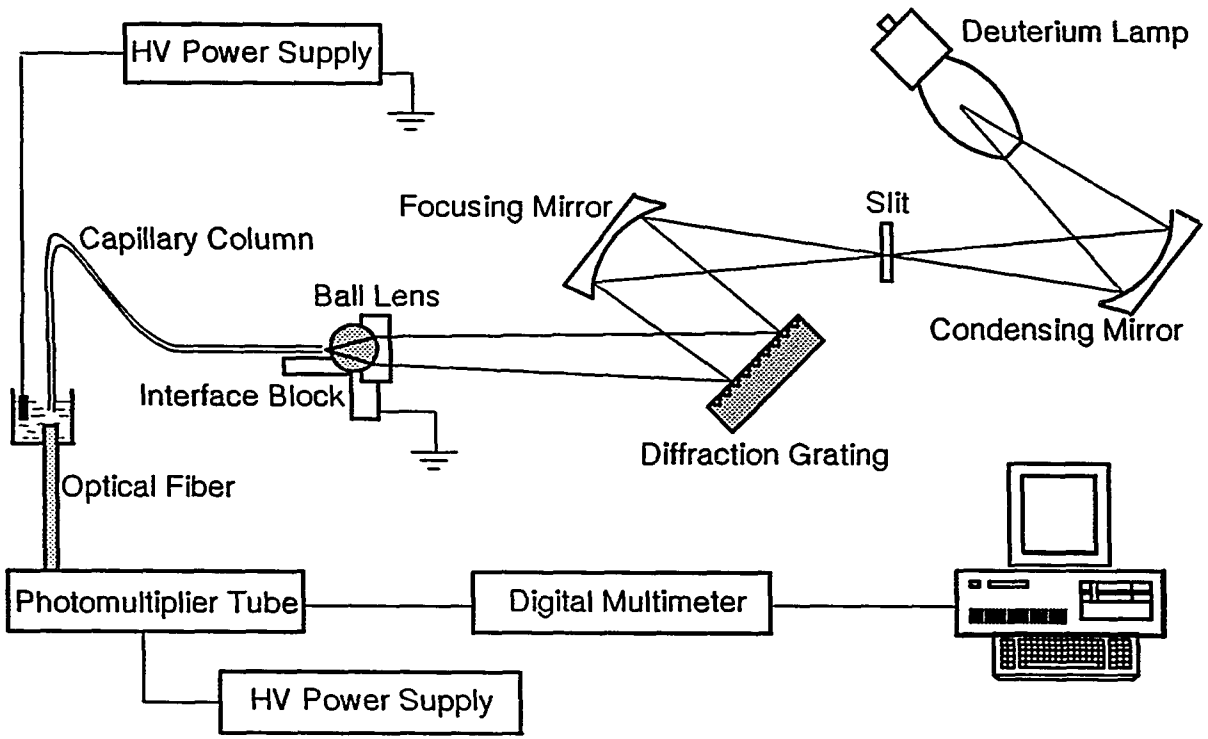
HV Power Supply
Deuterium Lamp
Focusing Mirror
Slit
Capillary Column
Ball Lens
Condensing Mirror
Interface Block
Diffraction Grating
Optical Fiber
Photomultiplier Tube
Digital Multimeter
HV Power Supply

amplified through a digital multimeter (Keithley Instruments, Cleveland, OH, model 160B). Data were collected and analyzed using an IBM AT computer with a 16 bit analog-to-digital conversion board (Data Translation, Marlboro, MA; model 2827).

Light coupling interface

For axial-beam on-column absorption detection, an interface block was designed and constructed in this laboratory to facilitate coupling light efficiently into the end of the capillary column. The interface block, as shown in Fig. 2, was attached to a modified capillary mounting cassette (ISCO, Inc., model 603854010) of the instrument, so that the cross-beam and axial-beam detection modes could be easily switched. Similar to the cross-beam detection, the capillary column was clamped by an aluminum plate onto the interface block, which was also made of aluminum to be electrically conductive and to maximize heat transfer away from the capillary. A groove was extremely carefully machined on the interface block to align and position the capillary column. An ultra-thin quartz cover slip (ESCO, Ork Ridge, NJ; 12 x 12 x 0.15 mm) was used as the window to protect the ball lens, since the electrophoresis buffer flew out from the interface end of the capillary. The interface block was aligned in both horizontal and vertical directions by adjusting two screws which were attached to the capillary mounting cassette of the instrument. The capillary alignment along the z direction, or the axial direction, was simplified by directly contacting the capillary end to the quartz window surface. The focal point of the light beam had been carefully designed to fall on the window

Figure 2. The interface block for coupling a conventional light source into a 50 μm i.d. capillary column. This assembly directly replaces the optical mount in a commercial variable wavelength absorption detector.

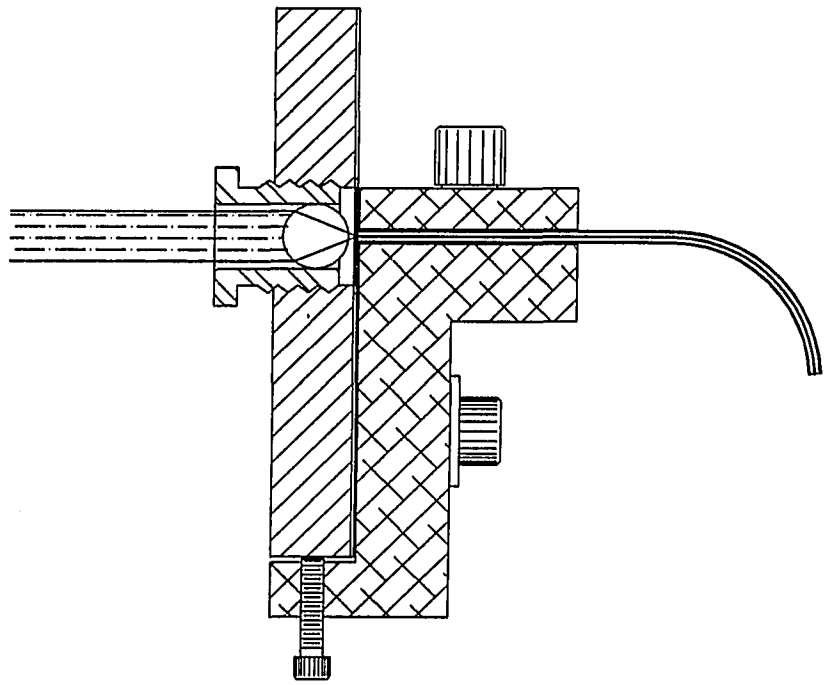

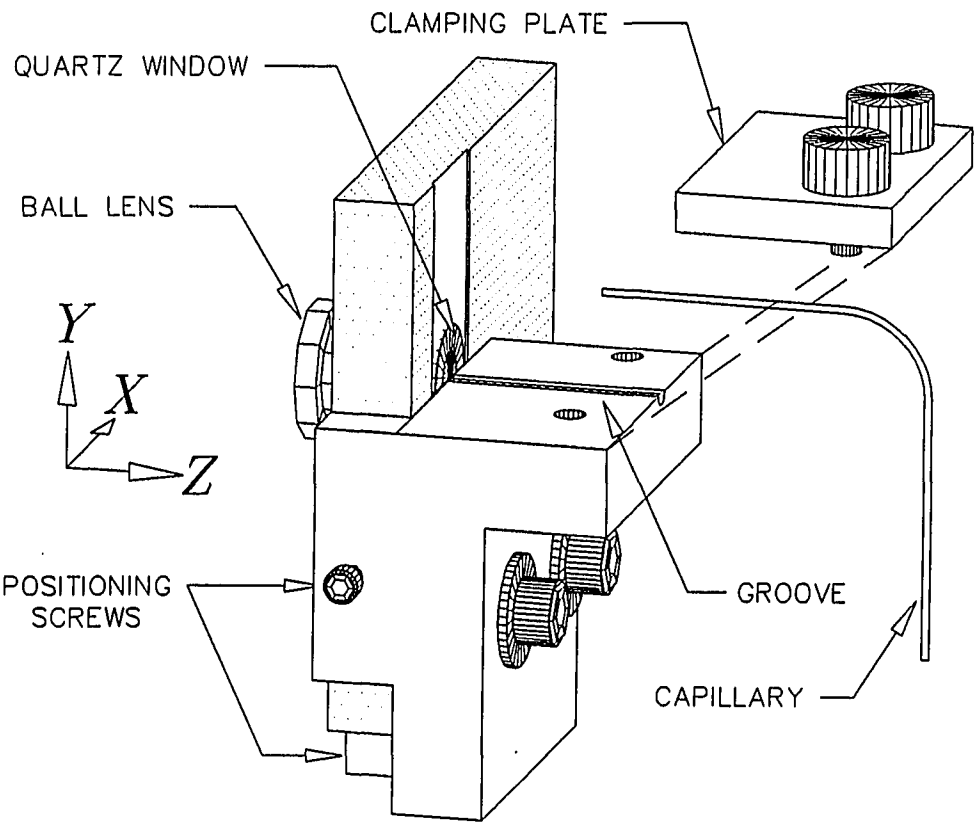
CLAMPING PLATE
QUARTZ WINDOW
BALL LENS
Y
X
Z
POSITIONING SCREWS
GROOVE
CAPILLARY

surface. The high potential loop of the electrophoresis was completed by grounding the interface block to the high voltage supply ground lead.

Collection of transmitted light

The transmitted light beam through the capillary column was collected at the high voltage end of the capillary. A plastic-clad silica optical fiber (Radiant Communication Corp., South Plainfield, NJ; model SPC-1000, 20 cm long) with large core diameter (1 mm) and numerical aperture (NA = 0.40) was used to efficiently collect the transmitted light beam. The optical fiber was inserted into the Teflon buffer reservoir, and the distance between the optical fiber and the capillary end was approximately 1 mm. A low vapor pressure resin (Varian, Lexington, MA) was used to seal the optical fiber and to eliminate electrical breakdown.

Electrophoresis medium and reagents

The running electrophoresis medium consisted of pure dimethyl sulfoxide (Fisher, Fair Lawn, NJ, certified grade), 25 mM tetramethyl ammonium bromide (Aldrich Chemical Co., Inc., Milwaukee, WI) and 10 mM hydrochloric acid (electronic grade). Both 3-amino quinoline and acridine were obtained from Aldrich and were used without further purification. All electrophoresis media and solutions were degassed in an ultrasonic bath and filtered with Nylon 66 filters (Alltech, Deerfield, IL, 0.2 μm).

Procedure

The capillary column was filled with the electrophoretic medium via syringe injection. It was confirmed that the electrophoresis medium from the interface end of the capillary contacted the interface block, and was thus grounded. The reservoir for the electrophoresis medium is at the positive potential end, where samples were injected. The medium was connected to a high voltage power supply (Glassman, Whitehouse Station, NJ; model PS/MJ30P0400-11) with a platinum wire electrode. The split-flow ratio of the injector was 1:2000, and a 10 μl injection would load about 5 nl of sample into the capillary. The separation of acridine and 3-amino quinoline was carried out in an untreated fused silica capillary (Polymicro Technologies, Phoenix, AZ, 365 μm o.d., 50 μm i.d. and 50 cm long) with an applied voltage of +30 kV.

RESULTS AND DISCUSSION

Light coupling and transmission

In the previous studies on axial-beam on-column absorption detection of OTCLC (22) and CE (23), lasers were used as the light source. It took advantage of the unique characteristics of the laser beam. The highly collimated output of the laser, because of the properties of a Gaussian profile, can be easily focused into extremely small diameters. The high intensity of the laser makes it much less important for efficient coupling of light into the capillary column. On the other hand, most commercial capillary electrophoresis instruments, where the cross-beam on-column detection is the standard arrangement, can only use 50 μm or larger diameter capillaries for absorption detection, due to poor focusing ability and low intensity of conventional light sources. Larger capillaries also increase the absorption pathlength. When the focused beam is much larger than the capillary i.d., the signal will be very sensitive to the refractive index change of solution and the distance between the capillary and photodetector (26). Also, the signal-to-noise ratio and the linear range of detection will be reduced (27).

In axial-beam detection, since the intensity of the dispersed deuterium light is so low, efficient coupling of the light beam into the capillary column is critical to improve on the shot-noise limited signal. However, the three dimensional alignment of the capillary column inside the capillary cell compartment of the instrument is not very straightforward. We have, as described in the experimental

section, constructed an interface block, which was attached to the original capillary mounting cassette of the cross-beam detector, to optimize the light coupling by aligning the capillaries in all three dimensions. At 900 V of photomultiplier tube voltage, we were able to detect ~2 μA and ~10 μA current transmitted through a 50 μm i.d. and 100 μm i.d. fused silica capillary column, respectively. In all cases, dimethylsulfoxide was used to fill the capillaries to facilitate total internal reflection of the coupled light beam. Interestingly, while the poor focusing ability of conventional light sources caused low light-coupling efficiency, the alignment actually became less critical than that for a tightly focused Gaussian beam. More importantly, the photobleaching of the analytes, due to long exposure time to radiation in capillaries, would be less a problem because of the very low intensity of the coupled light in the capillaries.

Electrophoresis

The electropherogram in Fig. 3 shows the separation of a test mixture acridine and 3-amino quinoline with the axial-beam absorption detection at 350 nm. At the beginning, the intensity of transmitted light was reduced due to the combined absorption of the two sample components. The separation of the two components was represented by two plateaus in the figure, which were due to the increase of the transmittance when the two components individually eluted out from the capillary. The features of this type of integrated electropherogram (chromatogram) have been discussed in detail earlier (22). Briefly, all the information, such

Figure 3. Electropherogram of acridine and 3-amino quinoline separated in a fused silica capillary column (365 μm i.d., 50 μm i.d. and 50 cm long). Electrophoresis medium: dimethyl sulfoxide with 25 mM tetramethyl ammonium bromide and 10 mM hydrochloric acid. Applied potential: + 30 kV. 5 nl injection. Sample concentration: acridine, 2.5×10^{-5} M; 3-amino quinoline, 2.0×10^{-4} M. An 11-point Golay smoothing is applied on the electropherogram.

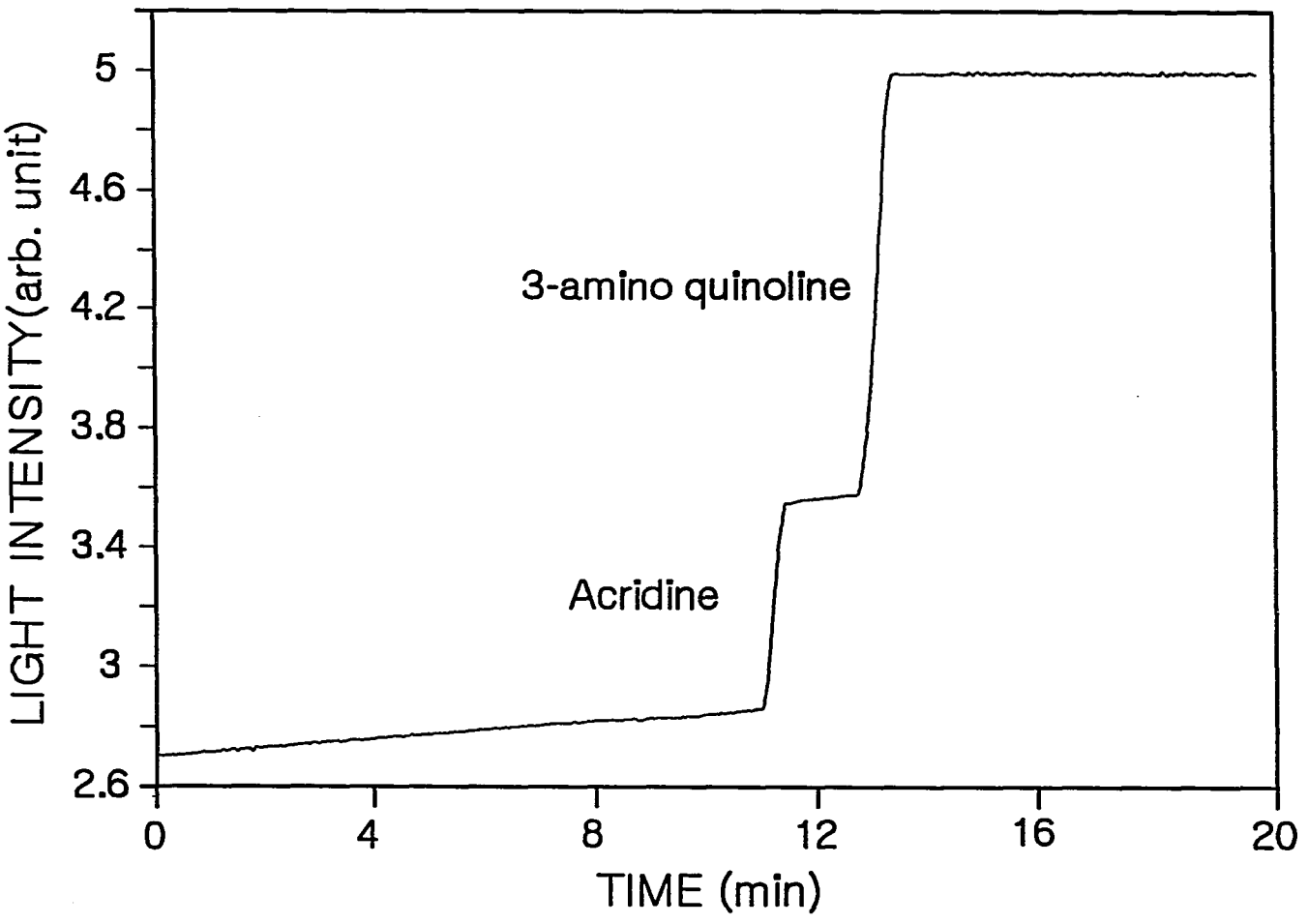
LIGHT INTENSITY(arb. unit)
5
4.6
4.2
3.8
3.4
3
2.6
3-amino quinoline
Acridine
0
4
8
12
16
20
TIME (min)

as resolution, sensitivity, peak width, peak area and elution time, have been preserved in the integrated electropherogram. The first derivative will give a "normal" electropherogram, but with poorer sensitivity (28).

Fig. 3 represents one of very few examples of electrophoresis separation in totally non-aqueous media (27). As indicated before (29), non-aqueous electrophoresis separation deserves further investigation, in order to extend CE to the application of a broader range of compounds. Electrophoresis separation in non-aqueous media will be particularly useful for samples that are insoluble in aqueous solution. For DMSO, up to a few percent of water can be added to allow applications to highly polar or charged analytes.

Analogous to an optical fiber (22), the light beam has to propagate through the capillaries of 10 to 50 μm i.d. by total internal reflection for efficient transmission. This limits the selection of electrophoresis media. Very few aqueous solutions can be used as buffer in CE in the optical waveguide mode since the refractive index of fused silica (RI = 1.458) is significantly larger than that of water (RI = 1.333). Moreover, the requirement on electrophoresis media with short cut-off wavelengths for UV absorption puts more constraint on the media selection, considering the long absorption pathlength (capillary length) in axial-beam scheme. Recently, a poly(tetrafluoroethylene-co-hexafluoropropylene) (FEP, RI = 1.338) tube has been used as a waveguide cell for spectrometry (30), and a Teflon capillary (RI = 1.350-1.380) has been employed for axial-beam absorption detection

in the total internal reflection scheme (23). For either FEP or Teflon capillaries, most aqueous solutions are suitable as the electrophoresis medium for axial-beam detection in the optical waveguide mode. In this study, we have tried to employ Teflon capillaries of 50 to 150 μm i.d. However, because Teflon capillaries are soft, they cannot be easily adapted to the commercial split flow injector where ferrules were used to tightly hold the capillary. Fig. 4 shows how a Teflon capillary was easily deformed while being clamped down in the mount. Obviously, light would be totally obstructed inside the deformed capillary. We were not able to detect any axial light transmission through the 50 to 150 μm i.d. Teflon capillary columns. The problem might be solved by designing a "jacket" for the Teflon capillary to make it more rigid. Then, most electrophoresis media can be used for axial-beam absorption detection in the optical waveguide mode.

Limit of detection

One of the major attractions of using a conventional light source instead of a laser is its high intensity stability. The noise level of the instrument for cross-beam detection was ~8.0×10^{-5} a.u. with high voltage active. For axial-beam detection, the noise was ~7.4×10^{-4} a.u. at S/N = 3. The degraded absorbance limit of detection (LOD) was due to electrostatic vibration of the capillary column, which was caused by the high potential field across the capillary. The LOD for cross-beam and axial-beam absorption detection can be compared by using the ratio of the absorbance LOD to the pathlength, A/b, which is independent of the molar

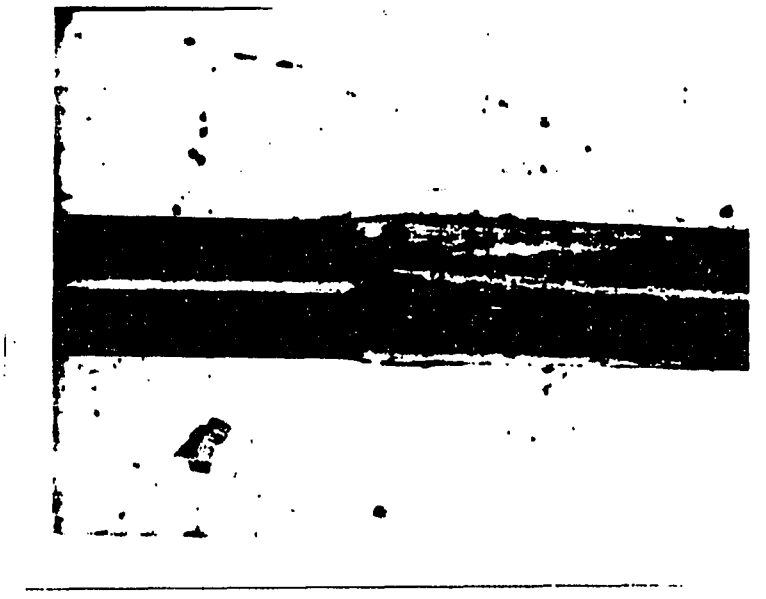

Figure 4. Deformation of Teflon capillary column as a result of clamping in the mount; 365 μm o.d. and 50 μm i.d.

absorptivity of the analyte. A/b = 1.6 x 10^{-2} a.u./cm for cross-beam detection in a 50 μm i.d. capillary. For axial-beam detection and 3 mm injected sample band, A/b = 2.5 x 10^{-3} a.u./cm, which is a seven-fold improvement over the cross-beam arrangement. Very often the length of the eluted zones are much larger than 3 mm, and the improvement provided by the axial-beam arrangement will be proportionately larger. Also, the improvement factor increases if smaller-diameter capillaries were used. We have demonstrated improved detection of acridine and 3-amino quinoline in Fig. 3 where 2.5 x 10^{-5} M and 2.0 x 10^{-4} M were injected. The concentration LOD were 1.9 x 10^{-7} M and 1.1 x 10^{-6} M, respectively. Note that these are injected concentrations, and not concentrations at the detector.

In conclusion, we have developed an axial-beam on-column absorption detector for capillary electrophoresis using a conventional light source. The detector is based on a modified commercial CE instrument. Similar modifications in any of the commercial CE instruments should be straightforward. The cross-beam and axial-beam detection geometries can be easily switched. The high intensity stability, variable wavelength, UV ability and simple design make this instrument attractive. Since the LOD here is apparently limited by capillary vibrations while the electric field is on, we expect even better results if the capillary can be held rigidly along its entire length. Improved LOD in axial-beam arrangement should make CE with absorption detection feasible to a wider range of applications.

LITERATURE CITED

1. Kuhr, W. G. Anal. Chem. 1990 62, 404R.
2. Ewing, A. G; Wallingford, R. A.; Olefirowicz, T. M. Anal. Chem. 1989, 61, 292A.
3. Jorgenson, J. W.; Lukacs, K. D. Science (Washington, D.C.) 1983, 222, 266.
4. Gordon, M. J.; Huang, X.; Pentoney, S. L.; Zare, R. N. Science (Washington, D.C.) 1989, 242, 224.
5. Bushey, M. M.; Jorgenson, J. W. Anal. Chem. 1989, 61, 491.
6. Nielson, R. J.; Sittampalam, G. S.; Rickard, E. C. Anal. Biochem. 1989, 177, 20.
7. Chen, Y. E.; Dovichi, N. Science (Washington, D.C.) 1988, 242, 562.
8. Righetti, P. G. J. Chromatogr. 1990, 516, 3.
9. Hjérten, S. J. J. Chromatogr. 1985, 347, 191.
10. Hjérten, S. J.; Elenbring, K.; Kilar, F.; Liao, J.; Chen, A.; Siebert, C.; Zhu, M. J. Chromatogr. 1987, 403, 47.
11. Jorgenson, J. W.; Lukacs, K .D. Anal. Chem. 1981, 53, 1298.
12. Guthrie, E. J.; Jorgenson, J. W. Anal. Chem. 1984, 56, 483.
13. Pentoney, S.; Zare, R.; Quint, J. Anal. Chem. 1989, 61, 1642.
14. Smith, R. A.; Olivares, J. A.; Nguyen, N. T.; Udseth, H. R. Anal. Chem. 1988, 60, 436.
15. Lee, E. D.; Mück, W.; Henion, J. D.; Covey, T. R. Biomed. Environ. Mass

Spectrom. 1989, 18, 844.

16. Moseley, M.; Deterding, L.; Tomer, K.; Jorgenson, J. J. Chromatogr. 1989, 480, 197.

17. Caprioli, R.; Moore, W.; Martin, M.; DaGue, B.; Wilson, K.; Moring, S. J. Chromatogr. 1989, 480, 247.

18. Mikkers, F.; Everaerts, F.; Verheggen, J. J. Chromatogr. 1979, 169, 11.

19. Huang, X.; Pang, T. K.; Gordon, M. J.; Zare, R. N. Anal. Chem. 1987, 59, 2747.

20. Wallingford, R. A.; Ewing, A. G. Anal. Chem. 1987, 59, 1762.

21. Yang, F. J. J. High Resolut. Chromatogr. Chromatogr. Commun. 1981, 4, 83.

22. Xi, X.; Yeung, E. S. Anal. Chem. 1990, 62, 1580.

23. Taylor, J.; Yeung, E. S. J. Chromatogr., 1991, accepted.

24. Grant, I. H.; Steuer, W. J. Microcol. Sep. 1990, 2, 74.

25. Yang, F. J. J. Chromatogr. 1982, 236, 265.

26. Vindevogel, J.; Schuddinck, G.; Dewaele, C.; Verzale, M. J. High Resolut. Chromatogr. Chromatogr. Commun. 1988, 11, 317.

27. Walboehl, Y.; Jorgenson, J. W. J. Chromatogr. 1984, 315, 135.

28. Synovec, R. E.; Yeung, E. S. Anal. Chem. 1985, 57, 2162.

29. Walbroehl, Y.; Jorgenson, J. W. Anal. Chem. 1986, 58, 479.

30. Tsunoda, K.; Nomura, A.; Yamada, J.; Nishi, S. Appl. Spectrosc. 1990, 44, 163.

SUMMARY AND DISCUSSION

We have discussed, in the earlier sections of this dissertation, both conceptual and technical challenges in the course of the development of novel detection methods for LC and CE. The new detectors, based on totally different physical principles from those normally associated with conventional instruments, will provide not only alternate detection methods to existing ones, but also more dimensions of information on the chemical properties and structures of the analytes. This is critical to meeting the increasing demands of separations and quantitative analysis of samples in complex matrices. Moreover, the improvements on the limits of detections (LOD) of the existing detectors are often hindered by the inherent limitations in the physical principles of the detection methods. For example, the LOD of RI detector is severely limited by fluctuations of pressure and temperature because refractive indices of compounds are extremely sensitive to pressure and temperature changes. It has been concluded that to improve the LOD of RI detection, temperature has to be maintained stable in 10^{-4}° range, which is unrealistic in most applications.

While looking for new physical properties of molecules, which are significant for developing novel LC detectors, we realized that the electrooptical and magnetooptical effects have rarely been exploited for the applications in LC detection. Table I gives the summary of electrooptical and magnetooptical effects. When an electric field is applied across a medium, the distribution of electrons

Table I. **Summary of Electrooptical and Magnetooptical Effects**

Field/light direction	Order	Description of effect	Name of effect	
			Elecrooptic	Magnetooptic
∥	1st	Polarization, plane rotated on transmission	---	Faraday
∥	1st	Polarization, plane rotated on reflection	---	Kerr, m-o
⊥	1st	Birefringence induced	Pockels	Voigt
⊥	2nd	Birefringence induced	Kerr, e-o	Cotton-Mouton
Any	---	Absorption edge shifted toward long λ	Franz-Keldysh	---
∥ & ⊥	All	Spectrum split	Stark	Zeeman

within it is disturbed and the polarizability of the medium is changed nonisotropically, even if the medium is originally isotopic. The medium becomes birefringent due to the applied field. The linear electrooptical effect, or Pockels effect, occurs only in crystals lacking a center of symmetry. The quadratic electrooptical effect, or electric Kerr effect, occurs in these, as well as in isotropic solids and in liquids. The Franz-Keldysh effect is an eletrooptical absorption effect. The applied electric field shifts the absorption band of some crystals toward the longer wavelength. Similar to an electric field, a magnetic field will also affect the optical processes in a medium. We have discussed Faraday effect in Section I in detail. The Faraday effects is a first-order magnetooptical effect and the magnetic field is parallel to the light direction. The magnetic Kerr effect is observed when plane polarized light is reflected on the surface of a crystal subjected to a parallel magnetic field. The rotation of the polarized plane has a linear relationship with magnetic field strength. For Cotton-Mouton effect and Voigt effect, the magnetic field is perpendicular to the light direction, and they are found in the liquid and gas phases, respectively.

Among all of these electrooptical and magnetooptical effects, the Stark and Zeeman effects are observed as spectrum splits in the gas phase; Pockels, magnetic Kerr, Franz-Keldysh and Voigt effects are only found in solid materials or in the gas phase. Obviously, they are not applicable for LC detection. On the other hand, the Cotton-Mouton effect, which is normally over two orders of magnitude weaker than the Faraday effect, does not have the sensitivity required for LC

detection. While we have successfully applied the Faraday effect in universal detection for LC, the electric Kerr effect deserves further exploration for application in LC detection. Using a derived approximate equation, we have recently estimated the potential LOD of the LC detector based on the electric Kerr effect [139]. Although the estimated LOD for favored molecules and strength of the applied electric field is similar to that of the detector based on Faraday effect, the distinct molecular property of the electric Kerr effect will provide complementary information on analytes' chemical properties and structures.

REFERENCES

1. Brown, P. R.; Hartwick, R. A., Ed.; High Performance Liquid Chromatography; John Wiley & Sons: New York, 1989.

2. Scott, R. P. W. Liquid Chromatography Detectors; Elsevier: Amsterdam, 1986.

3. Yeung, E. S. In Analytical Applications of Lasers; Piepmeier, E. H. Ed.; John Wiley & Sons: New York, 1986.

4. Vickery, T. M., Ed.; Liquid Chromatography Detectors; Marcel Decker: New York, 1983.

5. Yeung, E. S., Ed.; Detectors for Liquid Chromatography; John Wiley & Sons: New York, 1986.

6. Ettre, L. S. J. Chromatogr. Sci. 1978, 16, 396.

7. Borman, S. A. Anal. Chem. 1982, 54, 327A.

8. Yeung, E. S. In Lasers in Chemical Analysis; Hieftje, G. M.; Travis, J. C.; Lytle, F. E., Eds.; Humana Press: Clifton, N.J., 1981.

9. Yeung, E. S.; Synovec, R. E. Anal.Chem. 1986, 58, 1237A.

10. Yeung, E. S. J. Res. Natl. Bur. Stand. 1988, 93, 502.

11. Dovichi, N. J.; Zarrin, F.; Nolan, T. G.; Bornhop, D. J. Spectrochim. Acta 1988, 43B, 639.

12. Day, W. R. High Perform. Liq. Chromatogr. Clin. Lab. 1986, 28, 122.

13. Larkins, L. A.; Westcott, S. G. Anal. Proc. (London) 1986, 23, 258.

14. Hoshimo, T.; Sanda, M.; Hondo, T.; Saito, M.; Tohei, S. J. Chromatogr. 1984, 316, 473.

15. Miller, J. C.; Geroge, S. A.; Willis, B. G. Science 1982, 218, 241.

16. Spino, L. A.; Han, S. M.; Armstrong, D. W.; Parrott, A. R. J. Liq.

Chromatogr. 1987, 10, 1603.

17. Brooks, H. B.; Thrall, G.; Tehrani, J. J. Chromatogr. 1983, 385, 55.

18. Carver, D. R.; Weinberger, S. R.; Hlousek, L. Am. Lab. (Fairfield, CT) 1987, 19, 64.

19. Jezorek, J. R.; Faltynski, K. H.; Finch, J. W. J. Chem. Ed. 1986, 63, 354.

20. Denton, M. S.; DeAngelis, T. P.; Yacynych, A. M.; Heineman, W. R.; Gilbert, T. W. Anal. Chem. 1976, 48, 20.

21. Lazaro, F.; Rios, A.; Luque de Castro, M. D.; Valcarcel, M. Analusis 1986, 14, 378.

22. Alfredson, T.; Sheehan, T. J. Chromatogr. Sci. 1986, 24, 473.

23. Bagon, D. A. Anal. Proc. (London) 1987, 24, 42.

24. Lefleur, A. L.; Monchamp, P. A.; Plummer, E. F.; Wornat, M. J. Anal. Lett. 1987, 20, 1171.

25. Yeung, E. S. Chem. Anal. 1986, 89, 1.

26. Riddick, J. A.; Bunger, W. B. In Techniques of Chemistry; Weissberger, A. Ed.; Wiley: New York, 1970.

27. Munk, M. N. In Liquid Chromatography Detectors; Vickrey, T. M., Ed.; Dekker: New York, 1983.

28. Bornhop, D. J.; Povich, N. J. Anal. Chem. 1986, 58, 504.

29. Wilson, S. A.; Yeung, E. S. Anal. Chem. 1985, 57, 2611.

30. Woodruff, S. D.; Yeung, E. S. Anal. Chem. 1982, 54, 2124.

32. Gauglitz, G.; Krause-Bonte, J. Git Fachz. Lab 1988, 32, 200.

33. Pawdiszyn, J. Anal. Chem. 1988, 60, 766.

34. Hancock, D. O.; Synovec, R. E. Anal. Chem. 1988, 60, 1915.

35. Hancock, D. O.; Synovec, R. E. Anal. Chem. 1988, 60, 2812.

36. Hancock, D. O.; Synovec, R. E. J. Chromatogr. 1989, 464, 83.

37. Yeung, E. S. Chem. Anal. 1986, 89, 204.

38. Purdie, N.; Swallows, K. A. Anal. Chem. 1989, 61, 77A.

39. Yeung, E. S.; Steenhoek, L. E.; Woodruff, S. D.; Kuo, J. C. Anal. Chem. 1980, 52, 1399.

40. Yeung, E. S. In Advances in Chromatography; Giddings, J. C.; Grushka, E.; Cazes, J.; Brown, P. R. Eds.; Marcel Dekker: New York, 1984, vol. 23.

41. Sepaniak, M. J.; Kettler, C. N. Chem. Anal. 1986, 89, 148.

42. Weinberger, R. Lab. Prat. 1987, 36, 65.

43. Brinkman, U. A. T.; DeJong, G. J.; Gooijer, C. Methodol. Surv. Biochem. Anal; 1988, 18, 321.

44. Gluckman, J. C.; Novotony, M. V. Chromatogr. Sci. 1989, 45, 145.

45. McGowan, L. B. Anal. Chem. 1989, 61, 839A.

46. Brinkman, U. A. T.: DeJong, G. J.; Gooijer, C. Pure Appl. Chem. 1987, 59, 625.

47. Froehlich, P. Biochromatography 1987, 2, 144.

48. Baker, D. R.; Williams, R. C.; Steichen, J. R. J. Chromatogr. Sci. 1974, 12, 499.

49. Lyons, J. W.; Hardesty, P. T.; Faulkner, L. R. Modern Fluorescence Spectroscopy; vol. 4; Wehry, E. G. Ed.; Plenum: New York, 1981.

50. Barth, H. G.; Berber, W. E.; Lochmuler, C. H.; Majors, R. E.; Regnier, F. E. Anal. Chem. 1988, 60, 387R.

51. Symovec, R. E.; Johnson, E. L.; Moore, L. K.; Penn, C. N. Anal. Chem. 1990, 62, 357R.

52. Stulik, K.; Pacakova, V. Prog. HPLC 1987, 2, 131.

53. Johnson, D. C.; Weber, S. G.; Bond, A. M.; Wrightman, R. M.; Sharp, R. E.; Krull, I. S. Anal. Chim. Acta 1986, 180, 187.

54. Gunasingham, H. Trends Anal. Chem. 1988, 7, 217.

55. Gunasingham, H.; Fleet, B. Electroanal. Chem. 1988, 16, 89.

56. Kissinger, P. T. J. Chromatogr. 1989, 488, 31.

57. Roston, D. A.; Shoup, R. E.; Kissinger, P. T. Anal. Chem. 1982, 54, 1417A.

58. Mefford, I. N. Methods Biochem. Anal. 1985, 31, 221.

59. Jiang, N. S.; Mochacek, D. Prog. HPLC 1987, 2, 397.

60. Hiemdahl, P. Methods Enzymal. 1987, 142, 521.

61. Moleman, P.; Borstrok, J. J. M. Biog. Amines 1985, 3(1), 33.

62. Welch, L. E.; Lacourse, W. R.; Mead, D. A. Jr.; Johnson, D. C.; Ha, T. Anal Chem. 1989, 61, 555.

63. Covey, T. R.; Lee, E. D.; Bruins, A. P.; Henion, J. D. Anal. Chem. 1986, 58, 1451A.

64. Crowther, J. B.; Covey, T. R.; Henion, J. D.; In Detectors for Liquid Chromatography; Yeung, E. S., Ed.; John Wiley & Sons: New York, 1986, 292.

65. Games, D. E. Adv. Chromatogr. 1983, 21, 1.

66. Guiochon, G.; Arpino, P. J. J. Chromatogr. 1983, 271, 13.

67. Vekey, K.; Edwards, D.; Zerilli, L. F. J. Chromatogr. 1989, 688, 73.

68. Bowers, L. D. Clin. Chem. 1989, 35, 1282.

69. Arpino, P. Mass. Spectrom. Rev. 1989, 8, 35.

70. Lankmayr, E. P. Mass Spectro. Biotechnol. Process Anal. Control; Plenum:

New York, 1987.

71. Barefoot, A. C.; Reiser, R. W.; Cousins, S. A. J. Chromatogr. 1989, 474, 39.

72. Koropchak, J. A.; Aryamanya-Mugisha, H. Anal. Chem. 1988, 60, 1838.

73. Huang, S. K.; Klein, D. H.; McLoughlin, M. Biomed. Environ. Mass Spectrom. 1989, 18, 106.

74. Odham, G.; Valeur, A.; Michelsen, P.; Aronsson, E.; McDowall, M. J. Chromatogr. 1988, 434, 31.

75. Volk, K. J.; Yost, R. A.; Brajter-Toth, A. J. Chromatogr. 1989, 474, 231.

76. Otsuka, K.; Mizuno, T.; Azumna, K.; Tsuchiya, M. Anal. Sci. 1988, 4, 467.

77. Vekey, K.; Edwards, D. M. F.; Zerilli, L. F. J. Chromatogr. 1989, 474, 317.

78. Pullen, F. S.; Ashton, D. S.; Baldwin, M. A. J. Chromatogr. 1989, 474, 335.

79. DeWitt, J. S.; Tomer, K. B.; Jorgenson, J. W. J. Chromatogr. 1989, 462, 365.

80. Levi, P. Analusis 1988, 16, XLVII-L.

81. Winkler, P. C.; Perkins, D. D.; Williams, W. K.; Browner, R. F. Anal. Chem. 1988, 60, 489.

82. Sakairi, M.; Kambara, H. Anal. Chem. 1988, 60, 774.

83. Sakairi, M.; Kambara, H. Anal. Chem. 1989, 61, 1159.

84. Moon, D. C.; Kelley, T. A. Biomed. Environ. Mass Spectrum. 1988, 17, 229.

85. Caprioli, R. M.; DaGue, B. B.; Wilson, K. J. Chromatogr. Sci. 1988, 26, 640.

86. Chen, K. H.; Cotter, R. J. Rapid Commun. Mass Spectrom. 1988, 12, 237.

87. Deterding, L. J.; Moseley, M. A.; Tomer, K. B.; Jorgenson, J. W. Anal. Chem. 1989, 61, 2504.

88. Yeung, E. S. Chromatogr. Sci. 1989, 45, 117.

89. Scott, R. P. W., Ed.; Small Bore Liquid Chromatography Columns: Their Properties and Use; Wiley: New York, 1984.

90. Kucera, P. Ed.; Microcolumn High-Performance Liquid Chromatography; J. Chromatogr. Libr.; Vol. 28; Elsevier: New York, 1984.

91. Novotny, M. V.; Ishii, D., Ed.; Microcolumn Separations: Columns, Instrumentation and Ancillary Techniques; J. Chromatgr. Libr.; Vol 30; Elsevier: New York, 1985.

92. Yeung, E. S. in Microcolumn Separations: Columns, Instrumentation and Ancillary Techniques; Novotny, M. V.; Ishii, D., Eds.; Elsevier: New York, 1985.

93. Sagliano, N., Jr.; Hartwick, R. A. J. Chromatogr. Sci. 1986, 24, 506.

94. Skogerbee, K. J.; Yeung, E. S. Anal. Chem. 1986, 58, 1014.

95. Buffet, C. E.; Morris, M. D. Anal. Chem. 1983, 55, 376.

96. Harris, J. M.; Leach, R. A. J. Chromatogr. 1981, 218, 15.

97. Collette, T. W.; Perekh, N. J.; Griffen, J. H.; Carrierra, L. A.; Rogers, L. B. Appl. Spectroscopy 1986, 40, 164.

98. Nolan, T. G.; Hart, B. K.; Dovichi, N. J. Anal. Chem. 1985, 57, 2703.

99. Yeung, E. S. J. Pharm. Biomed. Anal. 1984, 2, 255.

100. Belenki, B. G. J. Chromatogr. 1988, 434, 337.

101. McGuffin, V.; Zare, R. N. Proc. Natl. Acad. Sci. U.S.A 1985, 82, 8315.

102. McGuffin, V.; Zare, R. N. in Chromatography and Separation Chemistry: Advances and Development; American Chemical Society: Washington, D. C., 1986.

103. Gluckman, J. C.; Shelly, D. C.; Novotny, M. V. J. Chromatogr. 1984, 317, 443.

104. Nagels, L. J.; Kauffmann, J. M.; Schuddinck, G.; DeWaele, C.; Pattriarche, G. J.; Verzede, M. J. Chromatogr. 1988, 459, 163.

105. Goto, M.; Shimada, K.; Takeuchi, T.; Ishii, D. Anal. Sci. 1988, 4, 17.

106. Caudill, W. L.; Ewing, A. G.; Jones, S.; Wightman, R. M. Anal. Chem. 1983, 55, 1877.

107. Lunte, C. E.; Kissinger, P. T.; Shoup, R. E. Anal. Chem. 1985, 57, 1541.

108. Henion, J. D.; Maylin, G. A. Biomed. Mass Spectrom. 1980, 7, 115.

109. Takeuchi, T.; Ishii, D.; Saito, A.; Ohki, T. J. High Resolut. Chromatogr. Commun. 1982, 2, 91.

110. Tijssen, R.; Bleamen, J. P. A.; Smit, A. L. C.; VanKreveld, M. E. J. Chromatogr. 1983, 218, 137.

111. Niessen, W. M. A.; Poppe, H. J. Chromatogr. 1985, 323, 37.

112. Alborn, H.; Stenhagen, G. J. Chromatogr. 1985, 323, 47.

113. Niessen, W. M. A. Chromatographia 1986, 21, 277.

114. Niessen, W. M. A. Chromatographia 1986, 21, 342.

115. Niessen, W. M. A.; Poppe, H. J.Chromatogr. 1987, 385, 1.

116. Niessen, W. M. A. J. Chromatogr. 1987, 394, 21.

117. Jorgenson, J.; Lukacs, K. D. Science 1983, 222, 266.

118. Gordon, M. J.; Huang, X.; Pentoney, S. L., Jr.; Zare, R. N. Science 1988, 242, 224.

119. Ewing, A. G.; Wallingford, R. A.; Olefirowicz, T. M. Anal. Chem. 1989, 61, 292A.

120. Wallingford, R. A.; Ewing, A. G. Adv. Chromatogr. 1989, 29, 1.

121. Kuhr, W. G. Anal. Chem. 1990, 62, 403R.

122. Mikkers, F. E. P.; Everaerts, F. M.; Verheggen, Th. P. E. M. J. Chromatogr. 1979, 169, 11.

123. Jorgenson, J. W.; Lukacs, K. D. Anal. Chem. 1981, 53, 1298.

124. Prusik, Z.; Kasicks, V.; Stanek, S.; Kuncova, G.; Hayer, M.; Vrkoc, I. J. Chromatogr. 1987, 390, 87.

125. Walbroehl, Y.; Jorgenson, J. W. J. Chromatogr. 1984, 315, 135.

126. Foret, F.; Deml, M.; Kahle, V.; Bocek, P. Electrophoresis 1986, 7, 430.

127. Kuhr, W.; Yeung, E. Anal. Chem. 1988, 60, 1832.

128. Kuhr, W.; Yeung, E. Anal. Chem. 1988, 60, 2642.

129. Huang, X.; Pang, T. K.; Gordon, M. J.; Zare, R. N. Anal. Chem. 1987, 59, 2747.

130. Wallingfor, R. A.; Ewing, A. G. Anal. Chem. 1988, 60, 258.

131. Wallingfor, R. A.; Ewing, A. G. Anal. Chem. 1988, 60, 1972.

132. Wallingfor, R. A.; Ewing, A. G. J. Chromatogr. 1988, 441, 299.

133. Olivares, T. A.; Nguyen, N. T.; Youker, C. R.; Smith, R. D. Anal. Chem. 1987, 59, 1230.

134. Smith, R. D.; Olivares, J. A.; Nguyen, N. T.; Udseth, H. R. Anal. Chem. 1988, 60, 436.

135. Smith, R. D.; Udseth, H. R. Nature 1988, 331, 638.

136. Smith, R. D.; Barinaga, C.; Udseth, H. R. Anal. Chem. 1988, 60, 1948.

137. Moseley, M.; Deterding, L.; Tomer, K.; Jorgenson, J. J. Chromatogr. 1989, 480, 197.

138. Moseley, M.; Deterding, L.; Tomer, K.; Jorgenson, J. Rapid Commun. Mass Spectrom. 1989, 3, 87.

139 Xi, X.; Yeung, E. S., Department of Chemistry, Iowa State University, unpublished results, 1991.

ACKNOWLEDGMENTS

This work was performed at Ames Laboratory under contract no. W-7405-eng-82 with the U. S. Department of Energy. The United States government has assigned the DOE Report number IS-T 1501 to this thesis.

It is difficult to acknowledge, in such a short section, all the aid and support I have received from many individuals during my graduate career at ISU.

First of all I would like to express my sincere appreciation to Dr. Edward S. Yeung, my research advisor, for the opportunity, insight, flexibility and patience provided during the course of this work. The completion of this graduate program would have been impossible without his guidance.

I am also thankful to my committee members, Dr. Dennis Johnson, Dr.Bernard Gerstein, Dr. Robert Jacobson and Dr. Walter Anderson for their time and advice.

The fellow graduate students and post-doctors in this research group deserve my thanks for some cheerful moments that made my life in Ames more enjoyable, and for sharing instruments, space and their knowledge and experience. I am especially graceful to Dr. Hirofumi Kawazumi for helpful discussion on the study of magneto-optical rotation.

I extend my thanks to staffs in Ames Lab Engineering Service, Ames Lab Student Machine Shop and Chemistry Glass Blowing Shop for their help.

A special note of appreciation goes to my friends in the ISU Table Tennis

Club, CSSU basketball and volleyball teams and the Sports Club Council for all the recreation and fun.

To my parents-in-law, I would like to express my deep gratitude. Their introduction and insight provided the opportunity of continuing my graduate career in the States. Without their encouragement, my adapting to such a different culture and society would have been more difficult.

For their unsurpassed encouragement and support during my long-time education, I am greatly indebted to my parents and sisters. To my mother, this thesis is dedicated for her love, understanding and sacrifice. Her unfailing love is so much more than I deserve.

Finally, to my wife Hui Wang, whose love and patience are an integral part of my success, I am thankful for the hope for our good life in the future.